EMP Theoretical Notes
Note 163

25 Jan 1972

The Ionospherically Propagated Exoatmospheric EMP Environment

Capt Michael A. Messier
Air Force Weapons Laboratory

Abstract

This note provides a basic understanding of the theory of pulse propagation through the ionosphere. It is intended for use by personnel involved in the design of simulators and in the development and application of testing and design criteria. The geometrical ray theory of propagation is used throughout. The propagation characteristics of two representative ionospheres are studied and the transfer functions of one of them is used to calculate the propagated time waveform. An analytic model for calculating the envelope of the propagated waveform is derived and the results are compared with the envelope predicted by Fourier transform methods. Finally, a discussion of energy and field coupling to systems with simple transfer functions is presented.

Foreword

The author started composing this note about two years ago when he was editing a technical report by William Karzas and John Darrah. That report was an exoatmospheric EMP criterion with some discussion about ionospheric propagation and system coupling. The report has not been published as yet, although the criterion has been disseminated. The criterion was strictly a Fourier transform and Karzas and Darrah were the first to point out the problems involved with using a time waveform.

The author decided that an unclassified note, which elaborated on the principles involved, would be useful to personnel involved with criteria or simulator development. This is that note.

The author wishes to thank Karzas and Darrah for unwittingly inspiring this note and for (also unwittingly) contributing some of the material in sections 4 and 2. The author also wishes to thank Capt. Gerard K. Schlegel for allowing him to proceed along this line of investigation while Capt. Schlegel was Lt. Messier's boss, and there were higher priority projects to pursue, and Mr. John Wood for making the difficult Fourier transform routines used to calculate the propagated waveforms a realistic method.

Contents

1. Introduction and Discussion of Exoatmospheric Criteria

The purpose of this note is to provide a general background for personnel involved with the survivability/vulnerability (S/V) assessment of satellite systems. This note is not intended to present criteria of any kind and the information presented should not be interpreted as such. The propagation of EMP through the ionosphere is examined as though it were a linear phenomenon, i.e., a transmission function can be determined through CW analysis and that transmission function is used with Fourier integrals in order to determine the transmitted pulse. The large electric field values involved actually cause nonlinearities and the real fields may be an order of magnitude different over large ranges of frequency or time. Therefore, good criteria cannot be established until this and other effects are considered.

Certain misconceptions exist which could take their toll in satellite S/V analysis and simulator design. The most common problem, and one which will repeatedly be referred to in the text of this note, is the idea that "EMP threats must be specified in volts/meter," or more exactly, that an EMP threat or criterion must be presented as a time waveform. This notion has caused no great difficulty in non-satellite criteria, except that it often results in an abbreviated thought process which accepts only peak electric field values as an input. This note will show that the ionosphere acts in two important ways upon a pulse which propagates through it. First, all frequency content, below a certain cutoff frequency, is filtered out. Second, the ionosphere causes dispersion of the pulse, i.e., the frequency components are separated in time. The result, in the time domain, is that the original pulse is transformed into an oscillating wavetrain. The envelope peak is much less than the peak of the undispersed signal, but this is compensated for by a much longer duration. The lower peak fields are commonly interpreted as meaning that the dispersed pulse is less a threat than the undispersed pulse. An immediate corollary is the belief that systems tested to the undispersed pulse are overtested to the exoatmospheric environment. This idea has about as much validity as the older idea that equipment protected against lightning is protected against EMP.

The use of a time waveform as a design or testing criterion, or as a specification for a simulator is unnecessary at best. No one will argue that a Fourier transform representation is entirely equivalent to a time waveform. The equivalence, of course, assumes that the time waveform is known for all time. One advantage of using the Fourier transform is that the user is forced to think more about what he is doing and cannot lean on the peak field crutch. A second advantage is that most coupling calculations are linear and the Fourier transform can be used directly. The transform of the ionospherically propagated pulse is more simply represented in the frequency domain and, most

importantly, less sensitive to the ionosphere parameters. Small changes in the dispersion result in small percentage errors in the phase of the transform and in the cutoff frequency. However, much larger percentage errors appear in the envelope magnitude, the peak value and width of peak, and in the instantaneous frequency seen at a given time. The work required to satisfy a time waveform specification could be much more than that required to satisfy the equivalent frequency space specification to the same degree of accuracy. Since the exact time waveform is probably not important, the extra work is wasted. The filtering of the ionosphere is beneficial in eliminating the need to calculate the late time signal before propagation because the low frequencies are removed from the spectrum. However, unknowns in the early time undispersed pulse are expanded to later times in the dispersed signal. Thus, if large uncertainties exist in the first nanosecond of the undispersed pulse, the same uncertainties can exist to many shakes in the dispersed pulse. The uncertainties will be exactly the same for the dispersed and undispersed pulses in the frequency domain. The only advantage to using a time domain specification is when non-linear phenomena are involved in a numerical study of the coupling. In the case of satellites, especially those at great orbiting distances, the nonlinearities are usually due to active logic circuits, as opposed to electrical breakdown (because of the low voltages involved). A computer study of the EMP effects would probably begin with a linear coupling to the satellite body anyway, with the resulting voltages and currents being applied to the active circuits.

The question of using the undispersed pulse as an "overtest" of a satellite system deserves careful consideration. Even though the undispersed pulse may, in fact, be an equivalent test pulse or an overtest in ninety percent of the systems tested, there is no a priori reason to believe that this will be true for any given system. It must be remembered that the environment predicted by linear methods is not correct, either, because of the non-linearities involved in the propagation of large fields through the ionosphere. Therefore, when deciding how to test, several factors must be considered. Figure 1-1 shows the block diagram for a hypothetical satellite system in order to demonstrate the types of equipment involved. If a failure mode depends on the field strength seen after coupling over a wide band, then the undispersed pulse will definitely be an overtest. If the failure mode depends on the total energy absorbed over a given bandwidth, then the undispersed pulse will either be an overtest or an equivalent test depending on whether or not the ionosphere has filtered out part of that bandwidth. If, however, the failure mode depends upon the time rate at which energy is applied, then the undispersed pulse can be a threat greater than, equal to, or less than the dispersed pulse. Some possible examples of the latter will be discussed in the next paragraph. The exact modes of failure may not be known until tests have been performed, but it should be possible to

study the satellite system beforehand in order to predict the most likely failure modes, especially for the active circuits. This study can then be used to design a proper test or series of tests. The pretest homework can then be compared with the test results to see if the system was really understood and a new series of tests devised, if necessary.

In order to speculate on failure modes which are more sensitive to the dispersed pulse, refer to the satellite model shown in figure 1-1. The EMP can couple into the satellite through antenna systems, through panels containing solar cells, by exciting the body of the satellite, or by penetrating through apertures in the skin, e.g., optical sensors. Certain satellites could act as high Q cavities and set up ringing modes which are driven by the dispersed signal. This would allow more time for components inside to absorb energy from the field. The fact that a satellite is such a small body means that any common grounding circuits behave much differently than what one normally thinks of here on earth. The ground itself is an antenna and highly varying potential differences can be superimposed upon the normal voltages by the oscillating waveform. These voltages can be reflected in a string of erroneous data being fed into the memory banks or transmitted back to the satellite's ground station. The undispersed pulse may only disturb a few bits. During the period when the satellite is coupling to frequencies near those of the clock which determines the sampling rate, or harmonics thereof, the entire sampling process could be thrown off. The telemetry unit, which determines the order in which data is returned to earth, could be unsynchronized and the ground station might not be able to decode the data. The power supply may see a quasi-D.C. signal corresponding to the envelope of the dispersed pulse and all systems would then operate with incorrect voltages for periods near a millisecond.

The last part of this section can be summed up by the statement that if one tests to the undispersed criteria, he has not tested to the correct environment; on the other hand, the dispersed environment calculated by linear theory isn't correct either.

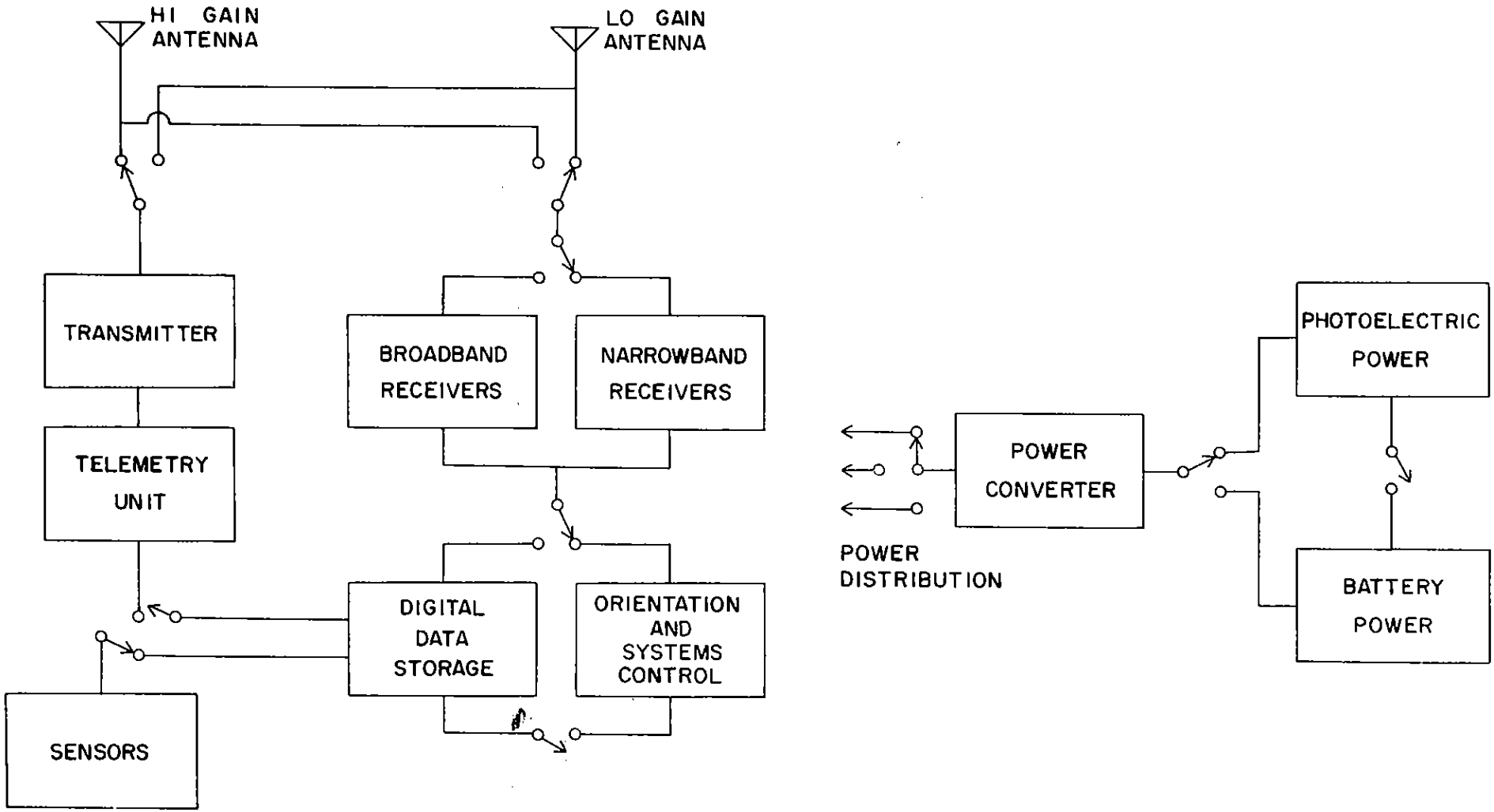

FIGURE 1-1 HYPOTHETICAL SATELLITE SYSTEM

2. Propagation Theory

This chapter presents a description of propagation in the ionosphere sufficient to understand the exoatmospheric EMP environment. The first section discusses the propagation of plane waves in a plasma. Here, basic concepts such as plasma frequency, absorption, and index of refraction are introduced. The following section discusses ray propagation in the ionosphere from the point of view of Snell's law. The relationship between angle of launch, electron density, and cutoff frequency is derived.

In chapter 3, the EMP environment will be determined using linear propagation theory. The initial pulse is Fourier transformed, operated on by a transfer function, and inverse transformed. The transfer function will be determined by considering the propagation of plane waves of various frequencies, thus putting chapter 2 to a useful purpose.

2.1 Propagation of a Plane Wave in a Plasma Medium

The currents produced in an ionized gas under the influence of an electromagnetic field are of two types: conduction and displacement. The first is characteristic of a metal and the second is characteristic of a nonconductor. We then expect to see properties common to both these types of matter in our study of plasma. These properties are described by the permittivity (ε), conductivity (σ), and magnetic permeability (μ). In all future discussion, μ will be assumed to be $\mu_o = 4\pi \times 10^{-7}$ henry/meter. Initially, only a homogeneous isotropic (no magnetic field) plasma will be considered. Also, the conductivity due to ions will be neglected, which is a good first order approximation due to their significantly lower mobility. The plasma state can then be characterized by two parameters for purposes of propagation study: plasma frequency (ω_p) and electron collision frequency (ν). The plasma frequency corresponds to an oscillation of the electrons under the influence of their combined electric field. A resonance effect occurs when the plasma is excited by an electromagnetic wave of frequency ω_p. ω_p is proportional to the square root of the electron density and is given by

$$\omega_p^2 = \frac{q^2}{\varepsilon_o m_e} N = 3182.8\ N \qquad (2.1\text{-}1)$$

where

q = electron charge (1.602×10^{-19} coulomb)

ε_o = permittivity of free space (8.842×10^{-12} farad/meter)

m_e = electron mass (9.108×10^{-31} kg)

N = electron density (electrons/meter^3)

In Hertz, the plasma frequency is given by

$$f_p^2 = 80.621\ N \qquad (2.1\text{-}2)$$

The electron collision frequency is the rate of energy loss collision of electrons with neutrals, assuming a slightly ionized gas. This is an energy loss mechanism and is responsible for the attenuation of EM radiation propagating through the medium.

The solution to Maxwell's equations for a lossy medium can be obtained by assuming either a complex dielectric coefficient or a complex conductivity. We will choose the latter and assume $\varepsilon = \varepsilon_o$. It is instructive, however, to look at the lossless case first, since the solution for current flow is analogous to

a simple LC circuit (Corson and Lorraine, 1962; p. 344). Neglecting collisions, conductivity is given by

$$\sigma = -i\varepsilon_o \frac{\omega_p^2}{\omega} \qquad (2.1\text{-}3)$$

The conductivity is imaginary and the conduction current lags the electric field intensity, E, by $\pi/2$ radians, the same as in an inductor. The displacement current,

$$\frac{\partial D}{\partial t} = i\omega\varepsilon_o E \ , \qquad (2.1\text{-}4)$$

leads E by the same amount, just as in a capacitor, so that the displacement and conduction currents are π radians out of phase. The total current is less than if no plasma were present. The total current density is given by

$$\frac{\partial D}{\partial t} + J = i\left[\omega\varepsilon_o E - \frac{\varepsilon_o \omega_p^2}{\omega} E\right]$$

$$= i\omega\varepsilon_o\left[1 - \left(\frac{\omega_p}{\omega}\right)^2\right]E \ . \qquad (2.1\text{-}5)$$

This shows a resonance phenomenon which makes the current zero at $\omega = \omega_p$. This case is mathematically similar to the solution for the current in a parallel LC circuit in which the total current is given by

$$I = i\omega CV - i\frac{V}{\omega L}$$

$$= i\omega C\left[1 - \frac{1/LC}{\omega^2}\right]V \ . \qquad (2.1\text{-}6)$$

The equation for the conductivity of the plasma can be derived from the Lorentz equation for the velocity of an electron under the influence of an electric field. The electron current is

$$J = qNv \qquad (2.1\text{-}7)$$

where

J = current density

q = electron charge

N = electron number density

v = electron velocity.

The current and electric field are related through Ohm's law

$$E = \sigma J \tag{2.1-8}$$

or

$$\sigma = qN\frac{v}{E} \tag{2.1-9}$$

The equation of motion of the electron in an electric field is

$$m\frac{dv}{dt} + mgv = qE(t) \tag{2.1-10}$$

where

m = electron mass

g = damping constant

= energy loss collision frequency (ν)

In the case of CW propagation,

$$E(t) = E_o e^{i\omega t} \tag{2.1-11}$$

and

$$v = \frac{q}{m}\frac{E}{g + i\omega} \tag{2.1-12}$$

or

$$\sigma = \frac{q^2 N}{m(g + i\omega)} \tag{2.1-13}$$

Since $g = \nu$, the electron energy loss collision frequency,

$$\sigma = \frac{q^2 N}{m(\nu + i\omega)} \tag{2.1-14}$$

or

$$\sigma = \frac{Nq^2}{m}\left[\frac{\nu}{\nu^2 + \omega^2} - i\frac{\omega}{\nu^2 + \omega^2}\right] \tag{2.1-15}$$

$$= \varepsilon_o \omega_p^2 \left[\frac{\nu}{\nu^2 + \omega^2} - i\frac{\omega}{\nu^2 + \omega^2}\right] \tag{2.1-16}$$

$$= \sigma_r - i\sigma_i \tag{2.1-17}$$

The real part (σ_r) causes absorption of the propagating wave, while the imaginary part (σ_i) is responsible for the frequency dependent propagation velocity.

Maxwell's radiation equations are

$$\nabla \times \vec{H} = \varepsilon_o \frac{\partial \vec{E}}{\partial t} + \sigma \vec{E} \tag{2.1-18}$$

$$\nabla \times \vec{E} = -\mu_o \frac{\partial \vec{H}}{\partial t} \tag{2.1-19}$$

Eliminating H to give the wave equation,

$$\nabla^2 \vec{E} = \varepsilon_o \mu_o \frac{\partial^2 \vec{E}}{\partial t^2} + \mu_o \sigma \frac{\partial \vec{E}}{\partial t} \, . \tag{2.1-20}$$

Let ℓ be the coordinate axis in the direction of propagation and assume a solution of the form

$$E(\ell, t) = E_o \exp[i(\omega t - k\ell)] \tag{2.1-21}$$

where E is transverse to ℓ and the vector notation has been dropped. Substitution yields an equation for k, the wave number,

$$k^2 = \varepsilon_o \mu_o \omega^2 \left(1 - i \frac{\sigma}{\varepsilon_o \omega}\right) . \qquad (2.1\text{-}22)$$

But $\varepsilon_o \mu_o = 1/c^2$, so that

$$k^2 = \frac{1}{\lambda\!\!\!^{-}_o^2} \left(1 - i \frac{\sigma}{\varepsilon_o \omega}\right) , \qquad (2.1\text{-}23)$$

where λ_o is the free space wavelength and $\lambda\!\!\!^{-}_o = \lambda_o/2\pi$. Using $k = k_r - ik_i$, $\sigma = \sigma_r - i\sigma_i$, and $\sigma' = \sigma/\varepsilon_o\omega$,

$$k_i = \frac{\sqrt{1 - \sigma_i'}}{\sqrt{2}\lambda\!\!\!^{-}_o} \left\{ \sqrt{1 + \left(\frac{\nu}{\omega}\right)^2 \left(\frac{\sigma_i'}{1 - \sigma_i'}\right)^2} - 1 \right\}^{1/2} \qquad (2.1\text{-}24)$$

$$k_r = \frac{\sqrt{1 - \sigma_i'}}{\sqrt{2}\lambda\!\!\!^{-}_o} \left\{ \sqrt{1 + \left(\frac{\nu}{\omega}\right)^2 \left(\frac{\sigma_i'}{1 - \sigma_i'}\right)^2} + 1 \right\}^{1/2} \qquad (2.1\text{-}25)$$

where

$$\sigma_i' = \frac{\omega_p^2}{\nu^2 + \omega^2} . \qquad (2.1\text{-}26)$$

k_r is related to the index of refraction (n) by

$$n = \lambda\!\!\!^{-}_o k_r \qquad (2.1\text{-}27)$$

so that

$$n = \sqrt{\frac{1 - \sigma_i'}{2}} \left\{ \sqrt{1 + \left(\frac{\nu}{\omega}\right)^2 \left(\frac{\sigma_i'}{1 - \sigma_i'}\right)^2} + 1 \right\}^{1/2} . \qquad (2.1\text{-}28)$$

For $\sigma_i' \ll 1$ and $\nu \ll \omega$,

$$n \approx \sqrt{1 - \sigma_i'} = \sqrt{1 - \left(\frac{\omega_p}{\omega}\right)^2} , \qquad (2.1\text{-}29)$$

while,

$$k_i = \frac{\omega}{2c}\sigma'_r = \frac{\omega_p^2}{2c}\frac{\nu}{\nu^2 + \omega^2} \tag{2.1-30}$$

or

$$k_i = \frac{q^2}{2\varepsilon_o m_e c}\frac{N\nu}{\nu^2 + \omega^2} \tag{2.1-31}$$

Looking at the expression for n, the index of refraction, we see that the phase velocity, $v_p = c/n$, is greater than the speed of light in vacuum. However, the group velocity, $v_g = nc$ (in an isotropic, lossless medium), which is the speed at which information is transmitted, is still less than the speed of light. The important point to be noted is that the velocities are frequency dependent, which leads to the phenomenon of dispersion, or spreading, of any pulse being propagated through the plasma. Using the binomial expansion, we see

$$v_p = c\left[1 + \frac{1}{2}\left(\frac{\omega_p}{\omega}\right)^2\right] \tag{2.1-32}$$

$$v_g = c\left[1 - \frac{1}{2}\left(\frac{\omega_p}{\omega}\right)^2\right] \tag{2.1-33}$$

for $\omega >> \omega_p$.

The attenuation is also frequency dependent. The attenuation factor is defined as

$$A = \frac{|E(\ell,t)|}{E_o} = \exp(-k_i\ell) \tag{2.1-34}$$

where we will refer to $(k_i\ell)$ as the attenuation index. The attenuation in decibels is given by

$$\begin{aligned} A(db) &= 10.(\log_{10}e)A \\ &= 10(\log_{10}e)k_i\ell \end{aligned} \tag{2.1-35}$$

so that, by equation 2.1-31, the attenuation in decibels per meter is

$$A(db/m) = 7.2 \times 10^{-9} \frac{\omega_p^2}{\nu^2 + \omega^2} \qquad (2.1\text{-}36)$$

or

$$A(db/m) = 2.29 \times 10^{-5} \frac{N\nu}{\nu^2 + \omega^2} \qquad (2.1\text{-}37)$$

For $\nu^2 << \omega^2$, the attenuation in decibels or decibels per meter is inversely proportional to the frequency. The attenuation factor, as a simple ratio, goes as e to a negative power which is inversely proportional to frequency, i.e.,

$$A = \exp\left(-\frac{W}{\omega^2}\right) , \qquad (2.1\text{-}38)$$

where W is a constant. In practice, W is easily found from ray trace programs and equation 2.1-38 can be used to model an ionospheric transmission function in conjunction with approximations for the dispersed phase. Experience shows that the model is quite good for realistic ionospheres down to frequencies close to the cutoff frequency (see section 2.2 for the definition of cutoff frequency).

If a plasma medium of variable electron density is involved and the density variations are not large over a wavelength of the frequency of interest, multiplications by ℓ can be replaced by an integration over ℓ. The restriction on the density gradient is necessary to ignore wave reflections in the media. Thus, in a variable medium, the electric field is described by

$$E(\omega,t) = E_o \exp[-\int k_i d\ell] \exp[i\int k_r d\ell] \, e^{i\omega t} \qquad (2.1\text{-}39)$$

and the attenuation in decibels becomes

$$A(db) = 2.29 \times 10^{-5} \int \frac{N\nu}{\nu^2 + \omega^2} d\ell \qquad (2.1\text{-}40)$$

Note that k_r and k_i exchange roles as phase and damping terms when

$$\omega_p^2 = \omega^2 + \nu^2 \qquad (2.1\text{-}41)$$

The presence of a magnetic field causes the conductivity to become a tensor quantity. In the direction parallel to the magnetic field, the equation for σ remains the same, namely

$$\underline{\text{parallel}}: \quad \sigma_o = \frac{Nq^2}{m(\nu + i\omega)} \, . \qquad (2.1\text{-}42)$$

However, the electron motion perpendicular to the magnetic field is modified by the $\vec{v} \times \vec{B}$ force yielding

$$\underline{\text{perpendicular}}: \quad \sigma_B = \frac{Nq^2(\nu + i\omega)}{m\left[(\nu + i\omega)^2 + \omega_e^2\right]} \qquad (2.1\text{-}43)$$

where ω_e is the gyrofrequency of the electron

$$\omega_e = \frac{Bq}{m} \, . \qquad (2.1\text{-}44)$$

The tensor quality of the conductivity causes the wave to be broken into two components, each propagating with a different velocity along a different path. These components are called the ordinary (O) and extraordinary (X) rays, the ordinary ray path being the path which would be taken in the absence of a magnetic field.

The magnetic field also causes the polarization of the wave to change from planar to elliptical. The wave propagates through the plasma by exciting free electrons into motion along the direction of the E field. If there is no ambient B field, the electrons will oscillate along this direction and reradiate the same signal, with the exception of whatever energy is absorbed through collisions with neutrals. The presence of an external B field induces an electron motion perpendicular to its original direction and the B field. If for example, the ray path is parallel to the magnetic field lines, the electrons will attempt to spiral in a circle about the ray, giving rise to an electric field with circular polarization.

The presence of ionic species can be accounted for by adding the ionic conductivity to the electron conductivity, i.e.,

$$\underline{\text{parallel}}: \quad \sigma_o = \left[\frac{N_e q_e^2}{m_e(\nu_e + i\omega)} + \frac{N_i q_i^2}{m_i(\nu_i + i\omega)}\right] \qquad (2.1\text{-}45)$$

perpendicular: $$\sigma_B = \left\{ \frac{N_e q_e^2 (\nu_e + i\omega)}{m_e \left[(\nu_e + i\omega)^2 + \omega_e^2 \right]} + \frac{N_i q_i^2 (\nu_i + i\omega)}{m_i \left[(\nu_i + i\omega)^2 + \omega_i^2 \right]} \right\}$$

(2.1-46)

The e subscripts denote electronic parameters and i subscripts denote ionic properties. The presence of ionic species causes new resonances to occur, but at much lower frequencies than the electron plasma frequency due to the large ionic mass. The ionic resonances can allow a small amount of the low frequencies to "leak" through.

In our discussion of the exoatmospheric environment, both the earth's magnetic field and the presence of ionic species will be ignored. Their consideration is not of immediate importance to S/V analysis.

2.2 Ray Propagation in the Ionosphere

In evaluating the threat to an exoatmospheric system, it will be possible to ignore many features of ionospheric propagation. Two such features, already mentioned, are X and O splitting and the presence of ionic species. This should be of little consequence. We will also ignore the electric field dependence of the ionospheric temperature which enters through the electron collision frequency (ν) and through the electron density (N), especially if the fields are large enough to induce electron avalanching. The presence of any field dependent quantity destroys the linearity of the problem and renders the Fourier transform methods used in sections 3 and 4 useless. The large fields produced by a high altitude burst, with their low geometric attenuation, could produce a significant field dependence. One more feature which will be ignored will be the wave-like nature of the signals which cause reflections in the ionosphere. We will assume that the gradients in the ionosphere's electron density profile are small compared to the wavelengths of the frequencies which propagate through. Under these conditions, we can use Snell's law to calculate the ray path of the propagating wave. The transfer functions developed for section 3 were calculated by a ray trace code using this technique. The phase and absorption are integrated along the path determined by Snell's law.

In a planar medium, Snell's law is

$$n \sin\theta = n_i \sin\theta_i \qquad (2.2\text{-}1)$$

where

n_i = index of refraction at the origin of the ray

θ_i = angle of incidence (measured from vertical)

n = index of refraction at any point

θ = angle of ray at any point.

If the ray originates in air ($n_i = 1$), Snell's law reduces to

$$n \sin\theta = \sin\theta_i \qquad (2.2\text{-}2)$$

In a medium with spherical symmetry, Snell's law takes on a form which takes into account the change in θ caused by moving from one reference radial to another, i.e.,

$$nR \sin\theta = n_i R_o \sin\theta_i \qquad (2.2\text{-}3)$$

where the new variables are

R_o = radius to the point of origin

R = radius to the point of interest.

When the ray originates in air,

$$nR \sin\theta = R_o \sin\theta_i \qquad (2.2\text{-}4)$$

The ionosphere cutoff frequency (ω_c) can be calculated directly from Snell's law. As will be shown, ω_c depends only upon the maximum electron density encountered along the path and θ_i. It does not depend upon the integral of any quantity along the path. Before proceeding, let us define two terms which are properly used in discussing the over-the-horizon (OTH) ionospherically propagated signal, but which the reader may encounter in general discussions of ionospheric propagation. The first term, MUF, is the maximum usable frequency for communication between two fixed locations. The second term, MOF, is the maximum observable frequency for propagation between two fixed points. The MOF, being higher than the MUF, but not useful, is probably caused by reflections from irregularities in the ionosphere. The MUF is obviously related to ω_c, but is properly used only with signals propagated between two points below the ionosphere. Given that same angle of launch, the MUF would also be the lower limit of frequencies propagated through the ionosphere.

Consider a planar ionosphere first. For a given angle of launch, the cutoff frequency is that for which the ray path makes a 90° angle at the altitude containing the largest electron density encountered to the point of interest. All higher frequencies will penetrate to higher altitudes. Let the maximum electron density be N_m. Let n_c be the index of refraction corresponding to N_m and let ω_{pm} be the corresponding plasma frequency. Then, by Snell's law,

$$n_c = \sin\theta_i \ . \qquad (2.2\text{-}5)$$

When ν is negligible,

$$n^2 = 1 - \left(\frac{\omega_{pm}}{\omega}\right)^2$$

and

$$n_c^2 = \sin^2\theta_i = 1 - \left(\frac{\omega_{pm}}{\omega_c}\right)^2$$

so that

$$\omega_c = \frac{\omega_{pm}}{\cos\theta_i} \quad . \tag{2.2-6}$$

From this equation we see that ω_c increases for increasing launch angles. For vertical incidence, $\omega_c = \omega_{pm}$, and ω_c becomes infinitely large as θ_i goes to 90°.

The plane ionosphere model breaks down for launch angles of about 60° and the spherical ionosphere model must be used. The same derivation using the spherical Snell's law yields

$$\omega_c = \frac{\omega_{pm}}{\sqrt{1 - \left(\frac{R_o}{R_c}\right)^2 \sin^2\theta_i}} \tag{2.2-7}$$

where R_c is the geocentric distance to N_m.

In order to complete the discussion of fundamental concepts, we must devote some time to define the wave and group phase as well as the associated delay and dispersion. A useful way to picture phase is the following. Imagine a vector attached to the ray path and perpendicular to it. The vector rotates at the signal frequency ω and accumulates a phase of 2π on each rotation. The vector slides along the ray path at the propagation velocity v. If the wave propagates at the free space velocity, c, the vector will accumulate a phase, ϕ_c, in moving between two fixed points. If the propagation velocity is faster, the vector will accumulate a smaller phase (ϕ_v) in moving between the two points because the rotation frequency is held constant and it simply has less time in which to accumulate phase. Likewise, if the propagation velocity is slower than c, a larger phase will be accumulated. The difference between ϕ_v and ϕ_c is the dispersed phase ϕ_d, i.e.,

$$\phi_d = \phi_v - \phi_c \quad . \tag{2.2-8}$$

In a plasma, the wave velocity is greater than c and the group velocity is less than c. Therefore, the dispersed wave phase is always a negative quantity and the dispersed group phase is

always greater than zero. This bit of information is useful in setting up a Fourier or Laplace transform calculation of the propagated signal since confusion often sets in while deciding what sign to give the dispersed phase in relation to the phase of the transform of the original signal.

The idea of a group phase is artificial, being calculated from the group velocity, which is, in turn, derived from the wave phase. The wave phase is defined by

$$\phi = \int k_r d\ell \ , \tag{2.2-9}$$

where k_r is the real part of the wave number and the integration is over the propagation path. Normally, one must distinguish between the phase path and group path, but they are the same if no magnetic field is considered. Since $k_i = \omega/v_p$ where v_p is the phase velocity (c/n),

$$\phi = \omega \int \frac{d\ell}{v_p} \ . \tag{2.2-10}$$

The phase delay is

$$\tau_p = \phi/\omega \tag{2.2-11a}$$

$$= \int \frac{d\ell}{v_p} \ . \tag{2.2-11b}$$

The phase velocity is the velocity at which a fixed point, or phase, of the sinusoidal signal moves through space. This is not the velocity at which information can be transmitted. Information cannot be carried by a purely sinusoidal wave. A wave which is purely sinusoidal cannot have a beginning in time because a truncated sinusoid requires other frequency components to give it its shape. The group velocity can be calculated as the velocity with which a characteristic feature of a wave packet, composed of a narrow band of frequencies centered on ω, propagates through space. This calculation is performed in most texts on ionospheric propagation or optics. The group velocity is shown to be

$$v_g = \frac{d\omega}{dk} \tag{2.2-12}$$

and the group delay is

$$\tau_g = \frac{d\phi}{d\omega} \tag{2.2-13a}$$

$$= \int \frac{d\ell}{v_g} \, . \tag{2.2-13b}$$

Finally, the dispersion is defined by

$$D = \frac{d^2\phi}{d\omega^2} \tag{2.2-14}$$

Given that $v_p = c/n$ and an equation for n, the index of refraction, equations for ϕ, τ, and D can be derived in terms of ω. The wave phase is

$$\phi = \omega \int \frac{n d\ell}{c} \tag{2.2-15}$$

and the dispersed phase is

$$\phi_d = \frac{\omega}{c} \int (n - 1) d\ell \tag{2.2-16}$$

which is negative as stated before. The phase delay is then

$$\tau_p = \frac{1}{c} \int n d\ell \tag{2.2-17}$$

while the dispersed phase delay is

$$\tau_{pd} = \frac{1}{c} \int (1 - n) d\ell \, . \tag{2.2-18}$$

The group delay is

$$\tau_g = \frac{1}{c} \int \left[n + \omega \frac{dn}{d\omega} \right] d\ell \tag{2.2-19}$$

when the variation in path length is ignored. This assumption is quite good except very near the cutoff frequency. The dispersed group delay is

$$\tau_{gd} = \frac{1}{c} \int \left[n + \omega \frac{dn}{d\omega} - 1 \right] d\ell \tag{2.2-20}$$

Under the same circumstances, the dispersion is

$$D = \frac{1}{c}\int\left[\omega\frac{d^2n}{d\omega^2} + 2\frac{dn}{d\omega}\right]d\ell \qquad (2.2\text{-}21)$$

In the absence of electron collisions, the index of refraction is given by

$$n = \sqrt{1 - \left(\frac{\omega_p}{\omega}\right)^2} \quad . \qquad (2.2\text{-}22)$$

In section 3.4, the group delay is calculated to be (eq. 3.4-20)

$$\tau_g = \frac{1}{c}\int\frac{d\ell}{n} \qquad (2.2\text{-}23)$$

which confirms that $v_g = nc$. The dispersed group delay is then

$$\tau_g = \frac{1}{c}\int\left[\frac{1}{n} - 1\right]d\ell \quad . \qquad (2.2\text{-}24)$$

The dispersion is

$$D = \frac{-1}{c}\int\frac{\omega_p^2}{(n\omega)^3}d\ell \qquad (2.2\text{-}25)$$

The "high frequency approximation" is useful for $\omega >> \omega_p$. In that case, n and powers of n can be approximated by the binomial theorem, e.g.,

$$n = 1 - \frac{1}{2}\left(\frac{\omega_p}{\omega}\right)^2$$

and

$$n^{-1} = 1 + \frac{1}{2}\left(\frac{\omega_p}{\omega}\right)^2$$

Under these assumptions, the dispersed phase is

$$\phi_d = \frac{-1}{2\omega c}\int \omega_p^2 d\ell \ , \tag{2.2-26}$$

the dispersed phase delay is

$$\tau_{pd} = \frac{-1}{2c\omega^2}\int \omega_p^2 d\ell \tag{2.2-27}$$

the dispersed group delay is

$$\tau_{gd} = \frac{1}{2c\omega^2}\int \omega_p^2 d\ell \tag{2.2-28a}$$

$$= -\tau_{pd} \tag{2.2-28b}$$

and the dispersion is (differentiating ϕ_d twice)

$$D = \frac{-1}{c\omega^3}\int \omega_p^2 d\ell \tag{2.2-29}$$

Note that the forms of the high frequency equations for dispersed quantities are the same as for the equations previously derived for the undispersed quantities with $n\omega$ replaced by ω in the high frequency case.

The high frequency approximation is useful because the equation for $n(\omega)$ does not appear explicitly, simplifying many calculations. The integral over ω_p^2 can be replaced by another parameter which is often used to characterize ionospheres, the "total electron content" or "TEC" with units of electrons/unit area. The term TEC is commonly used in two ways. The first way is in characterizing a particular ionosphere by giving the number of electrons in a tube of unit area cross section where the tube stretches from the earth, through the ionosphere to infinity. This type of measurement is also called the "vertical TEC." More generally, the term TEC is used as a measure of the electron density encountered along the propagation path. In the high frequency approximation, this converts directly to dispersion characteristics. The TEC is defined by

$$TEC = \int N d\ell \tag{2.2-30}$$

where N is the electron density and the integration is along some path through the ionosphere, most likely a propagation path. Since

$$\omega_p^2 = (2\pi)^2 f_p^2$$

$$= (2\pi)^2 \ 80.621 \ N \qquad (2.2\text{-}31)$$

the high frequency equations reduce to

$$\phi_d = \frac{-\pi(80.6)}{fc} (TEC) \qquad (2.2\text{-}32)$$

$$\tau_{pd} = \frac{-80.6}{2f^2c} (TEC) \qquad (2.2\text{-}33)$$

$$\tau_{gd} = \frac{80.6}{2f^2c} (TEC) \qquad (2.2\text{-}34)$$

$$D = \frac{-80.6}{2\pi f^3 c} (TEC) \qquad (2.2\text{-}35)$$

where we have converted from ω (rad/sec) to f (Hz) in the process.

The ionosphere transmission function is formed from the attenuation and phase functions, i.e.,

$$T(\omega) = A(\omega) \ e^{i\phi(\omega)} \ . \qquad (2.2\text{-}36)$$

Assuming that linear theory is valid, the propagated time waveform is given by the inverse Fourier transform as

$$E(t) = \frac{1}{2\pi} \int_{-\infty}^{\infty} \hat{E}(\omega) A(\omega) \ \exp[i(\psi(\omega) + \phi(\omega))] \ e^{i\omega t} d\omega \qquad (2.2\text{-}37)$$

where $\hat{E}(\omega)e^{i\psi(\omega)}$ is the Fourier transform of the pulse which enters the ionosphere.

This transform can be performed numerically if great care is used in the treatment of the cutoff frequency and the phase. The amplitude must be allowed to approach small values near the cutoff frequency such that the change in amplitude is not too large over the frequency step size. Otherwise, modulations will appear in the envelope of the waveform. Even more important is the treatment of the total phase, i.e., $\phi(\omega) + \psi(\omega) + \omega t = \Phi(\omega)$. It is important to normalize $\Phi(\omega)$ after it is calculated. In the calculation of the waveforms shown in section

3.3, the total phase was set equal to zero at the first frequency point of integration and Φ was translated the same amount for all other frequencies. It was found that the transform was very sensitive to discontinuities in even the second and third derivatives of Φ and we found it most efficient to fit $\phi(\omega)$ by a power series, the lowest term of which was the high frequency approximation. $\phi(\omega)$ is the dispersed phase, which eliminates the time lag corresponding to the time required for the signal to reach the observer. Such discontinuities in the phase produce large gliches in the envelope of the time waveform corresponding to the delay of the frequency at which the discontinuity occurred. Finally, care must be taken in the calculation of integrals of $\sin\Phi$ and $\cos\Phi$ because Φ can go through many cycles between the limits of integration. Normal integration schemes do not take this into account and give incorrect values to the integral. The value of the integral will vary wildly from increment to increment and the value of the total integral will vary randomly from one time to another. The integration scheme must take into account the quadrants of the end points of integration and the direction of phase increase.

3. The Exoatmospheric Fields

In this section, the basic concepts developed in section 2 are used to predict the exoatmospheric environment produced by an ionospherically propagated pulse. The section is divided into four parts: 1) a general description of the fields, 2) a detailed description of the characteristics of a specific ionosphere which will be used to produce 3) specific time waveforms representing environments likely to be seen by exoatmospheric systems, and 4) a method for analytically calculating, to a good approximation, the envelope of an ionospherically propagated pulse along with instantaneous frequency as a function of delay.

Up to this time, it has been the custom in survivability/vulnerability assessments to use the time waveform of the threat extensively. This trend is changing more to frequency space analysis, which is, of course, entirely equivalent when both are used properly. However, one disadvantage of time waveform analysis has been that workers in the field have been caught in the trap of thinking in terms of peak fields. In sections 3.3 and 3.4, it will be seen that the ionospheric dispersion greatly reduces the magnitude of the peak fields. This can lead to the catastrophic conclusion that the threat to a system is also reduced accordingly. The fact of the matter is that almost all of the energy above the ionospheric cutoff frequency is still present; the only difference is that it is now delivered over a much longer period of time with a considerably different time history. Whether this is a lesser or greater threat depends entirely upon the nature of the system. In short, do not underestimate the threat of the ionospherically propagated environment.

The exoatmospheric environment is best represented in the frequency domain for two reasons. The first reason is that it eliminates the danger of falling into the peak field trap. Secondly, the representation in terms of frequency amplitude and phase is much less sensitive to ionospheric characteristics than is the time waveform. There is very little need to ever use the time history of the propagated signal, even when simulating it on the computer for coupling analysis or as specifications for a simulator or as a system or testing criterion. An additional problem encountered when using the time waveform is the extremely good resolution required over long periods of time. This results in a requirement for an enormous amount of time points in the waveform. The time waveforms presented in this section are produced to satisfy the reader's (and author's) curiosity and it is hoped that they will be used with caution, if at all.

3.1 Characteristics of Exoatmospheric EMP

1. The ionosphere acts like a high-pass filter in transmitting a signal.

2. Three propagation effects are of importance to the study of the exoatmospheric signal: refraction, absorption, and dispersion.

a. Refraction is the bending of the path of an EM wave. It is frequency dependent with the higher frequencies bending less. Total reflection will occur for frequencies below a certain value called the critical frequency. The cutoff frequency increases with the ionosphere's electron density and with the obliqueness at which the wave is transmitted with respect to the ionosphere.

b. Absorption is due to the finite conductivity of the ionospheric plasma and increases with the electron energy loss collision frequency and electron density. Absorption occurs in the lower regions of the ionosphere and its effects are seen only in the lowest transmitted frequencies. It is not a major concern for S/V analysis.

c. Dispersion is the variation of the signal propagation velocity with frequency. The group velocity of high frequencies is closest to c, the free space velocity. Lower frequencies travel more slowly, down to the cutoff frequency, which has infinite delay. The dispersion, or frequency separation, increases with electron density and with the time of propagation in the plasma.

3. In addition to the ionospheric effects, the signal strength is reduced by the geometric, or 1/R, attenuation typical of the far field dipole radiation.

4. Since the ionospheric characteristics are most easily described in terms of their frequency dependence, the simplest approach to studying the EXO environment is in the frequency domain. The environment will later be presented in the time domain.

a. The Fourier transform of a time waveform can be described in terms of an amplitude and a phase, both of which are affected by the ionosphere.

b. The amplitude will first be modified by removing all content below the cutoff frequency. The sharpness of the cutoff will be reduced by absorption, providing a smooth roll-off. This action by itself, without modifying the phase, will be reflected in the time domain as the original time waveform with strong oscillations superimposed, the frequency of which will be equal to the cutoff frequency. As an example of this,

an impulse function filtered in this way yields the following time waveform:

$$A(t) = \delta(t) - \frac{\cos\omega_c t}{t} , \qquad (3.1\text{-}1)$$

where $\delta(t)$ is the impulse function.

c. Geometric attenuation will reduce the amplitude uniformly for all frequencies in the same way that it does for free space propagation.

d. The phase of the Fourier transform will be modified by the addition of a term which varies as $1/\omega$ for frequencies much greater than the cutoff frequency. The phase dispersion is the most important factor in determining the form of the propagated time waveform. If the ionosphere is approximated as a slab with constant electron density, and if the high frequency approximation for the phase is used, the impulse response of the ionosphere can be calculated as

$$I(t) = \delta(t) - \sqrt{\frac{k}{2}} \frac{\omega_p}{\sqrt{t}} J_1(\omega_p \sqrt{2kt}) , \qquad (3.1\text{-}2)$$

where ω_p is proportional to the square root of the electron density, $k = L/c$, where L is the path length, c is the speed of light in vacuum, and J_1 is the Bessel function of order one. This impulse response has been used to calculate the propagated time waveform of exoatmospheric signals, using convolution methods, with great success. This method considers only the phase dispersion and does not modify the Fourier amplitude.

5. The exoatmospheric time waveform can be characterized as follows:

a. The signal will initially rise in the same way as the nondispersed signal. The length of time that the signal retains its original shape depends on how much the high frequencies are dispersed.

b. After the initial rise, the signal breaks into a high frequency oscillation. The envelope of the waveform will continue to rise to a peak. Increasing dispersion will cause the envelope to peak at lower values, to occur later in time, and to become less distinct.

c. The oscillation frequency will continually decrease down to the cutoff frequency, which has an infinite delay.

3.2 Useful Ionosphere Models

This section presents certain characteristics of two ionospheric models which could serve as standards for studying variations in the exoatmospheric EMP environment. The ionospheres, a daytime, sunspot maximum and a nighttime, sunspot minimum are adapted from (Johnson, 1965). They were detailed in (Messier, 1971), but because the collision frequency model was in error below 100 km, as published, the model is reproduced here with minor corrections. The ionosphere models consist of the data points given in Tables 3.2-1 and 3.2-2 and an exponential interpolation between points. Since the data above 1000 km or below 60 or 80 km is not too important for predicting EMP environments, one can assume the electron density is zero or extrapolate with the appropriate exponential functions. The electron collision frequency function will extrapolate well to the ground. Tables 3.2-3 and 3.2-4 give the appropriate constants for interpolation assuming functions of the following form:

$$N = N_o \exp(a_N h) \tag{3.2-1}$$

$$\nu = \nu_o \exp(a_\nu h) \tag{3.2-2}$$

where

N is electron density (m^{-3})

ν is electron (momentum transfer) collision frequency (sec^{-1})

h is altitude (km).

Figure 3.2-1 shows the electron density and electron collision frequency profiles. Figures 3.2-2 and 3.2-3 are the transmission functions of the nighttime and daytime ionospheres for ray launch angles of 0°, 60°, 75°, and 90° from the vertical. Figure 3.2-4 is a plot of delay versus frequency for both ionospheres and launch angles of 0° and 90°. Multiplying delay by frequency will give useful values of phase. The phase and transmission functions together define the ionosphere transfer functions. Section 3.4 presents a method of calculating the delay versus frequency curves for any ionosphere and launch angle. Figure 3.2-5 shows the minimum ionosphere penetration frequency as a function of launch angle for both ionospheres. The same is also shown for a planar nighttime ionosphere in order to show where the plane ionosphere approximation breaks down. Figures 3.2-6 and 3.2-7 show the cutoff frequency as a function of altitude for both ionospheres and for launch angles of 0°, 30°, 45°, 60°, 75°, and 90°. Figures 3.2-8 and 3.2-9 show the total electron content (TEC) as a

Altitude (km)	Electron Density (m^{-3})	Electron Collision Frequency (sec^{-1})
80	1.0(8)	1.5(6)
90	1.0(9)	3.9(5)
100	2.0(9)	1.0(5)
150	2.0(8)	5.0(2)
200	9.0(8)	4.5(1)
225	1.0(10)	2.0(1)
250	7.0(10)	1.0(2)
275	1.9(11)	4.0(2)
300	2.0(11)	5.0(2)
350	1.8(11)	4.0(2)
500	3.0(10)	1.0(2)
700	1.6(10)	4.0(1)
1000	8.5(9)	2.5(1)

Table 3.2-1. Nighttime, Sunspot Minimum Ionosphere Profile

Altitude (km)	Electron Density (m^{-3})	Electron Collision Frequency (sec^{-1})
60	1.0(8)	2.3(7)
100	4.0(9)	1.0(5)
130	2.0(11)	6.0(3)
160	3.0(11)	1.5(3)
230	6.0(11)	6.0(2)
280	2.0(12)	1.4(3)
1000	1.0(11)	8.0(1)

Table 3.2-2. Daytime, Sunspot Maximum Ionosphere Profile

Altitude Interval (km)	N_o (m^{-3})	a_N (km^{-1})	ν_o (sec^{-1})	a_ν (km^{-1})
80-90	1.000(0)	2.303(-1)	8.104(10)	-1.361(-1)
90-100	1.953(6)	6.931(-2)	8.104(10)	-1.361(-1)
100-150	2.000(11)	-4.605(-2)	4.000(9)	-1.060(-1)
150-200	2.195(6)	3.008(-2)	6.859(5)	-4.816(-2)
200-225	3.874(0)	9.632(-2)	2.956(4)	-3.244(-2)
225-250	2.478(2)	7.784(-2)	1.024(-5)	6.438(-2)
250-275	3.225(6)	3.994(-2)	9.537(-5)	5.545(-2)
275-300	1.081(11)	2.052(-3)	2.436(1)	8.926(-3)
300-350	3.763(11)	-2.107(-3)	1.907(3)	-4.463(-3)
350-500	1.177(13)	-1.195(-2)	1.016(4)	-9.242(-3)
500-700	1.444(11)	-3.143(-3)	9.882(2)	-4.581(-3)
700-1000	7.000(10)	-2.108(-3)	1.198(2)	-1.567(-3)

Table 3.2-3. Interpolation Parameters for Nighttime Ionosphere

Altitude Interval (km)	N_o (m^{-3})	a_N (km^{-1})	ν_o (sec^{-1})	a_ν (km^{-1})
60-100	3.953(5)	9.222(-2)	8.104(10)	-1.361(-1)
100-130	8.686(3)	1.304(-1)	1.183(9)	-9.378(-2)
130-160	3.451(10)	1.351(-2)	2.438(6)	-4.621(-2)
160-230	6.153(10)	9.902(-3)	1.218(4)	-1.309(-2)
230-280	2.360(9)	2.408(-2)	1.218(1)	1.694(-2)
280-1000	6.412(12)	-4.161(-3)	4.261(3)	-3.975(-3)

Table 3.2-4. Interpolation Parameters for Daytime Ionosphere

function of altitude for the same launch angles. Finally, figures 3.2-10 and 3.2-11 show the attenuation constant, W, as a function of altitude for both ionospheres and the same launch angles. The attenuation constant, W, is defined by equation 2.1-38.

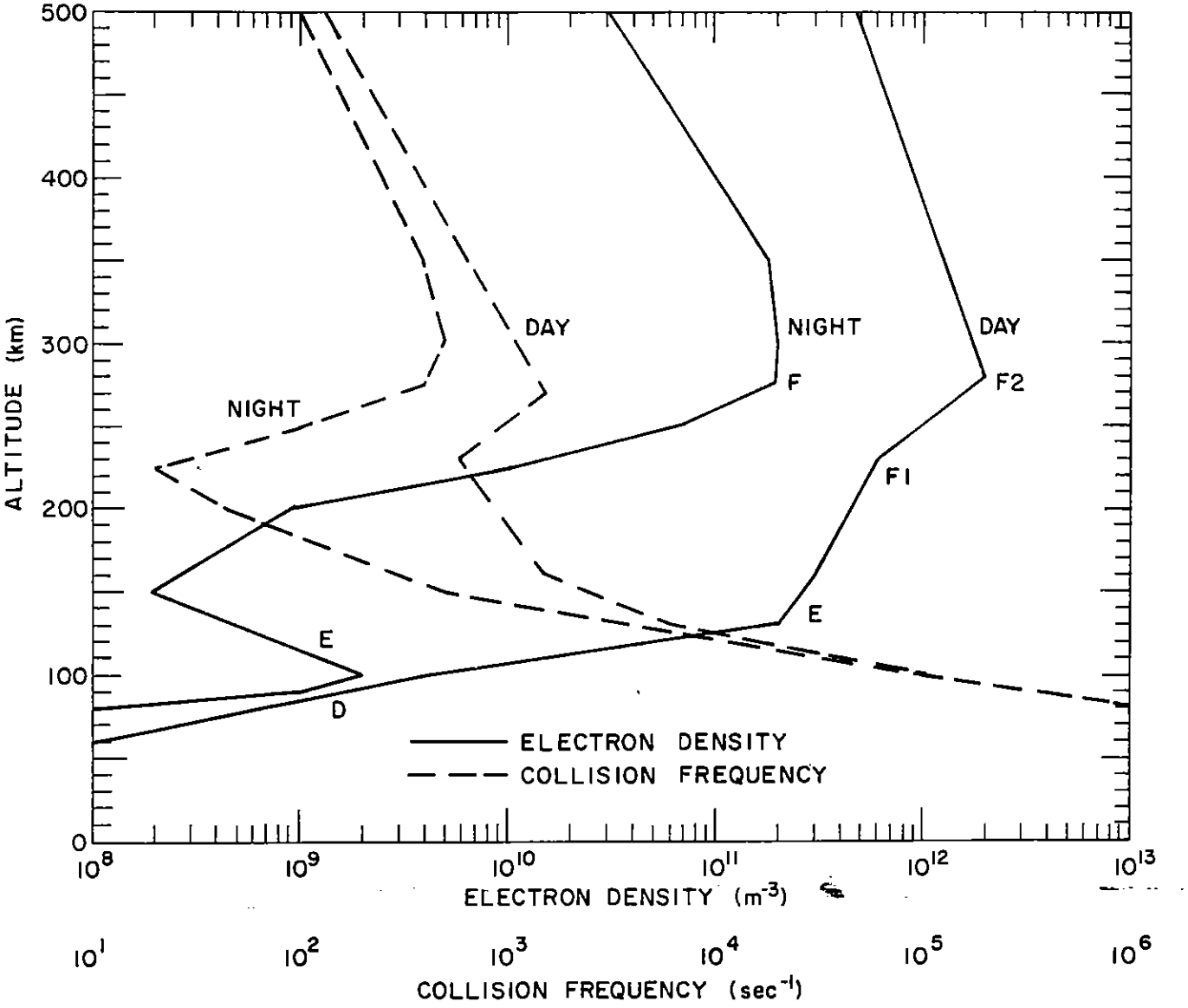

FIGURE 3.2-1 IONOSPHERIC MODELS

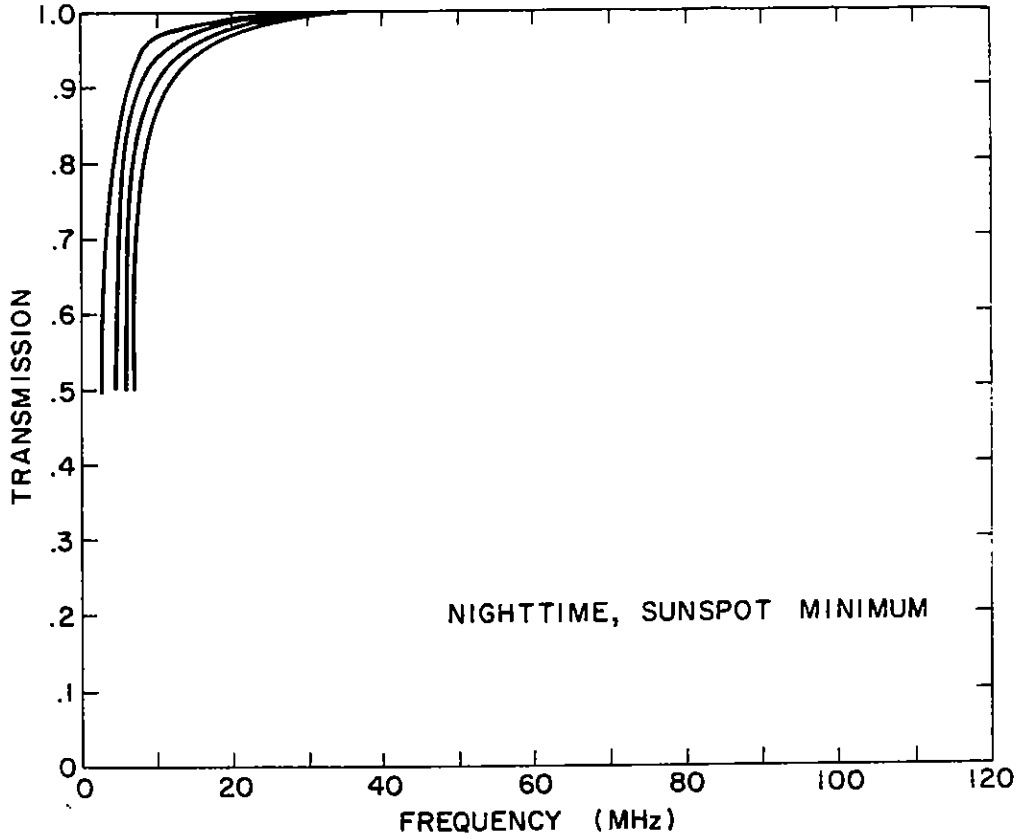

FIGURE 3.2-2 TRANSMISSION vs FREQUENCY FOR LAUNCH ANGLES OF 0°, 60°, 75°, 90°

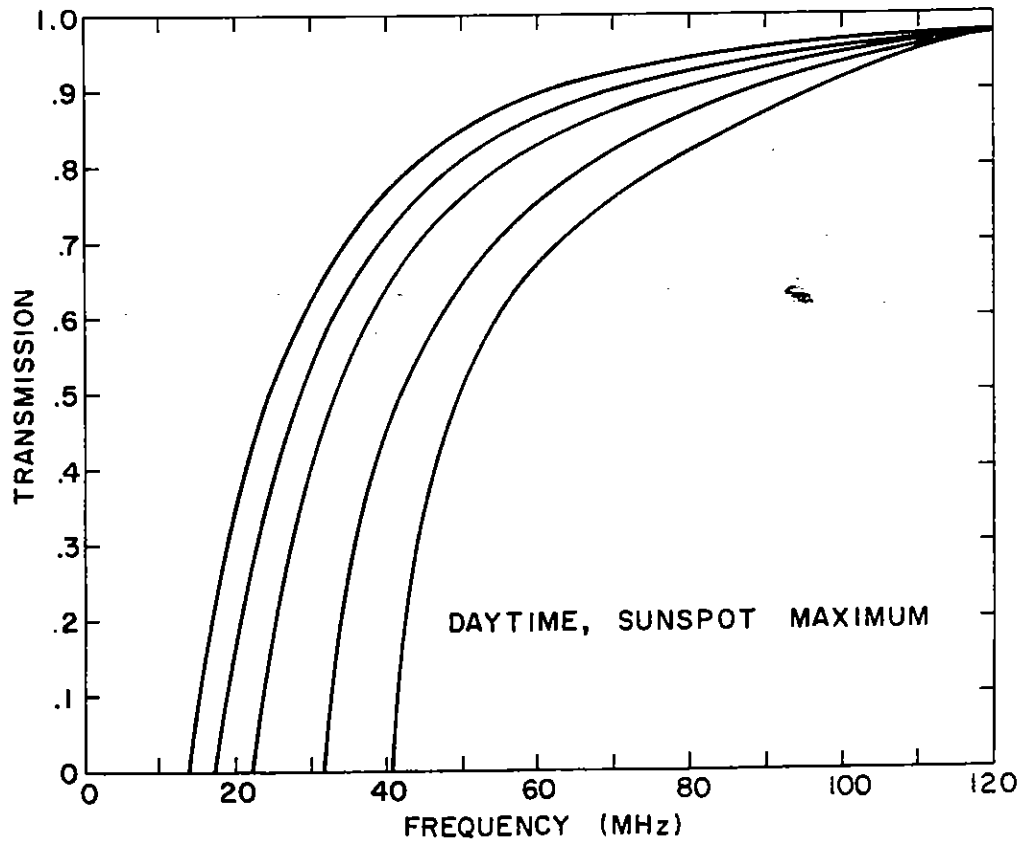

FIGURE 3.2-3 TRANSMISSION vs FREQUENCY FOR LAUNCH ANGLES OF 0°, 45°, 60°, 75°, 90°

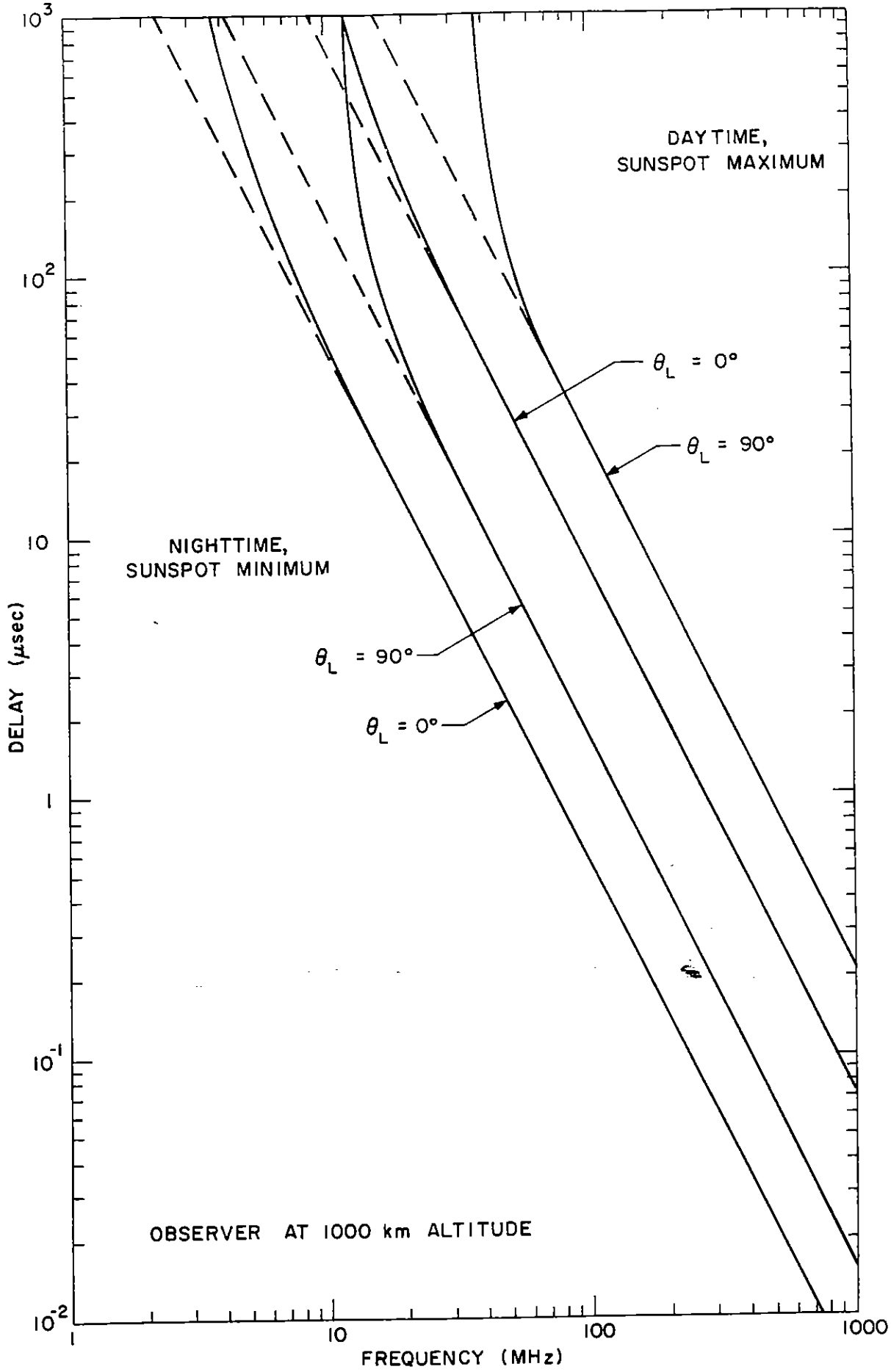

FIGURE 3.2-4 DISPERSED DELAY vs FREQUENCY

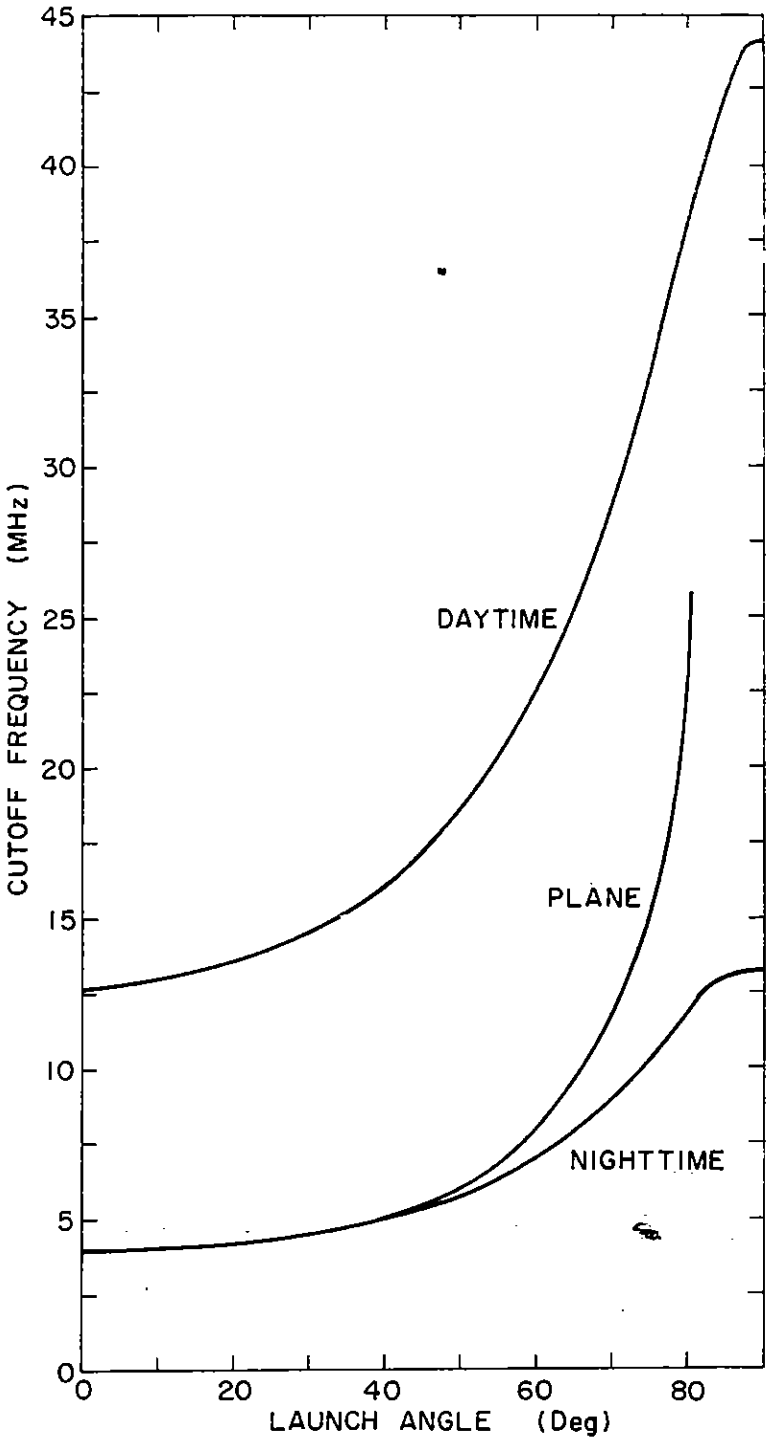

FIGURE 3.2-5 MINIMUM IONOSPHERE PENETRATION FREQUENCY vs LAUNCH ANGLE

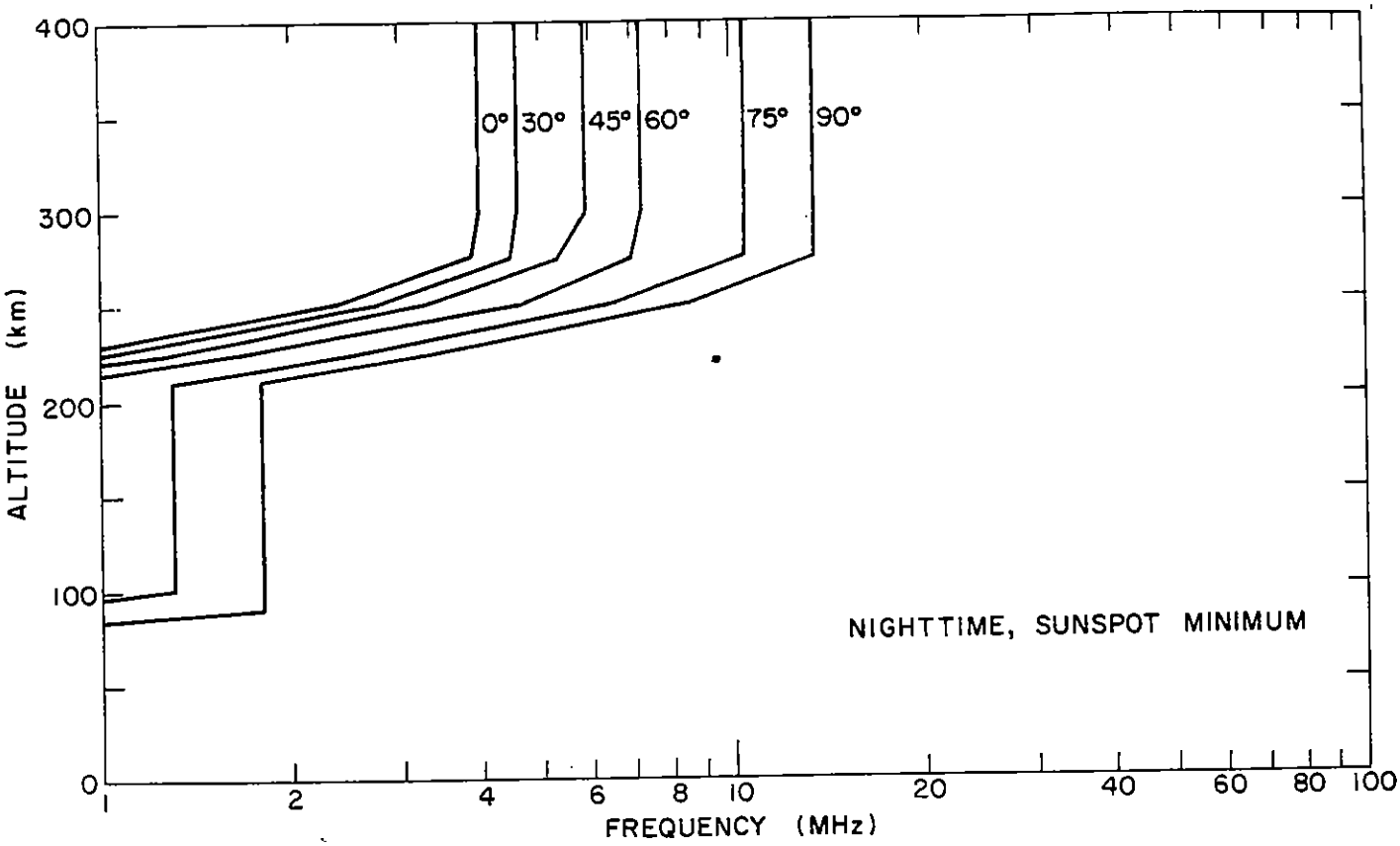

FIGURE 3.2-6 ALTITUDE vs CUTOFF FREQUENCY FOR VARIOUS LAUNCH ANGLES

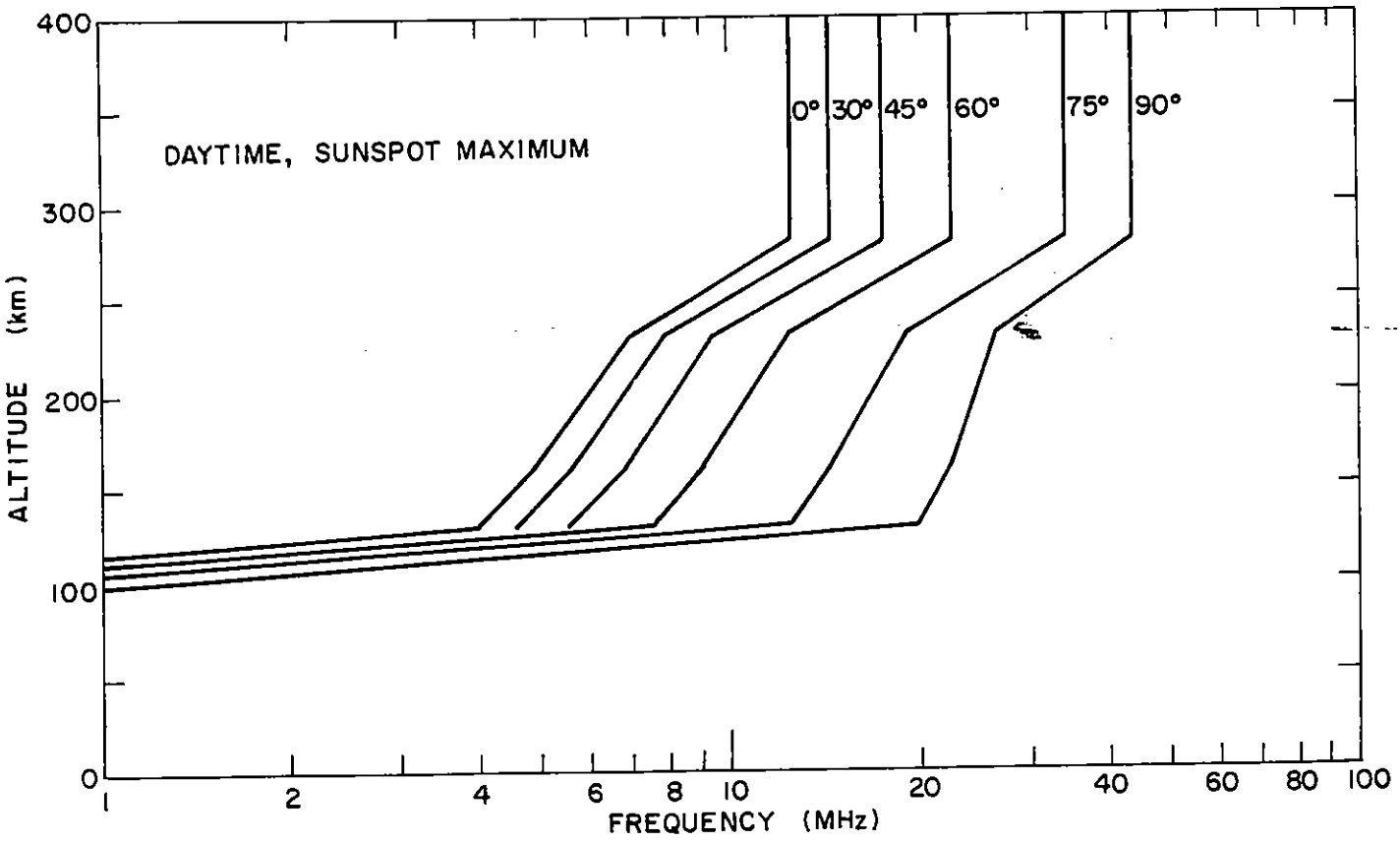

FIGURE 3.2-7 ALTITUDE vs CUTOFF FREQUENCY FOR VARIOUS LAUNCH ANGLES

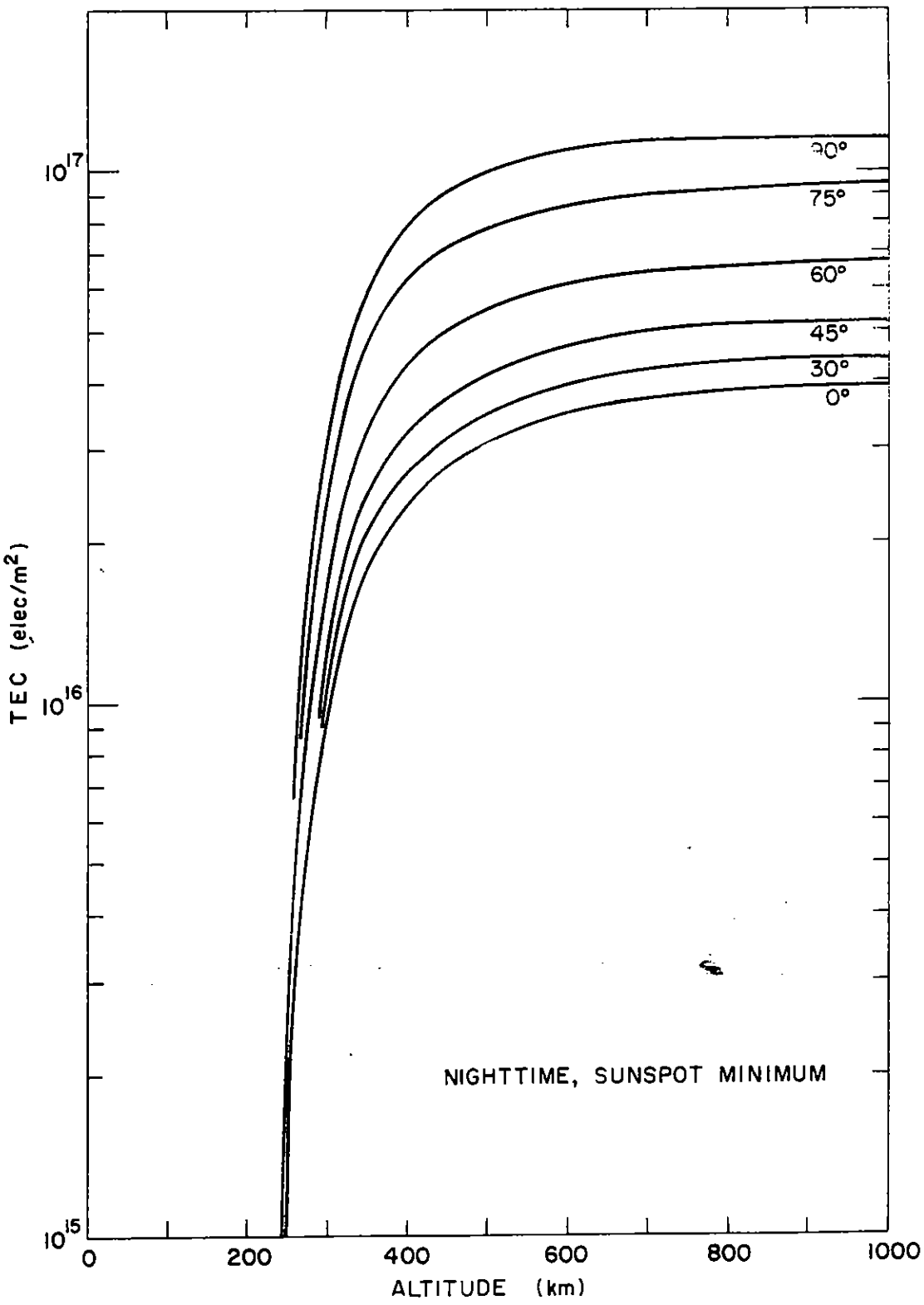

FIGURE 3.2-8 TEC vs ALTITUDE FOR VARIOUS LAUNCH ANGLES

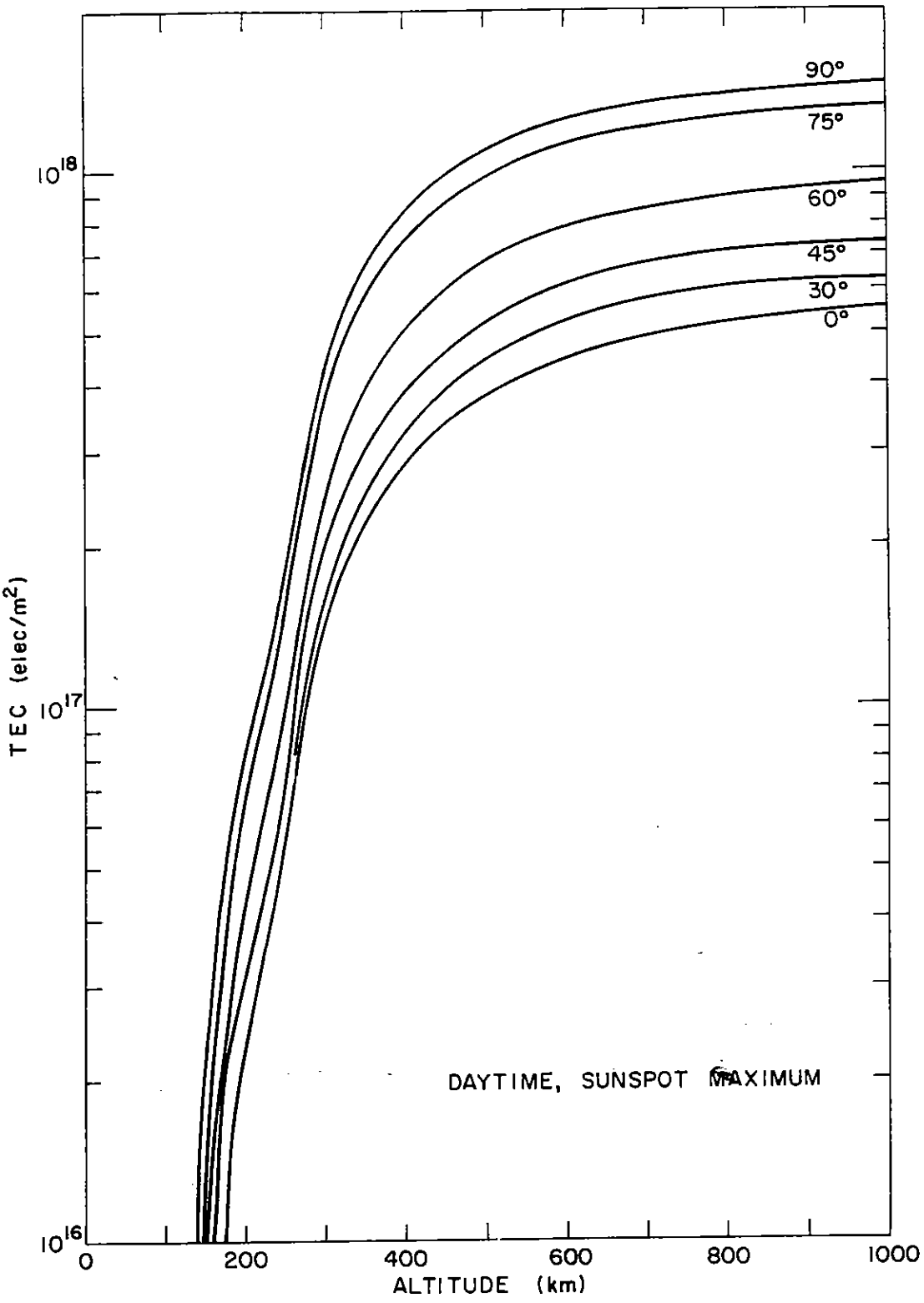

FIGURE 3.2-9 TEC vs ALTITUDE FOR VARIOUS LAUNCH ANGLES

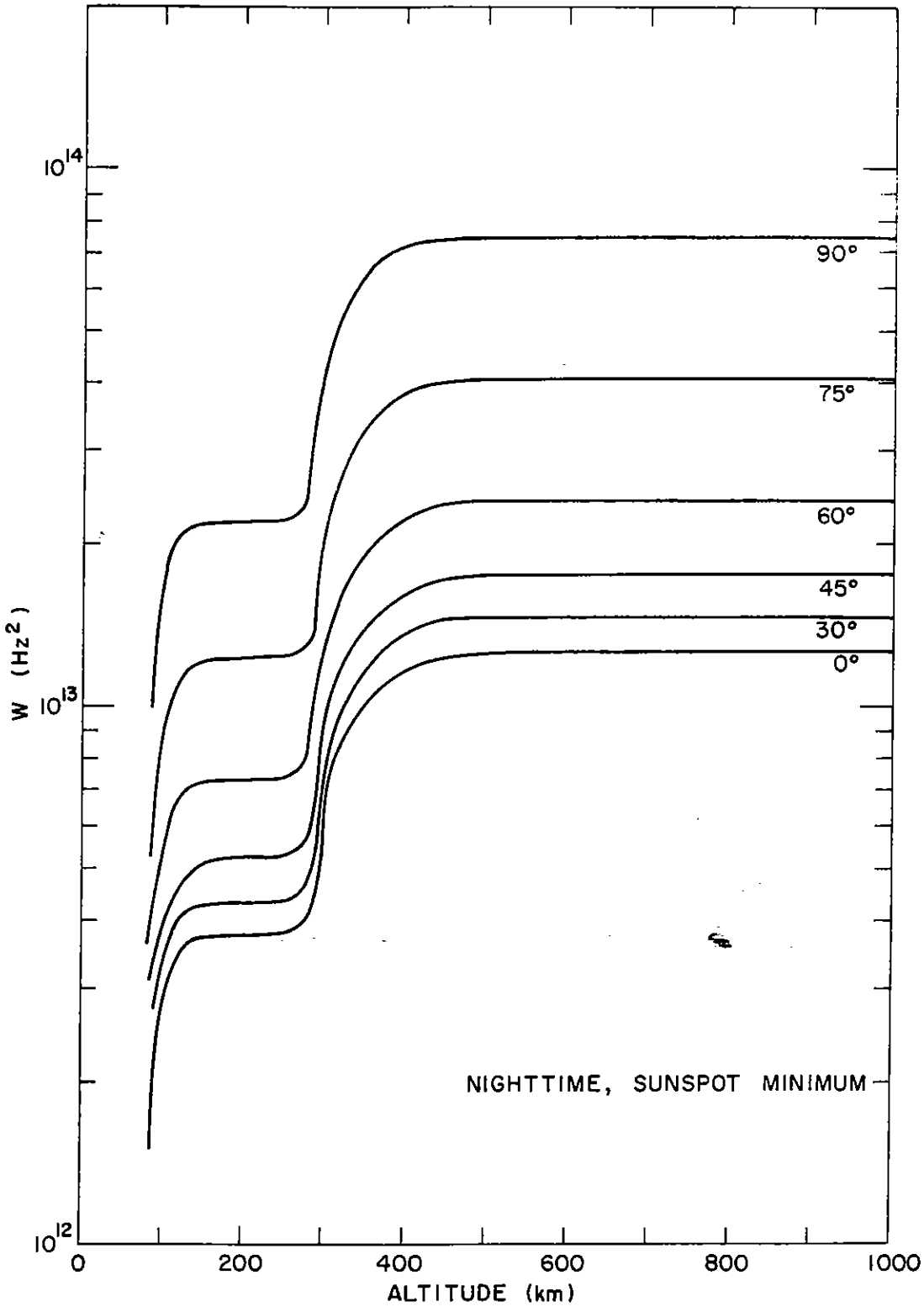

FIGURE 3.2-10 W vs ALTITUDE FOR VARIOUS LAUNCH ANGLES

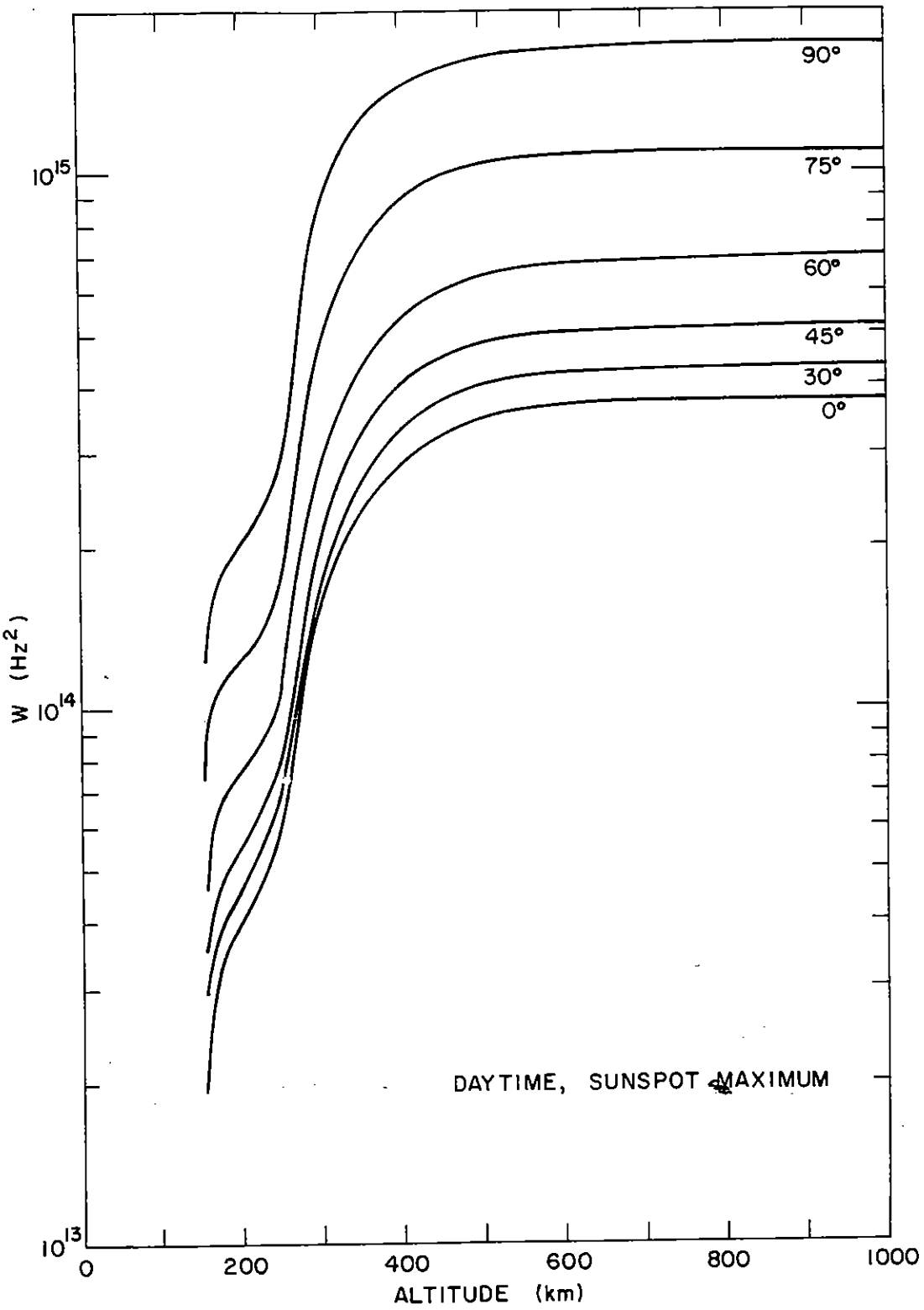

FIGURE 3.2-11 W vs ALTITUDE FOR VARIOUS LAUNCH ANGLES

3.3 Exoatmospheric Time Waveforms

In this section, the ionosphere transfer functions and time waveforms are presented for pulse propagation to four different observer altitudes in the nighttime ionosphere. The time waveforms do not include geometric attenuation. Two launch angles are used: 0° and 90°. The observer altitudes in each case are 100 km, 200 km, 300 km, and 1000 km. Since 1000 km is essentially out of the ionosphere, the time waveform will not vary significantly for greater distances.

Figure 3.3-1 shows the transmission functions for the 0° launch angle and figure 3.3-2 shows the transmission functions for the 90° launch angle. Figures 3.3-3 and 3.3-4 show the group delay versus frequency for the 0° and 90° launch angles respectively. The unfiltered waveform is shown in figure 3.3-5 and is of the form

$$E(t) = E_o[e^{-\beta t} - e^{-\alpha t}] \qquad (3.3\text{-}1)$$

where

$$E_o = 52$$

$$\alpha = 4.76 \times 10^8 \text{ sec}^{-1}$$

$$\beta = 4. \times 10^6 \text{ sec}^{-1}.$$

Figures 3.3-6 through 3.3-9 are the propagated time waveforms at observer altitudes of 100, 200, 300 and 1000 km respectively and for a vertical launch angle (0°). Figures 3.310 through 3.3-13 show the same for a 90° launch angle.

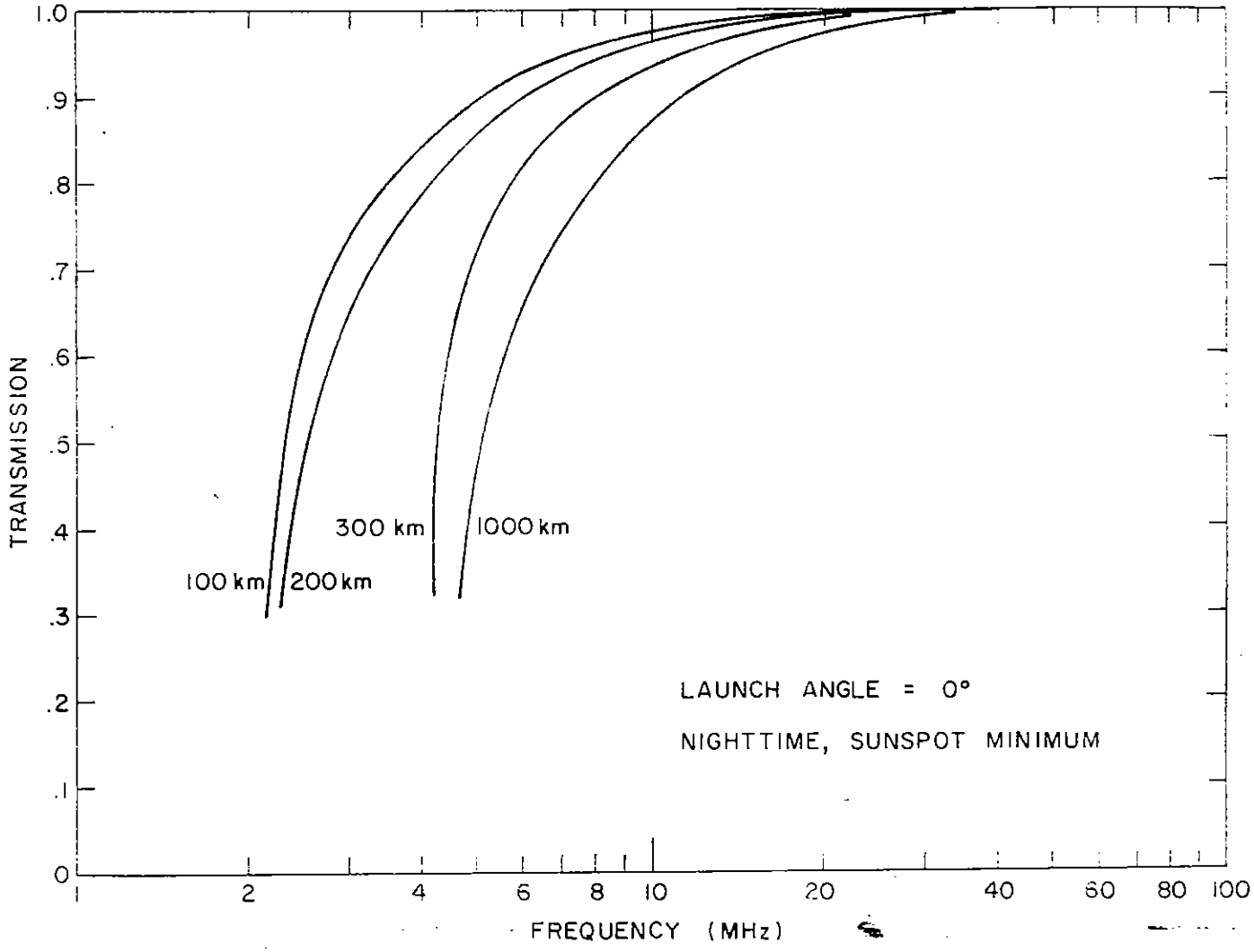

FIGURE 3.3-1 TRANSMISSION vs FREQUENCY FOR VARIOUS OBSERVER ALTITUDES

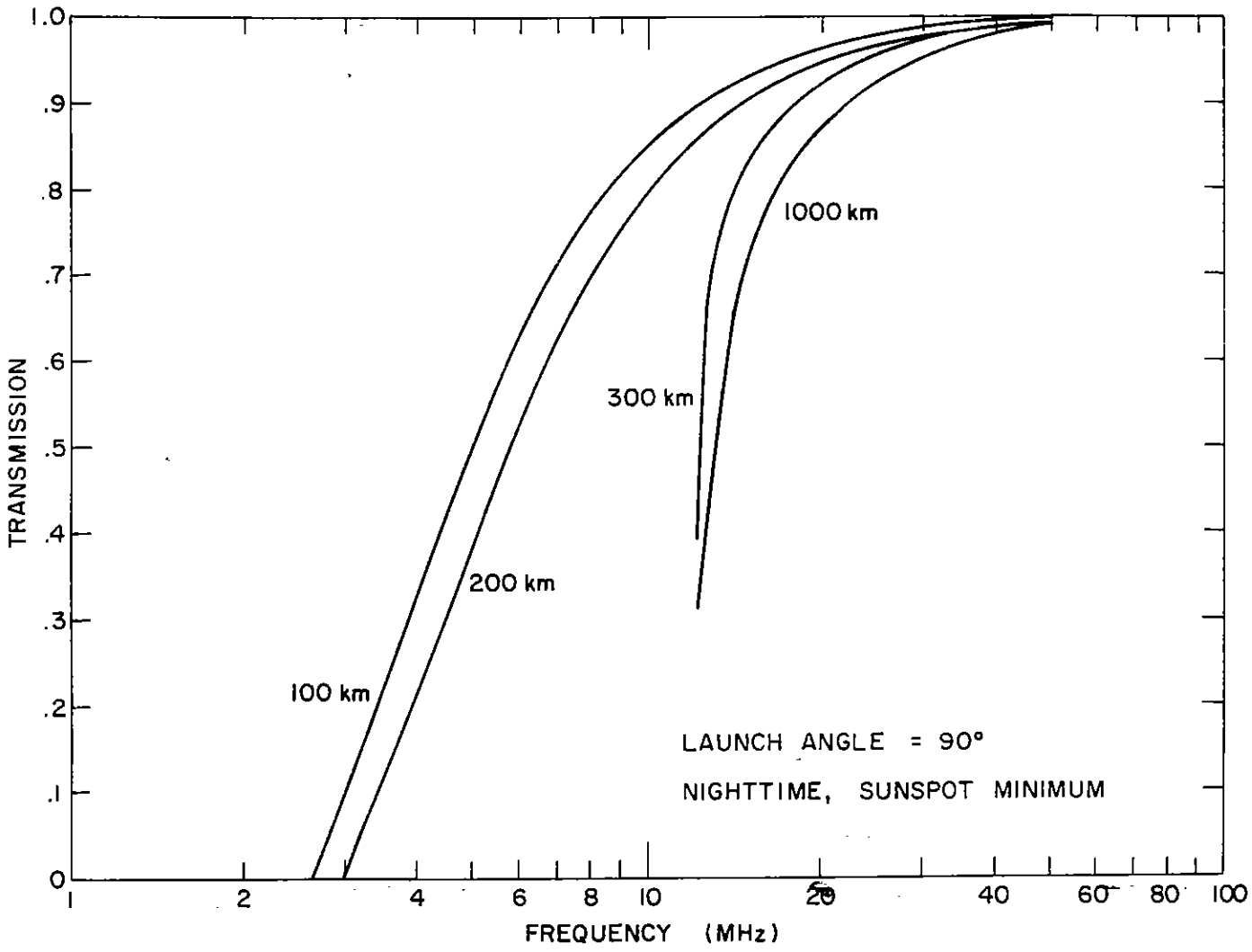

FIGURE 3.3-2 TRANSMISSION vs FREQUENCY FOR VARIOUS OBSERVER ALTITUDES

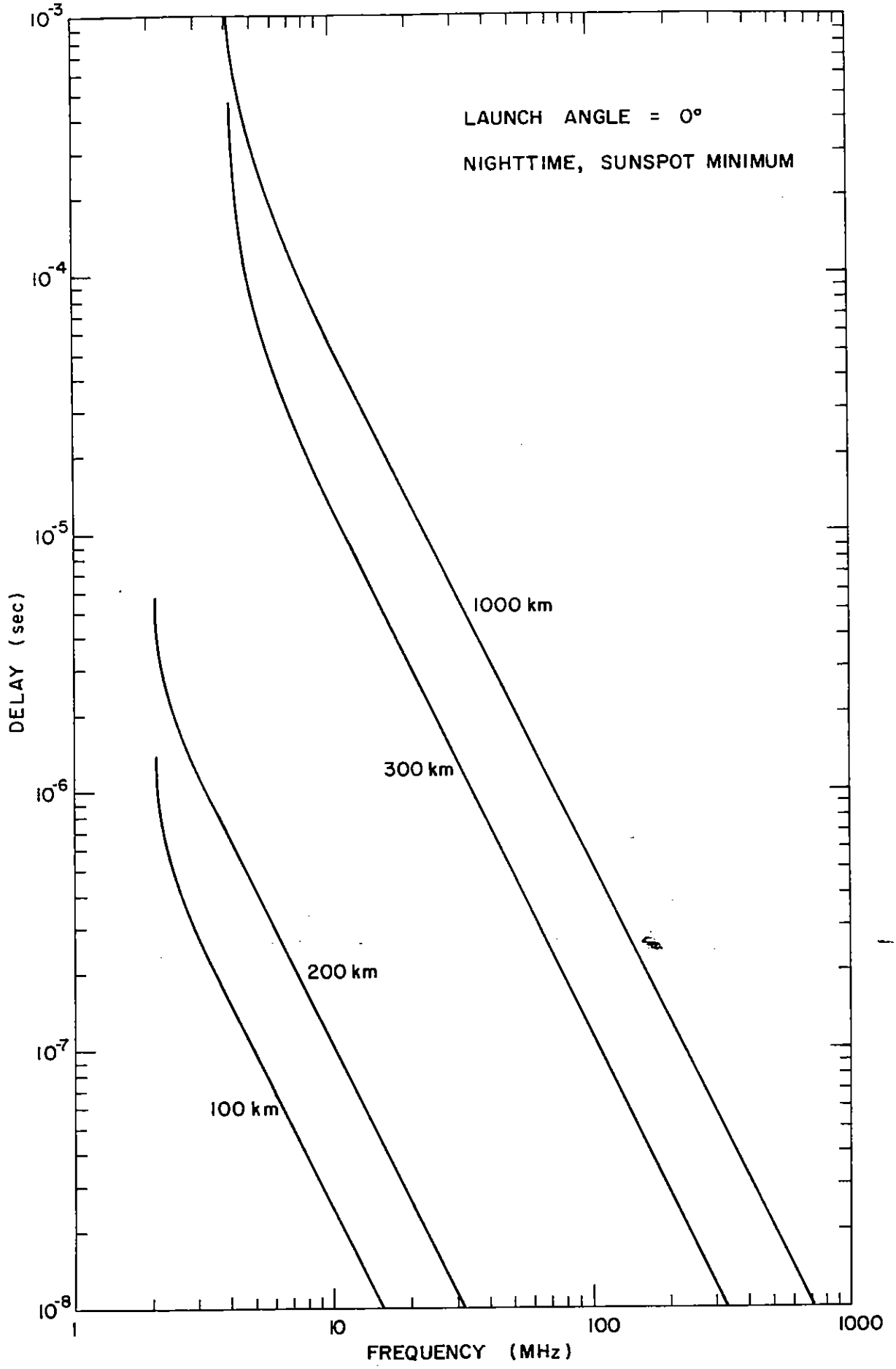

FIGURE 3.3-3 DELAY vs FREQUENCY FOR VARIOUS OBSERVER ALTITUDES

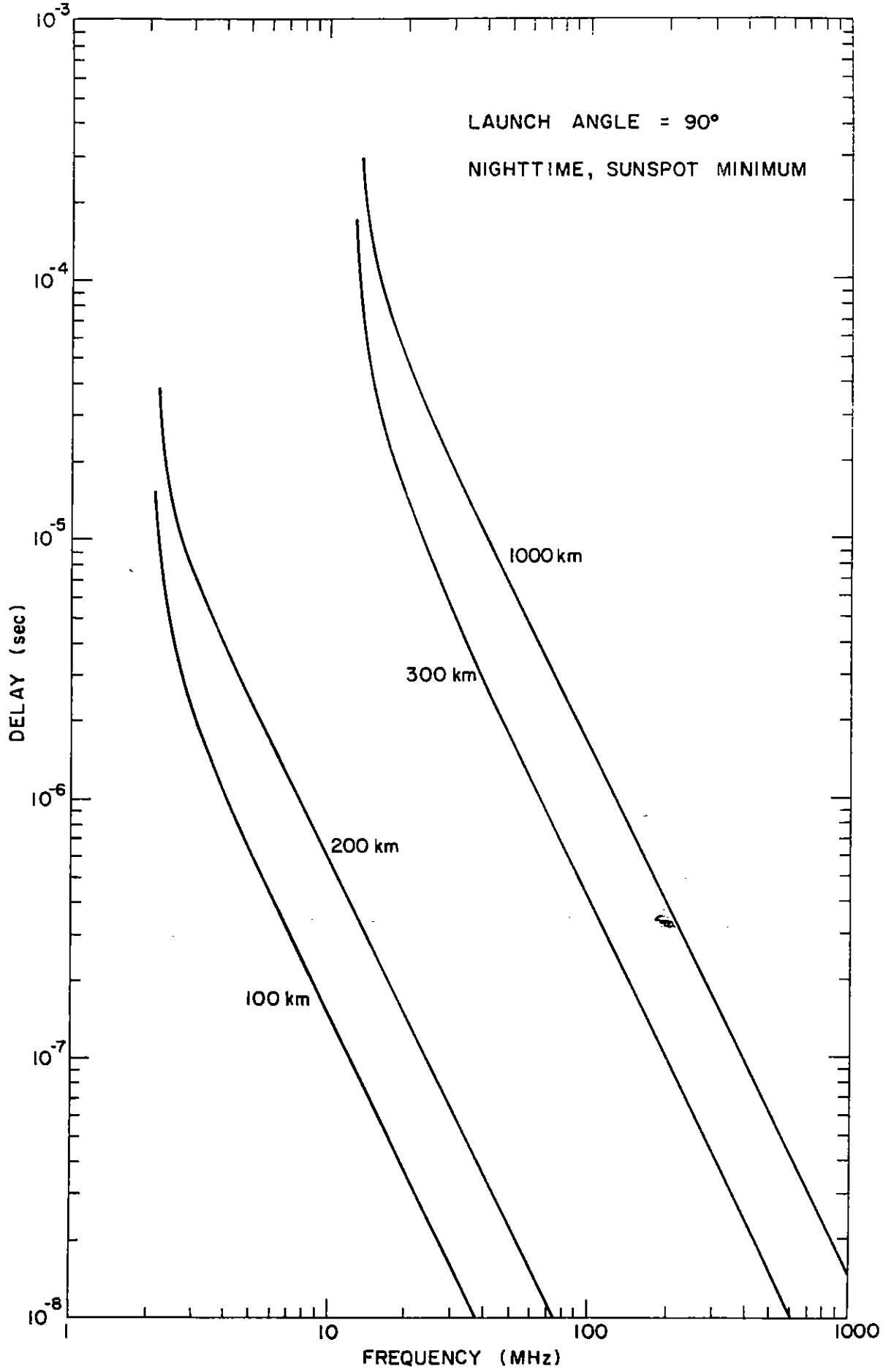

FIGURE 3.3-4 DELAY vs FREQUENCY FOR VARIOUS OBSERVER ALTITUDES

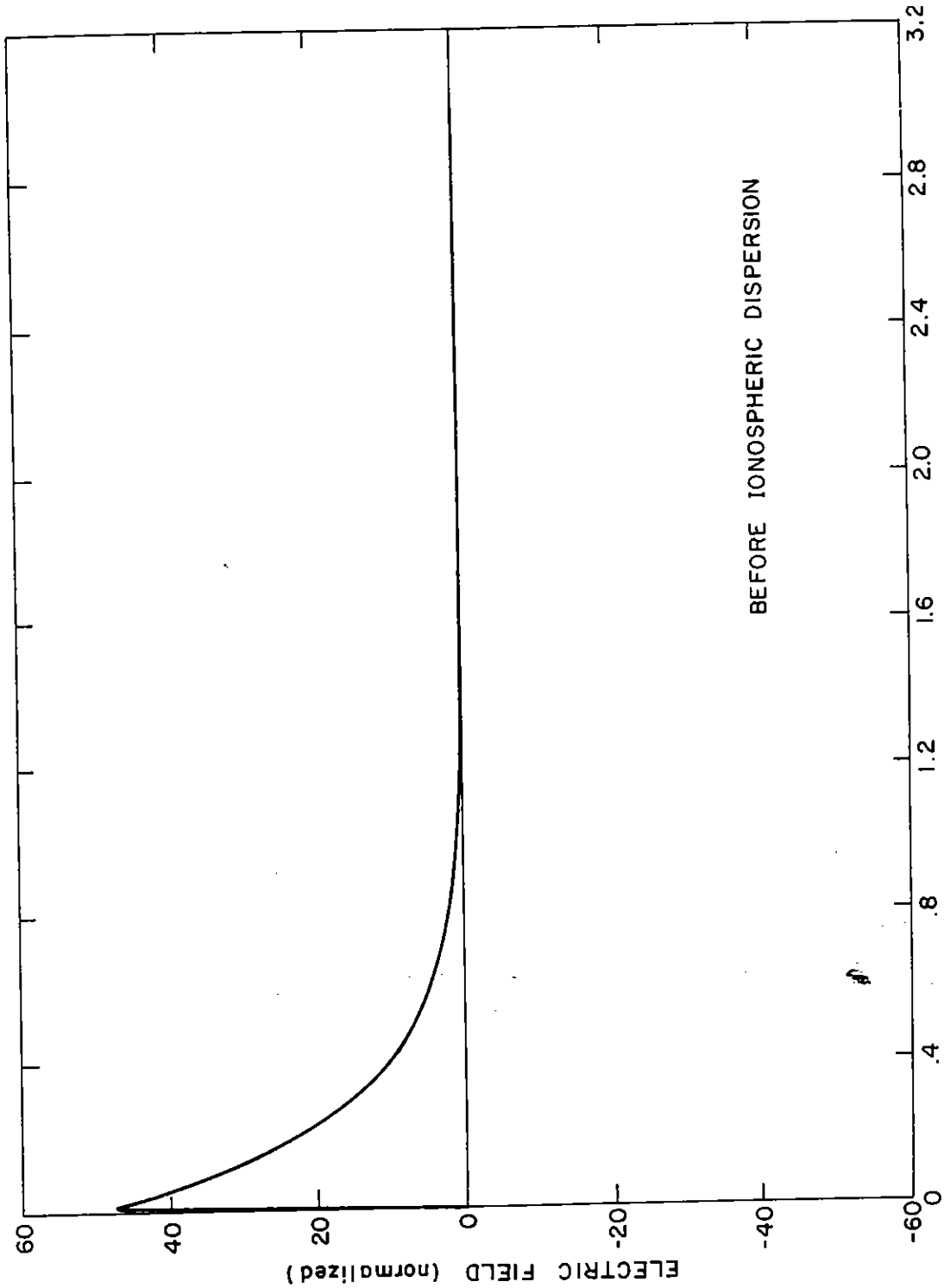

FIGURE 3.3-5 ORIGINAL PULSE

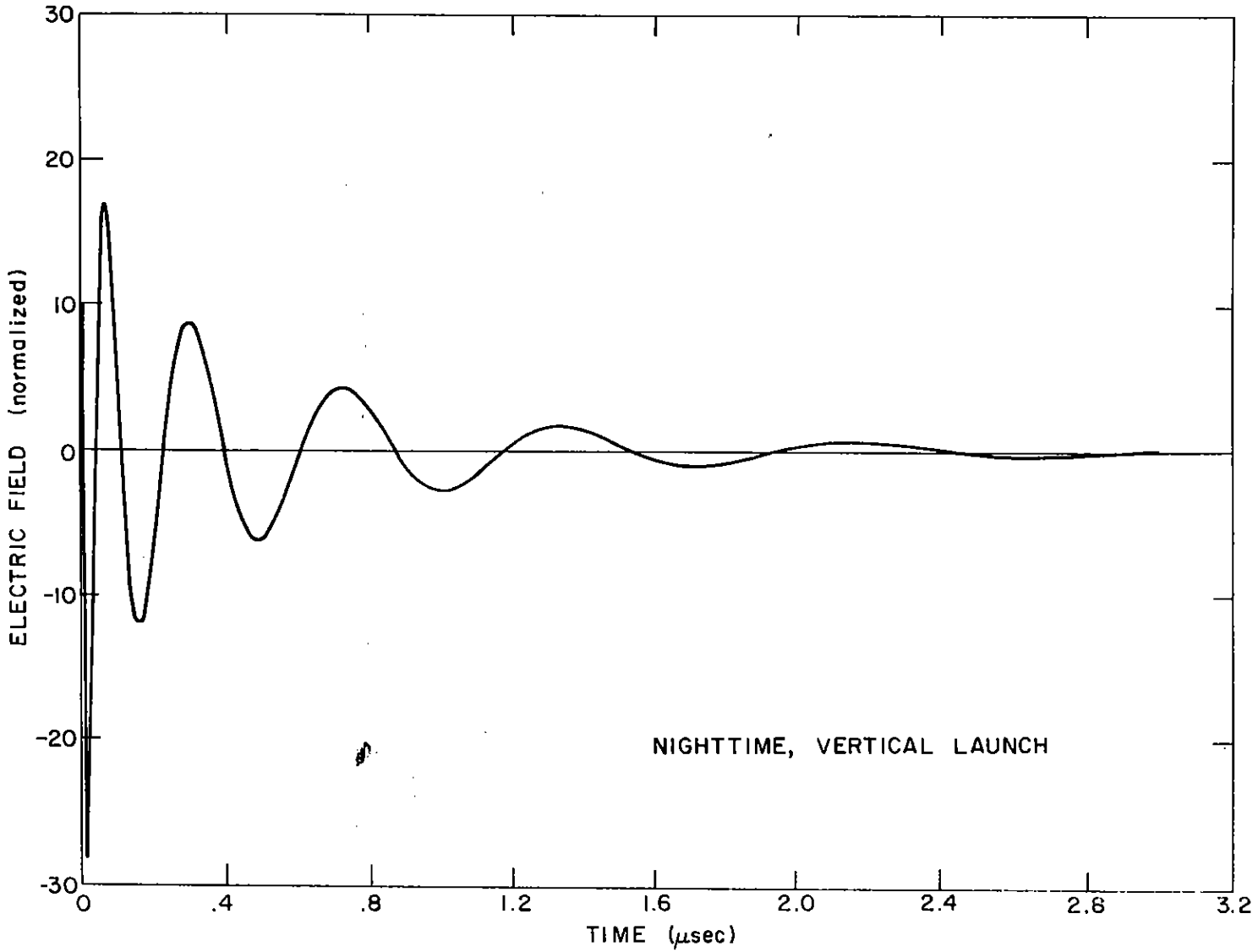

FIGURE 3.3-6 ELECTRIC FIELD AT 100 km

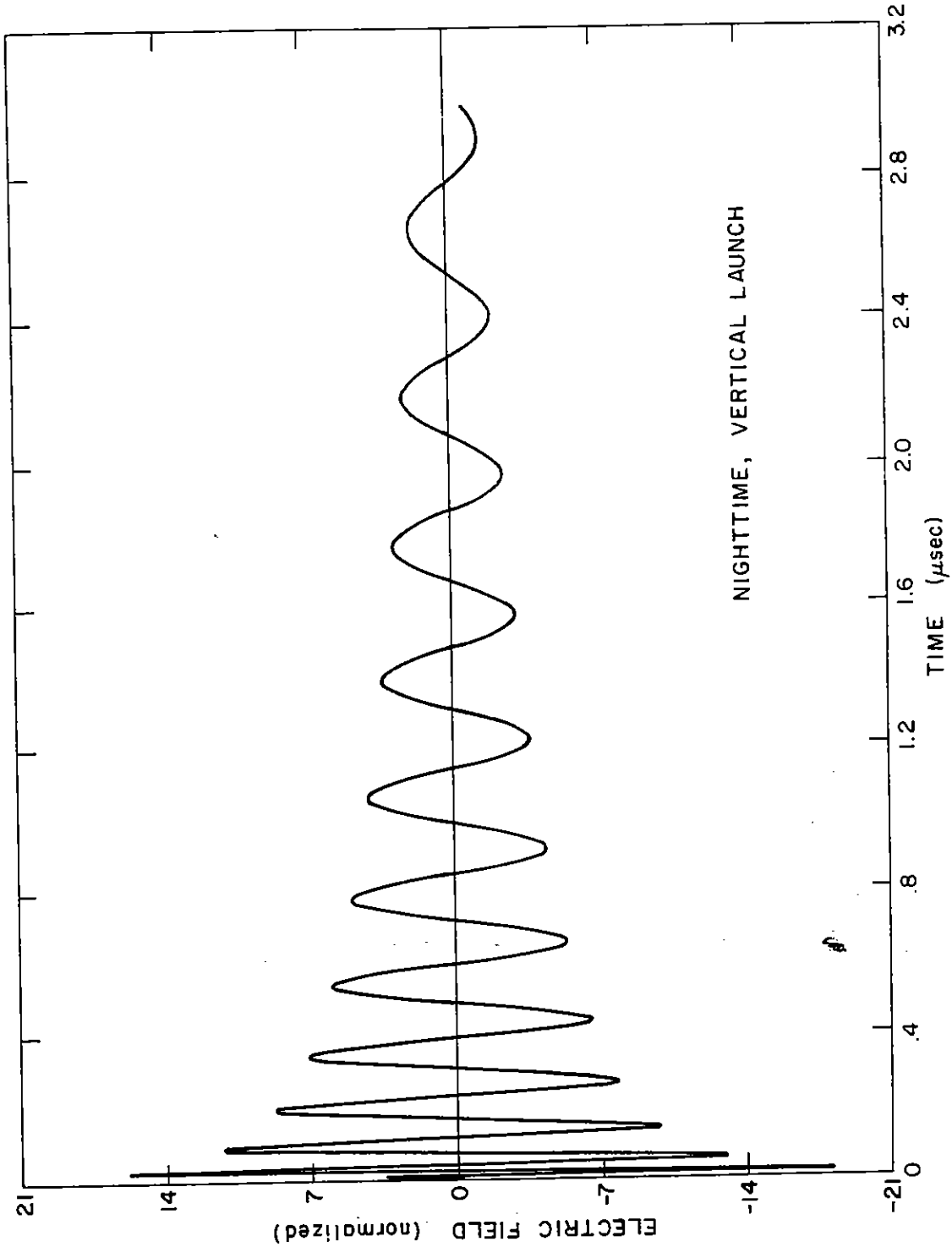

FIGURE 3.3-7 ELECTRIC FIELD AT 200 km

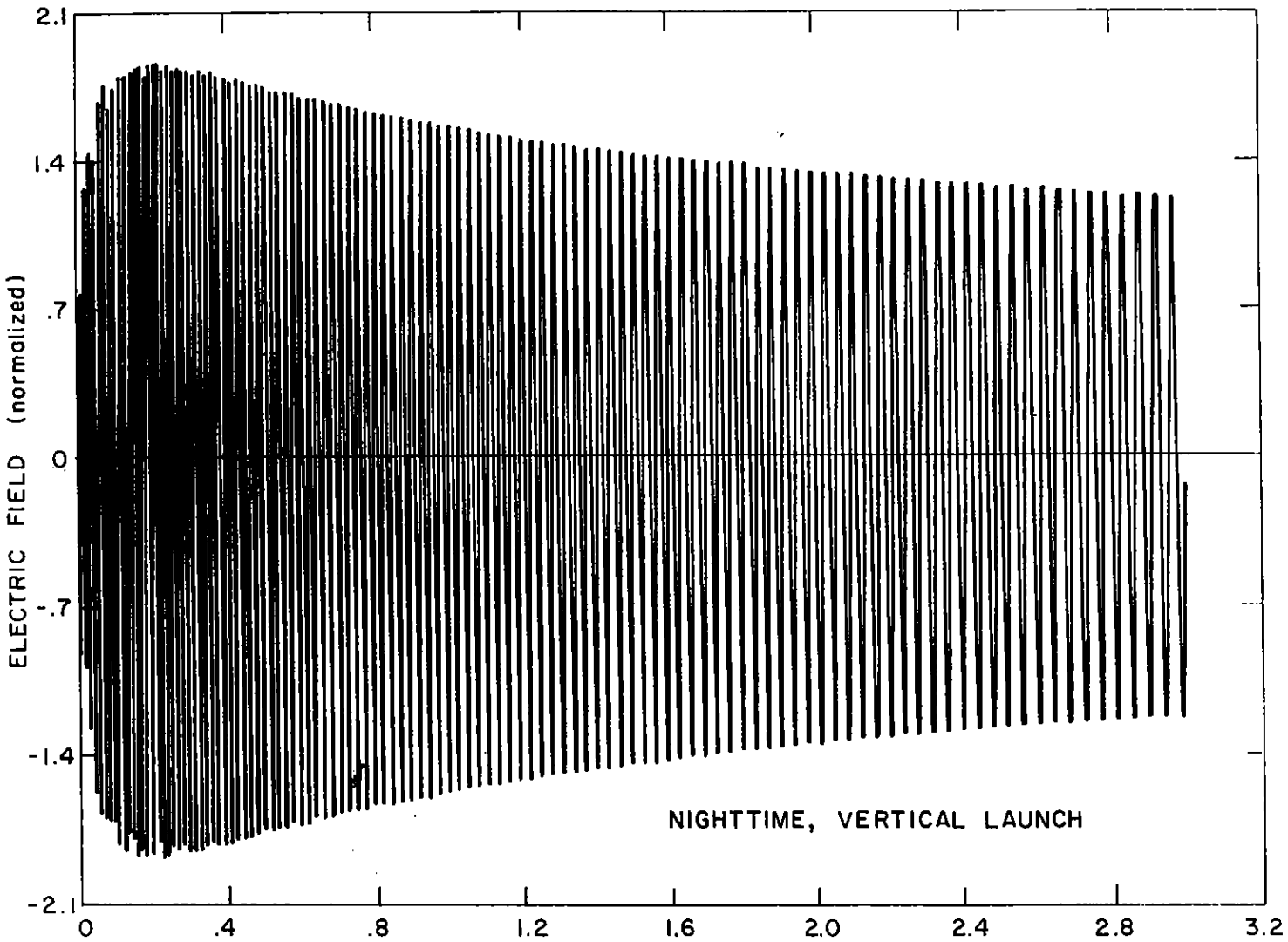

FIGURE 3.3-8 ELECTRIC FIELD AT 300 km

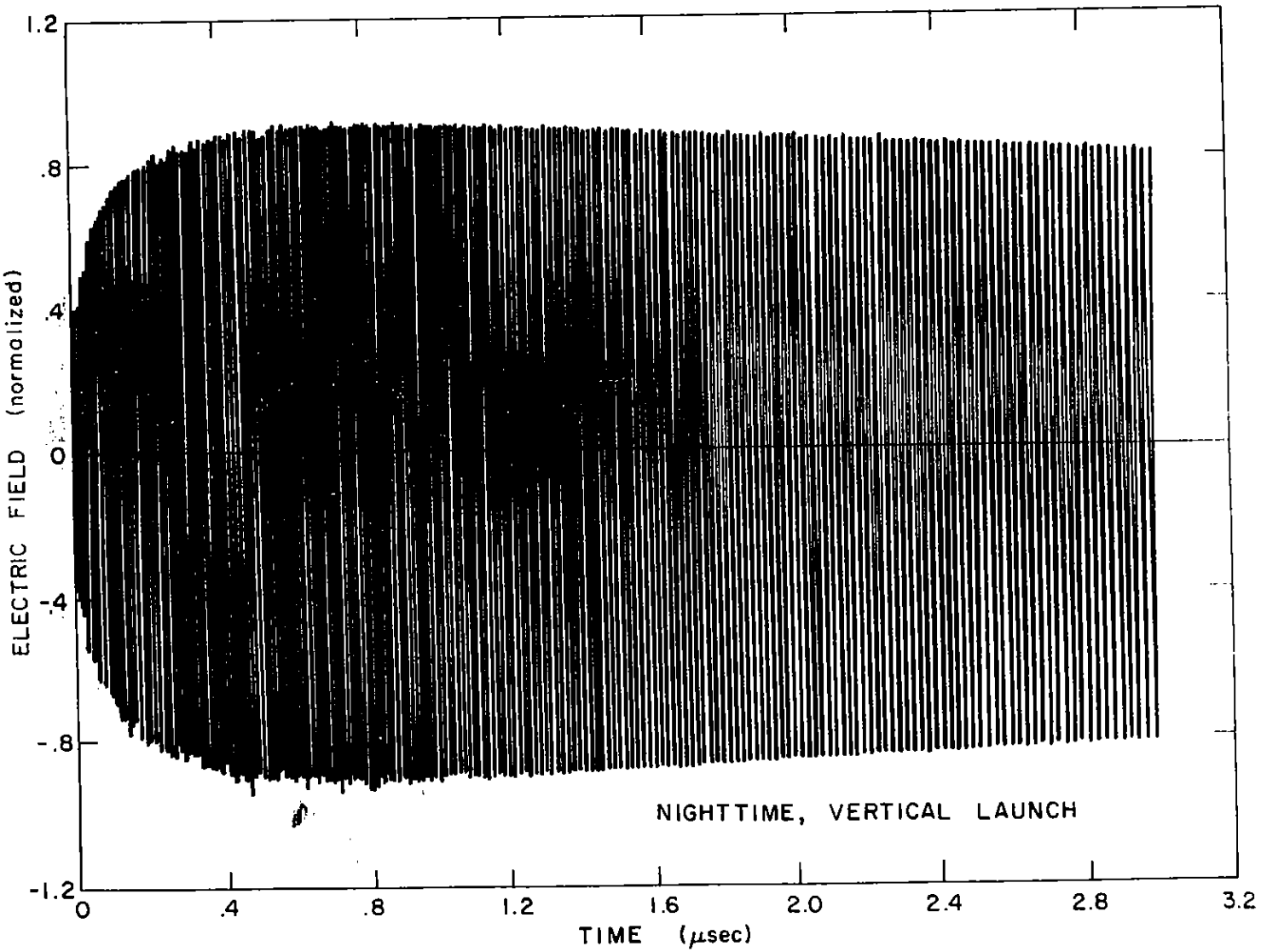

FIGURE 3.3-9 ELECTRIC FIELD AT 1000 km

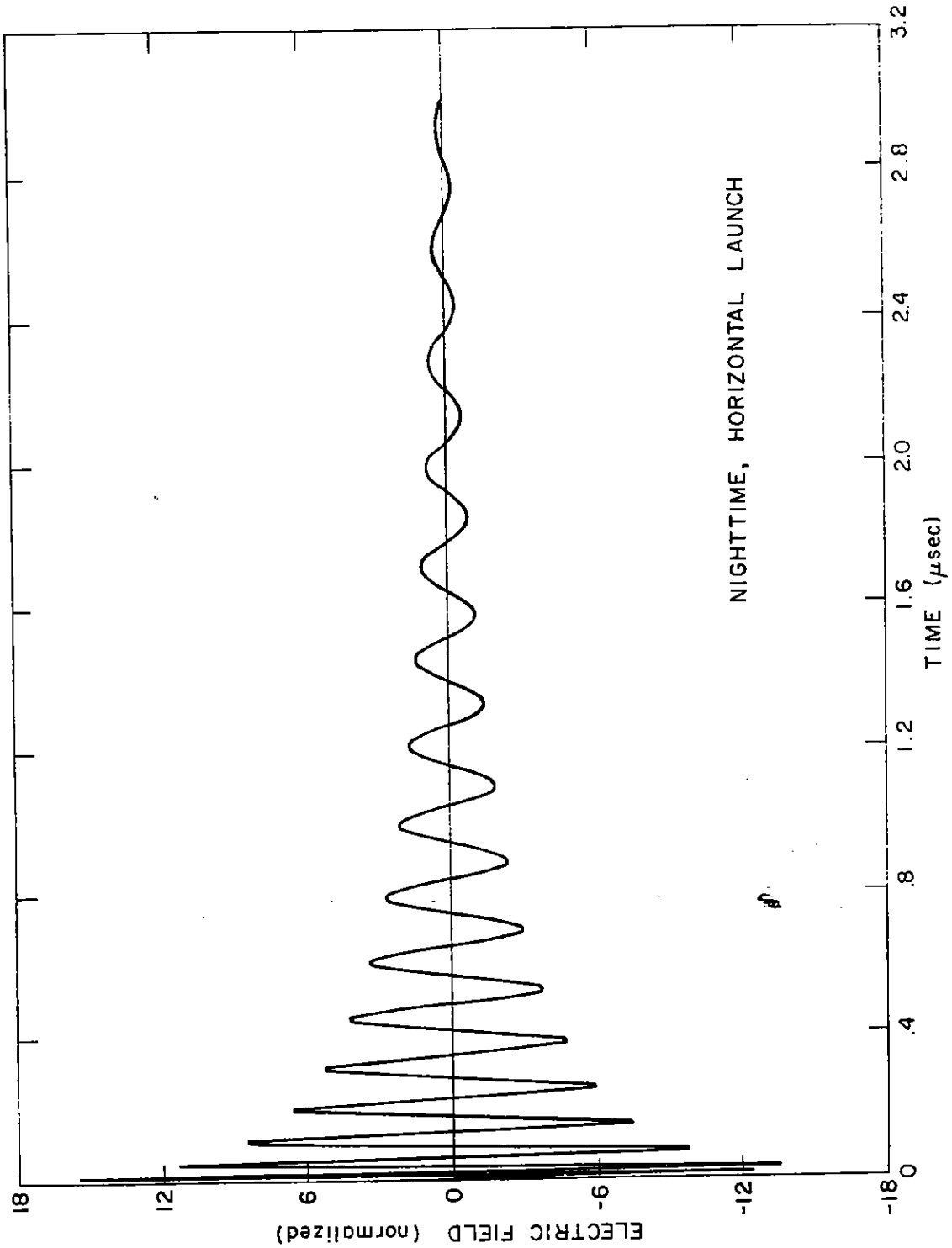

FIGURE 3.3-10 ELECTRIC FIELD AT 100 km

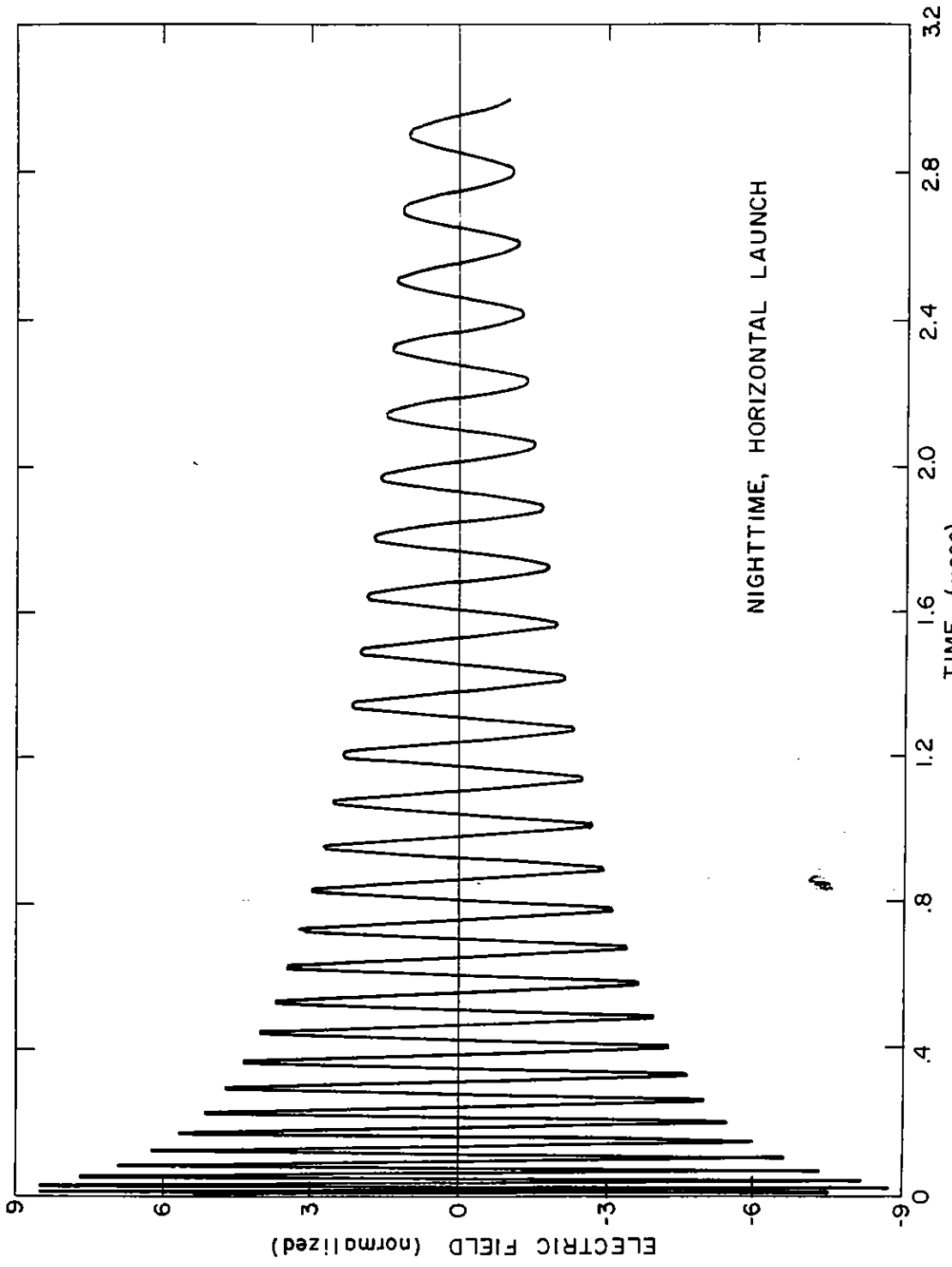

FIGURE 3.3-11 ELECTRIC FIELD AT 200 km

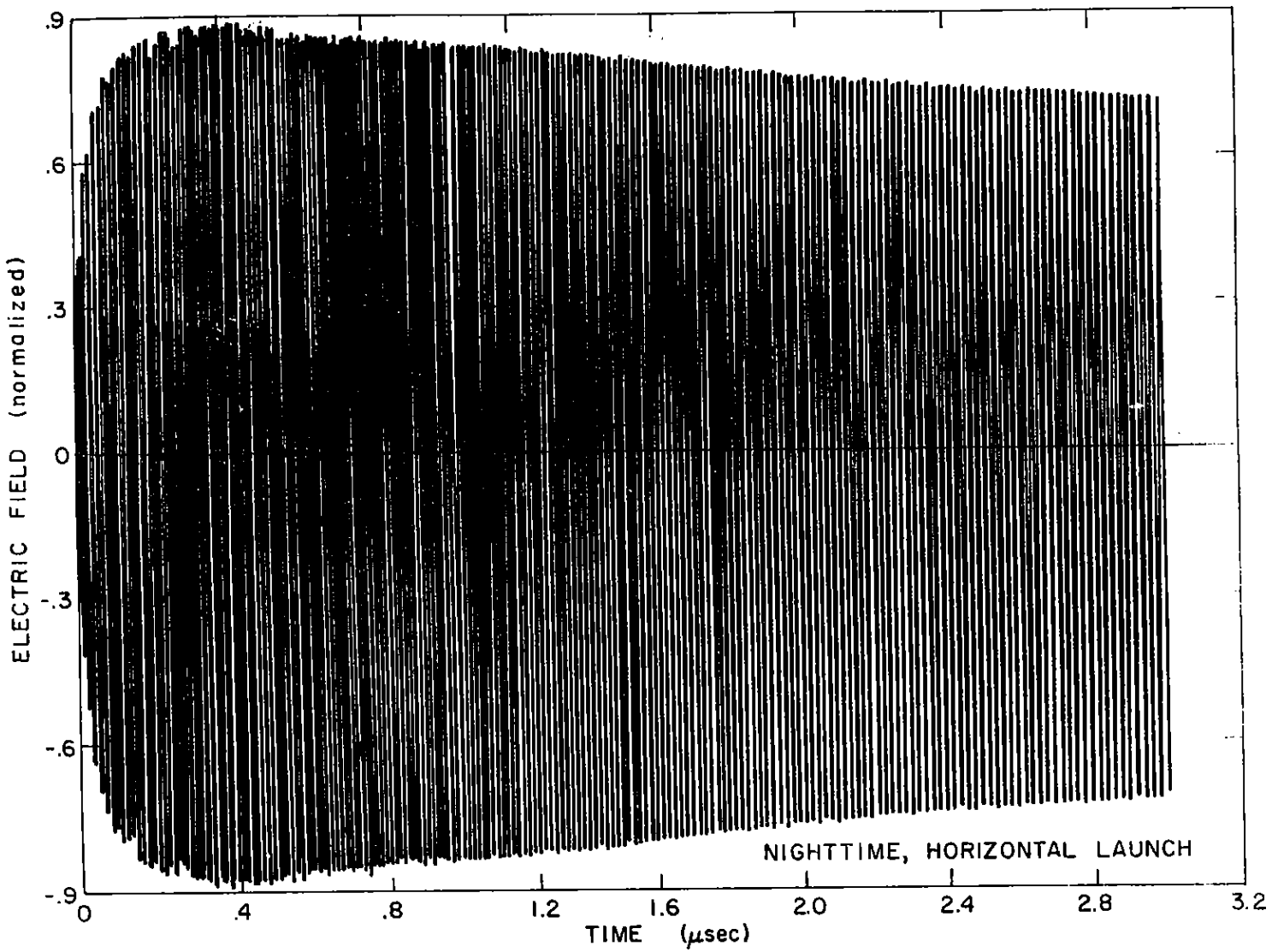

FIGURE 3.3-12 ELECTRIC FIELD AT 300 km

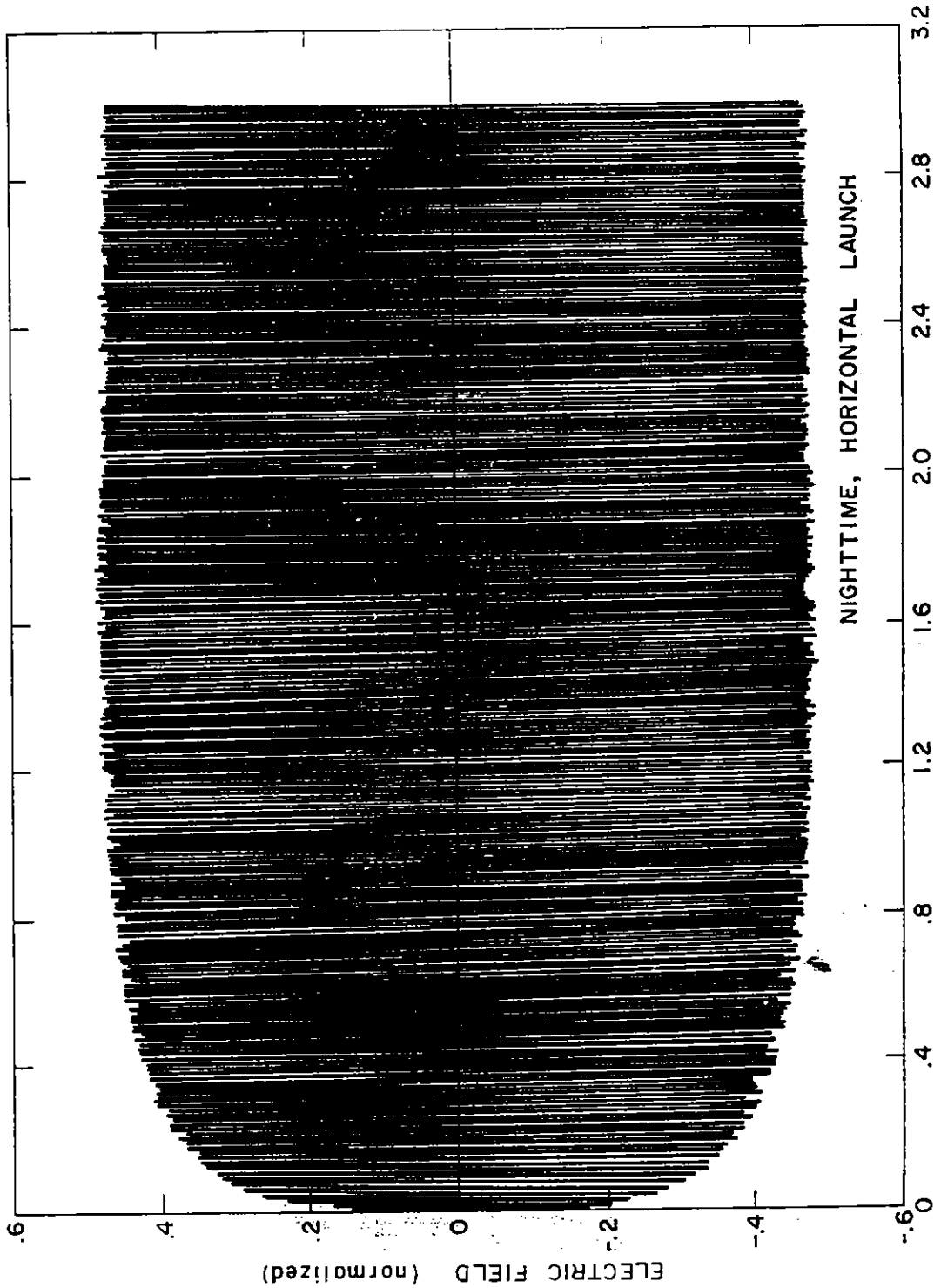

FIGURE 3.3-13 ELECTRIC FIELD AT 1000 km

3.4 Approximate Calculation of the Envelope of a Pulse Propagated through a Slab Ionosphere

This section presents a rather unusual method for calculating the envelope of a pulse propagated through a slab ionosphere. The fact that a slab ionospheric model is used is no real constraint since the TEC and cutoff frequency derived from an arbitrary ionosphere can be used to construct a slab model which produces nearly the same effects, except very close to the cutoff frequency where ray bending and reflections become important. For purposes of S/V analysis, the errors near the cutoff frequency are negligible. The comparisons shown and others not shown indicate that the envelope calculations are extremely good and certainly more than adequate for our purposes.

In section 4.2, it is shown that the peak field seen by a narrow band receiver, with center frequency ω_o, is independent of the receiver for large ionospheric dispersion (if the receiver induced dispersion is negligible). The peak electric field is given by

$$E_M = \frac{|\hat{E}(\omega_o)|}{\pi} \Delta \qquad (3.4\text{-}1)$$

where the "effective" or "ionospheric" bandpass is given by

$$\Delta = \sqrt{\frac{2\pi}{D(\omega_o)}}$$

and

$D(\omega_o)$ is the ionospheric dispersion at ω_o

$|\hat{E}(\omega_o)|$ is the amplitude of the Fourier transform of the signal reaching the receiver.

The dispersion is the second derivative of the phase with respect to ω. D can include a term to account for the dispersion due to a receiver function, in which case E_M will not reflect the pure ionospherically propagated waveform. With the exception noted above, E_M is independent of the receiver, and appears to be the magnitude of the dispersed pulse envelope at the time that the instantaneous frequency ω_o arrives in the system bandwidth. Since we can calculate the group delay for ω_o, we will know both frequency and envelope amplitude as a function of time.

We will start with the high frequency approximation for dispersion since, in doing some representative calculations, it will be useful to make comparisons and see how late the high

frequency approximation breaks down. In the high frequency approximation

$$\phi(\omega) = \frac{\omega_p^2 L}{2c\omega} \tag{3.4-2}$$

$$\tau(\omega) = \frac{\omega_p^2 L}{2c\omega^2} = \phi/\omega \tag{3.4-3}$$

$$D(\omega) = \frac{\omega_p^2 L}{c\omega^3} = 2\phi/\omega^2 \ , \tag{3.4-4}$$

where L is the slab thickness, ω_p is the plasma frequency corresponding to the electron density, N, c is the speed of light in vacuo, and ω is the signal frequency (ω (rad/sec) = $2\pi f$ (Hz)). The L/c free space delay has been removed from these expressions so that $\tau = 0$ is the observer's local time starting when the highest frequencies would reach him. The parameters L and ω_p can be replaced by the total electron content (TEC) in the high frequency approximation as follows:

$$\omega_p^2 L = (2\pi)^2 \ 80.6 \ NL$$

$$\omega_p^2 L = (2\pi)^2 \ 80.6 \ (TEC) \tag{3.4-5}$$

where the TEC is in units of electrons/m^2.

Solving equation 3.4-3 for frequency as a function of time,

$$f = B\sqrt{\frac{(TEC)}{\tau}} \tag{3.4-6}$$

where

$$B = \sqrt{\frac{80.6}{2c}}$$

and

$$\tau = t - L/c \ .$$

The effective bandwidth is given by

$$\Delta = \frac{\sqrt{2}\pi}{B} \frac{f^{3/2}}{\sqrt{TEC}} \tag{3.4-7}$$

so that the value of the envelope at the time a given frequency, f, arrives is

$$E_M(f) = \frac{\sqrt{2}}{B} |\hat{E}(f)| \frac{f^{3/2}}{\sqrt{TEC}} . \tag{3.4-8}$$

In terms of time, this becomes

$$E_M(\tau) = \sqrt{2}\sqrt{B}|\hat{E}(f)| \frac{(TEC)^{1/4}}{\tau^{3/4}} \tag{3.4-9}$$

As a test, consider the envelope of a propagated impulse function. Then $|\hat{E}(f)| = 1$ for all f and

$$I_M(\tau) = \sqrt{2}\sqrt{B} \frac{(TEC)^{1/4}}{\tau^{3/4}} \tag{3.4-10}$$

which agrees exactly with the envelope of the waveform predicted by equation I-17 (Appendix I).

Equation 3.1-1 can be used to determine the frequency corresponding to the envelope peak (f_M) by differentiating with respect to ω. Once the frequency is known, the amplitude and delay can be found. Then, using equation 3.4-4 for $D(\omega)$, f_M must satisfy

$$\frac{d}{d\omega} |\hat{E}(\omega)| \Big|_{\omega_M} = -\frac{3}{2} \frac{|\hat{E}(\omega_M)|}{\omega_M} \tag{3.4-11a}$$

or

$$\frac{d}{d\omega} \ln(|\hat{E}(\omega)|) \Big|_{\omega_M} = -\frac{3/2}{\omega_M} \tag{3.4-11b}$$

Note that $\omega_M = 2\pi f_M$ is independent of the ionospheric dispersion and therefore, the envelope peak will always correspond to the

same frequency; f_M depends only upon the initial time waveform (and ionospheric absorption to a smaller degree).

As an example, consider the initial time waveform to be the double exponential

$$E(t) = E_o[e^{-\beta t} - e^{-\alpha t}] \tag{3.4-12}$$

with $\alpha >> \beta$. We intuitively expect f_M to be one of the high frequencies, certainly above the cutoff frequency (on the order of 5-10 MHz for vertical propagation). The amplitude of the Fourier transform of E(t) is approximated by

$$|\hat{E}(\omega)| = E_o \frac{\alpha}{\omega \sqrt{\alpha^2 + \omega^2}} \tag{3.4-13}$$

for frequencies near α (see Appendix IV). Then

$$\frac{d}{d\omega}|\hat{E}| = -|\hat{E}|\left[\frac{1}{\omega} + \frac{\omega}{\alpha^2 + \omega^2}\right]$$

and equation 3.4-11 yields

$$\alpha = \omega_M \tag{3.4-14}$$

or

$$f_M = \alpha/2\pi$$

The delay is given by equation 3.4-3 (after converting to TEC) as

$$\tau(f_M) = B^2(2\pi)^2 \frac{TEC}{\alpha^2} \tag{3.4-15}$$

where

$$B^2 = \frac{40.3}{c} = 1.34 \times 10^{-7}$$

Evaluating the constants,

$$\tau(f_M) = (5.30 \times 10^{-6}) \frac{TEC}{\alpha^2} \qquad (3.4\text{-}16)$$

Let $\alpha = 4.76 \times 10^8$ rad/sec or $\alpha^2 = 2.27 \times 10^{17}$. Then

$$\tau(f_M) = 2.34 \times 10^{-23} \ (TEC) \ . \qquad (3.4\text{-}17)$$

Ionosphere vertical TEC's range from 10^{16} to 10^{18} electrons/m^2, with typical values being 5×10^{16} to 5×10^{17}. The lower values correspond to nighttime ionospheres and the higher ones to daytime ionospheres. Non-vertical paths will have higher TEC's. Table 3.4-1 shows the time of the envelope peak and the ratio of the peak amplitude to E_o for various TEC's. The peak of the original waveform (with $\beta = 4 \times 10^6$ sec^{-1}) was about 1×10^{-8} sec.

TEC (elec/m^2)	τ (μsec)	E_{peak}/E_o
1.E16	.234	1.89E-2
2.E16	.468	1.34E-2
5.E16	1.17	8.46E-3
1.E17	2.34	5.98E-3
2.E17	4.68	4.23E-3
5.E17	11.7	2.67E-3
1.E18	23.4	1.89E-3

Table 3.4-1. Magnitude and Time of the Envelope Peak for the Double Exponential Pulse with α = 4.76E8

The expressions for $E_M(f)$ and $f(\tau)$ will now be calculated without resorting to the high frequency approximation. The phase is given by

$$\phi(\omega) = \frac{\omega L}{v(\omega)} \qquad (3.4\text{-}18)$$

where

v = phase velocity

= c/n

n = index of refraction

$$= \sqrt{1 - (\omega_p/\omega)^2}$$

$$= \sqrt{1 - (f_p/f)^2}$$

The group delay is given by

$$t = \frac{d\phi}{d\omega} = \frac{L}{c}\left[n + \omega \frac{dn}{d\omega}\right] , \qquad (3.4\text{-}19)$$

where

$$\frac{dn}{d\omega} = \frac{\omega_p^2/\omega^3}{n}$$

so that

$$\frac{d\phi}{d\omega} = \frac{L}{nc} \qquad (3.4\text{-}20)$$

The dispersion is given by the second derivative as

$$D = \frac{d}{d\omega}\left(\frac{d\phi}{d\omega}\right)$$

$$= \frac{L}{c} \frac{d}{d\omega}\left(\frac{1}{n}\right)$$

$$D = -\frac{L\omega_p^2}{c\omega^3 n^3} \qquad (3.4\text{-}21)$$

Note that the expression for D is of the same form as in the high frequency approximation, with ω replaced by ωn. Converting to TEC and f instead of ω_p, L, and ω,

$$D = \frac{1}{\pi}\left[\frac{40.3}{c}\right]\frac{(TEC)}{f^3 n^3} \qquad (3.4\text{-}22)$$

Similarly, the expression for E_M is identical to that for the high frequency approximation with f replaced by fn, i.e.,

$$E_M = \frac{\sqrt{2}}{B} \left| \hat{E}(f) \right| \frac{(fn)^{3/2}}{\sqrt{TEC}} \qquad (3.4\text{-}23)$$

Returning to the expression for group delay,

$$t = \frac{L}{nc}$$

$$= \frac{L}{c} \frac{1}{\sqrt{1 - (f_p/f)^2}}$$

$$f^2 = \frac{f_p^2 (ct)^2}{(ct + L)(ct - L)} \qquad (3.4\text{-}24)$$

This delay includes the free space delay, L/c. Shifting the time frame by this amount, let

$$\tau = t - L/c \ , \qquad (3.4\text{-}25)$$

$$f^2 = \frac{f_p^2 (L + c\tau)^2}{(2L + c\tau)(c\tau)}$$

$$f = B\left[1 + \frac{c\tau}{L}\right] \sqrt{\frac{(TEC)}{\tau\left(1 + \frac{c\tau}{2L}\right)}} \qquad (3.4\text{-}26)$$

where $B = \sqrt{40.3/c}$, as before. The equation reduces to the high frequency approximation for

$$\tau << L/c \ .$$

A relation for L must now be found. Equation 3.4-26 shows that L is responsible for determining the times for which the relation between τ and f deviates from the high frequency approximation. In the limit of $\tau >> L/c$, equation 3.4-26 reduces to

$$f = \sqrt{\frac{80.6\ (TEC)}{L}} \qquad (3.4\text{-}27)$$

which must correspond to the cutoff frequency for the ionosphere and launch angle under consideration. This will be true if L is defined by

$$L = \frac{TEC}{N_p} \tag{3.4-28}$$

where N_p is related to the cutoff frequency by

$$f_c^2 = 80.6\ N_p \tag{3.4-29}$$

For vertical propagation, N_p is simply the peak electron density. Let us consider vertical propagation first. For the nighttime, sunspot minimum ionosphere presented in section 3.2, the vertical TEC is 4.32E16 elec/m^2 and the peak electron density is 2.E11 elec/m^3. Therefore, for vertical propagation through the ionosphere, L = 216 km. The TEC to 300 km is 9.E15 elec/m^2. The peak electron density is the same so that for propagation to 300 km, L = 45 km. The vertical TEC for the daytime, sunspot maximum ionosphere is 5.78E17 elec/m^2 and the peak electron density is 2.E12 elec/m^3. Then, for vertical propagation through the daytime ionosphere, L = 289 km. The vertical TEC to 300 km is 1.4E17 elec/m^2, N_p is the same so that L = 70 km for propagation to 300 km. A reasonable average L for propagation vertically through the ionosphere is 255 km. An average value for propagation to 300 km is not reasonable.

The general effect on L due to increasing the launch angle (θ_i) can be seen by considering propagation through a planar slab ionosphere. In this case, the TEC varies as $1/\cos\theta_i$. The cutoff frequency also varies as $1/\cos\theta_i$ so that N_p varies as $1/\cos^2\theta_i$. Then, L varies as $\cos\theta_i$. The fact that the effective slab thickness, L, decreases with increasing launch angle is rather unexpected because we associate L with the physical propagation path length. However, L was defined in such a way as to reflect the dispersion characteristics near the cutoff frequency and it was left to the TEC term to account for the increased dispersion due to the longer path length.

The expressions for τ and D must also be modified to reflect the fact that, for non-vertical incidence, they both must be infinite at the cutoff frequency and not the plasma frequency. For this purpose, we introduce an "effective index of refraction," n'. In terms of TEC and L, instead of the plasma frequency, the index of refraction becomes

$$n = \left[1 - \frac{80.6\ (TEC)}{Lf^2}\right]^{1/2} \tag{3.4-30}$$

For non-vertical angles, with L defined as above, this is equivalent to

$$n' = \left[1 - \left(\frac{f_c}{f}\right)^2\right]^{1/2} \qquad (3.4\text{-}31)$$

which reduces to n for vertical incidence. As f approaches the cutoff frequency, n' goes to zero, delay and dispersion go to infinity, and the effective bandwidth goes to zero.

Figure 3.4-1a shows $f\sqrt{L/c(TEC)}$ vs. $\tau c/L$, i.e., normalized frequency vs. normalized delay. This is a plot of equation 3.4-26. Figure 3.4-1b shows

$$\sqrt{TEC}\,\frac{E_M(f)}{|\hat{E}(f)|}$$

vs. fn', i.e., normalized envelope value vs. normalized frequency. This is a plot of equation 3.4-23. In order to calculate the envelope and instantaneous frequency as a function of time for a given ionosphere, one must first characterize that ionosphere in terms of TEC and L (considering launch angle) and use figure 3.4-1a to determine frequency as a function of delay. Then, using the Fourier transform of the original signal times the amplitude of the ionosphere transfer function, $|\hat{E}(f)|$, and figure 3.4-1b, the magnitude of the envelope as a function of frequency and time can be found. Remember that this approach assumes large dispersion and will not be valid for very early times (depending upon D) and it does not account for the variation of path length with frequency and will be invalid at late times (depending upon launch angle). At late times, the ray propagation theory breaks down anyway, owing to the wave propagation characteristics involved with frequencies near the cutoff frequency. Finally, remember that the entire linear theory will fail if the electric field is too large.

Figures 3.4-2 through 3.4-7 show various envelope calculations and some comparisons with the envelopes of certain Fourier transform type calculations. Figures 3.4-2 and 3.4-3 show calculations of the ionosphere's impulse function response as a function of time for vertical TEC's of 1, 2, 5, 10, 20, 50, and 100 (in units of 10^{16} electrons/m^2). The first graph is the set of calculations using the high frequency approximation while the second set uses the "correct" equations. Figures 3.4-4 and 3.4-5 use the double exponential used to construct table 3.4-1 with $E_o = 52$. None of the calculations in this section includes a geometric attenuation. Again, the first set of this pair uses the high frequency approximation while the second set does not. Figure 3.4-6 compares envelope calculations for TEC's of 5×10^{16} and 1×10^{17} with the envelopes of Fourier transform calculations. The transfer functions for the Fourier transform calculation are for vertical propagation. Finally, figure 3.4-7

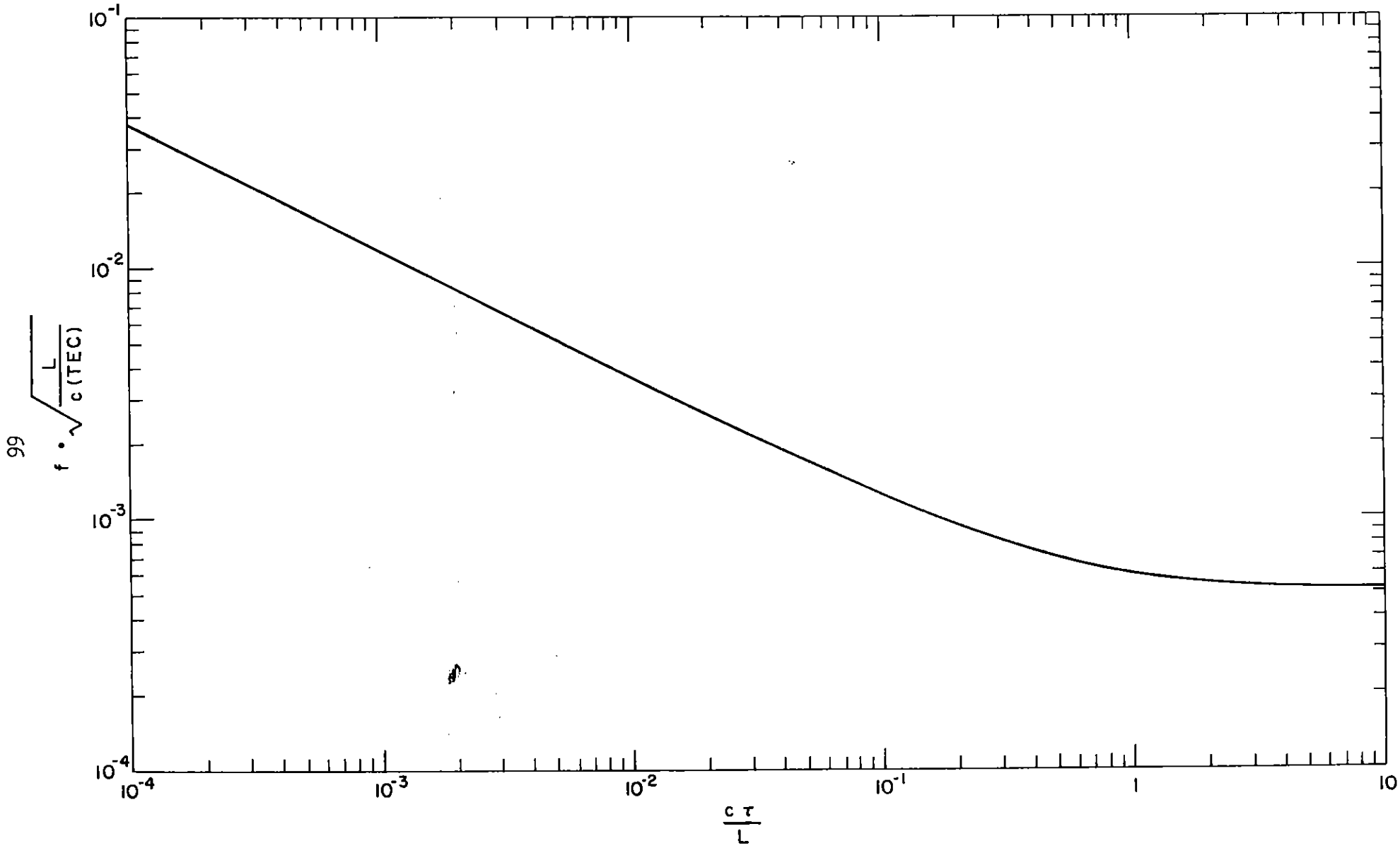

FIGURE 3.4-1a NORMALIZED FREQUENCY vs NORMALIZED DELAY

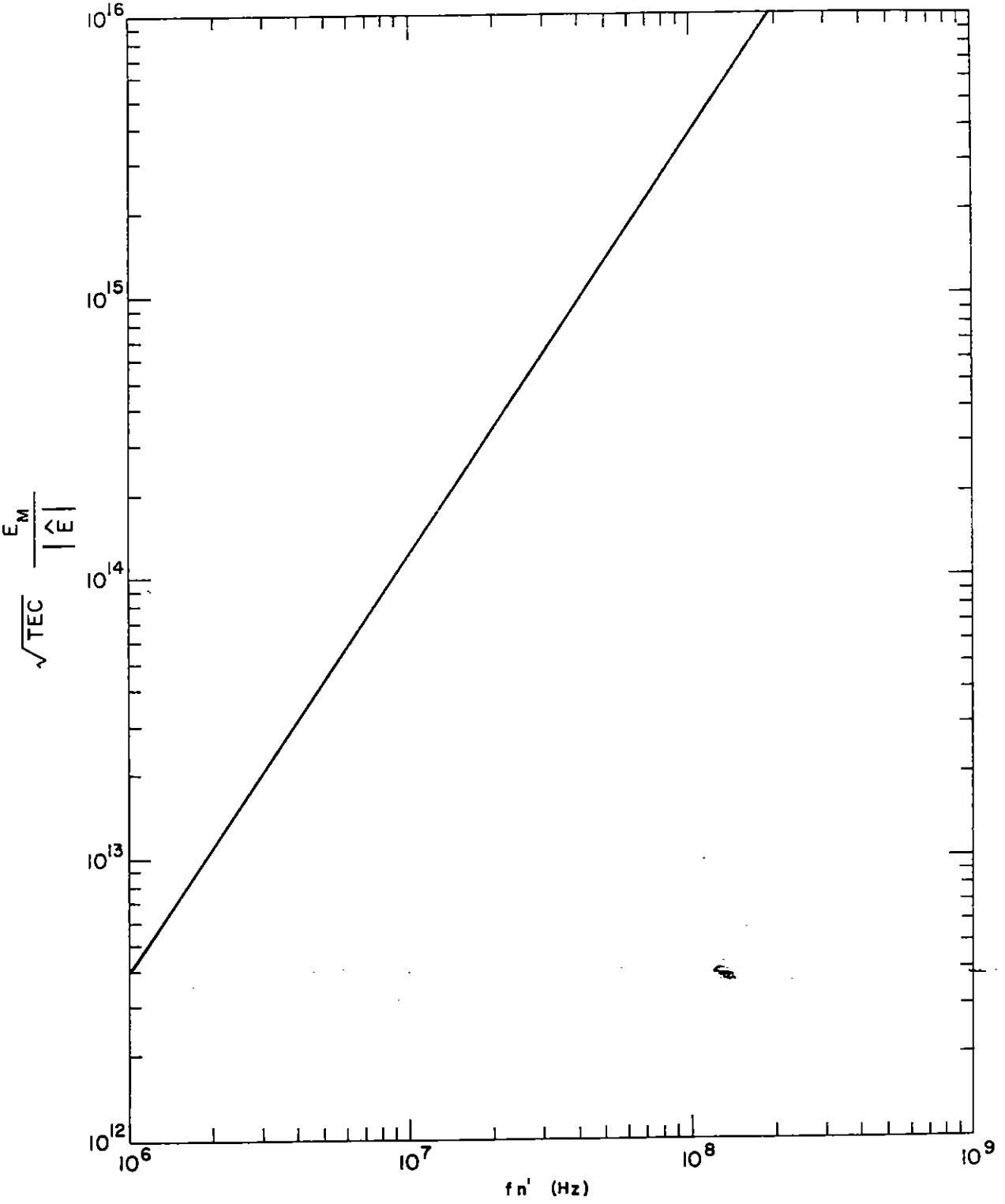

FIGURE 3.4-1b NORMALIZED AMPLITUDE vs FREQUENCY TIMES INDEX OF REFRACTION

compares envelope calculations with the envelope of a Fourier transform calculation for a pulse with a 90° launch angle at the earth's surface. The TEC for the 1000 MHz ray path is 1.17×10^{17} elec/m^2. In this comparison, absorption was considered in the analytic calculation by using equation 2.1-38 and $W = 7.47 \times 10^{13}$. In addition, a correction factor was used to decrease the transmission factor rapidly near the cutoff frequency. The cutoff frequency for this calculation was 13.5 MHz and the instantaneous frequency seen at 10^{-4} sec. is 17.4 MHz so that the late-time divergence between the analytic and Fourier calculations is in large part due to the artificial truncation of the transfer function. At these times, the frequency dependence of the ray bending should also start being significant. This effect increases the dispersion for low frequencies and is not included in the analytic calculation.

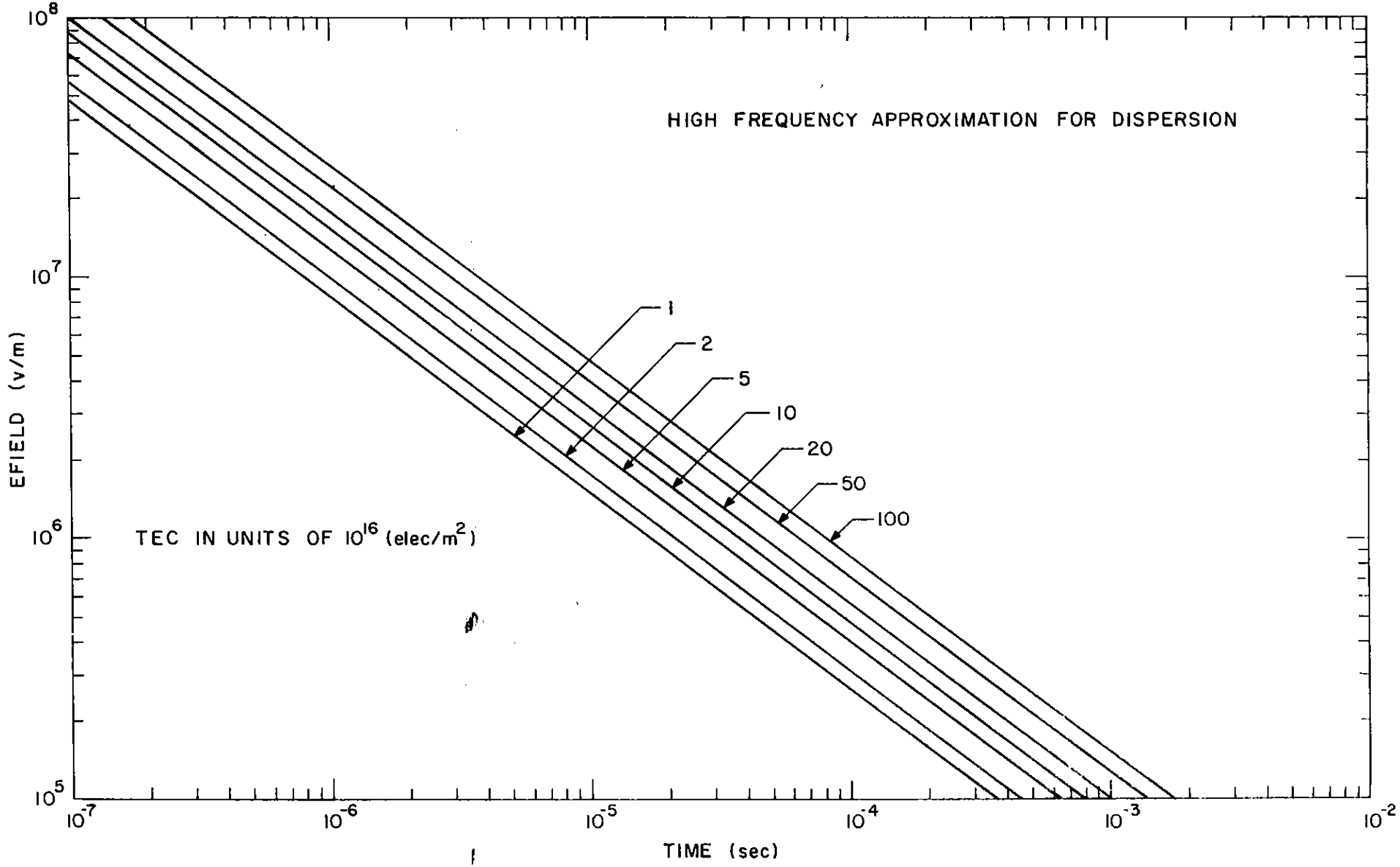

FIGURE 3.4-2 EFIELD vs TIME IMPULSE RESPONSE

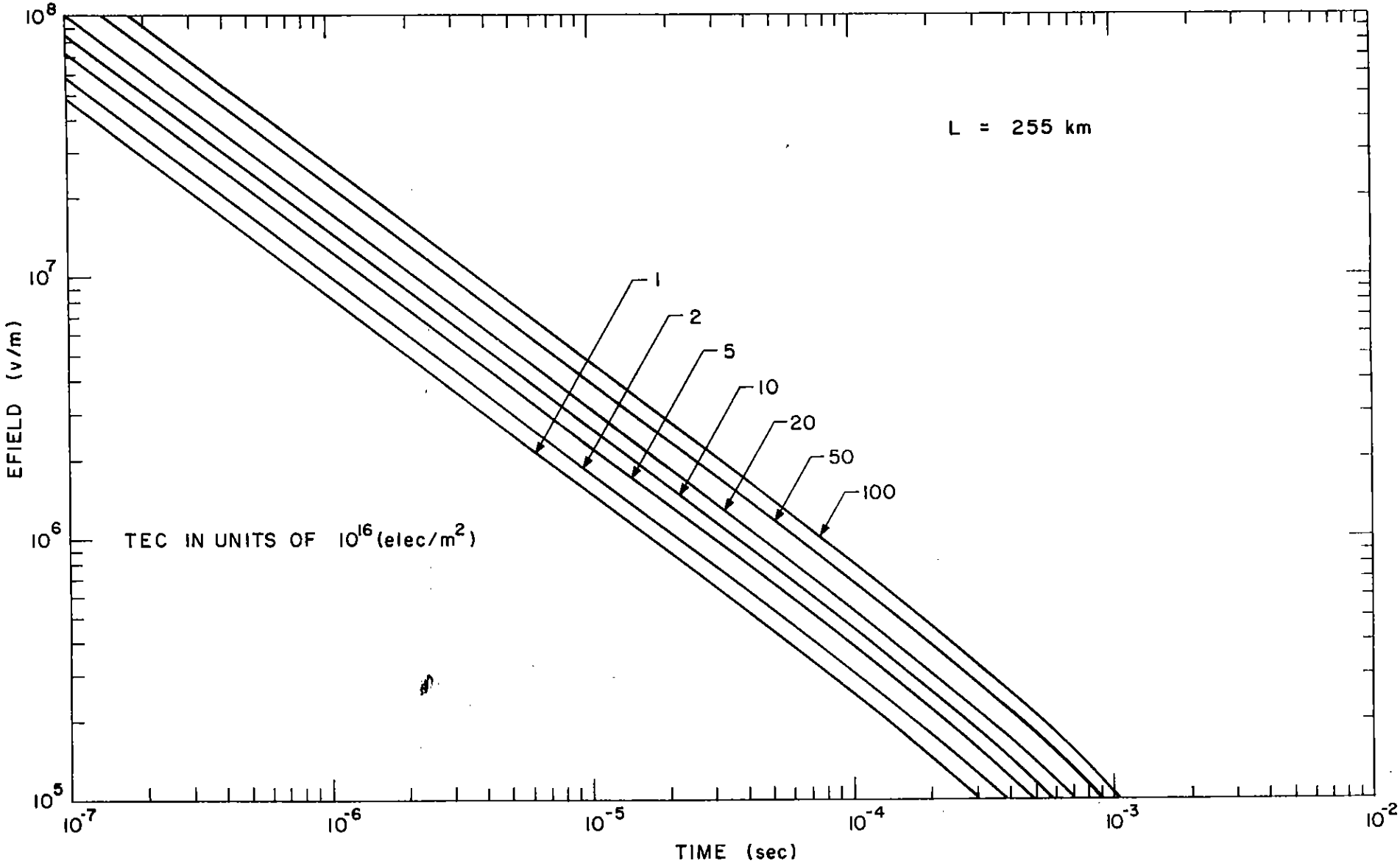

FIGURE 3.4-3 EFIELD vs TIME FOR IMPULSE RESPONSE

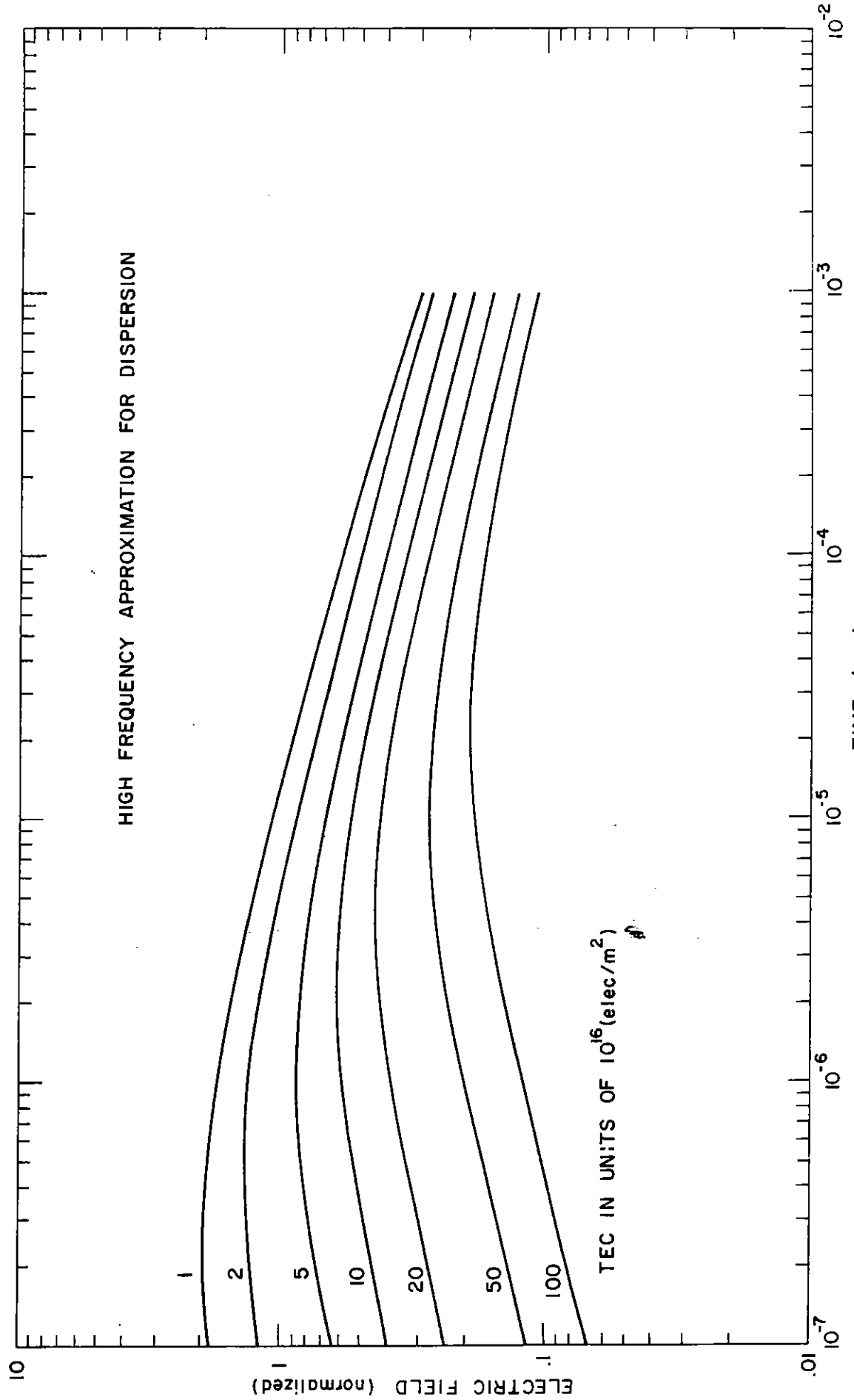

FIGURE 3.4-4 EFIELD vs TIME FOR DOUBLE EXPONENTIAL PULSE

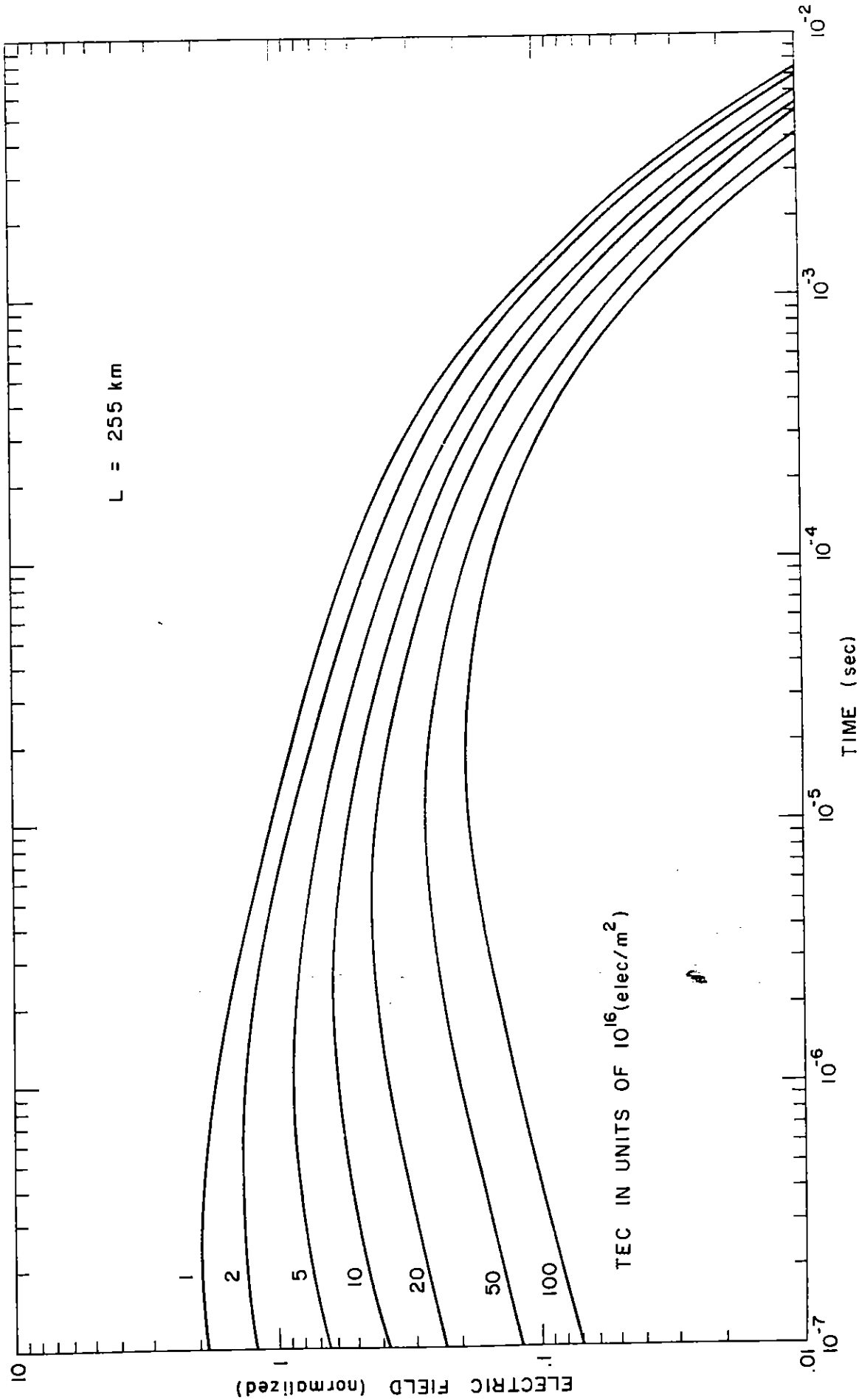

FIGURE 3.4-5 EFIELD vs TIME FOR DOUBLE EXPONENTIAL PULSE

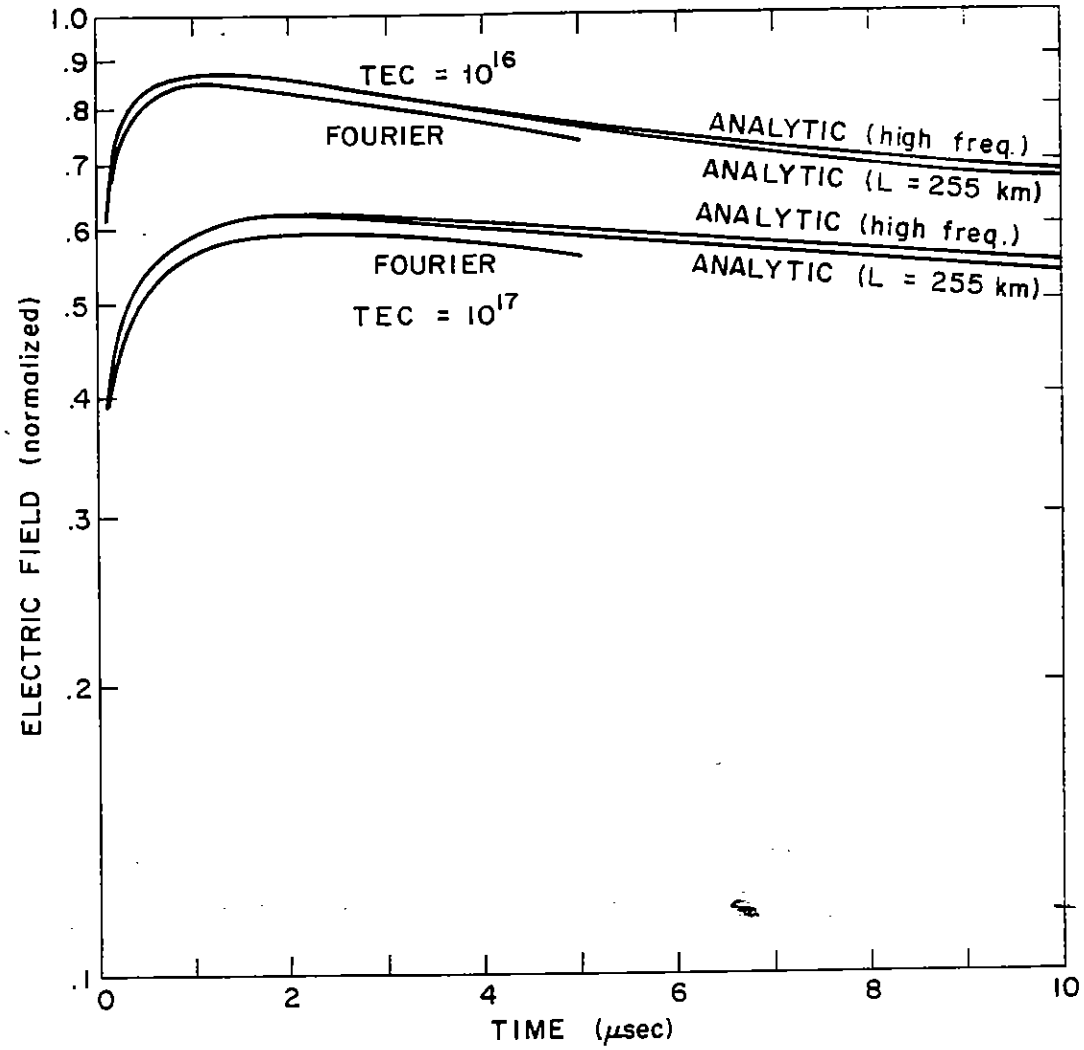

FIGURE 3.4-6 COMPARISON WITH FOURIER TRANSFORM

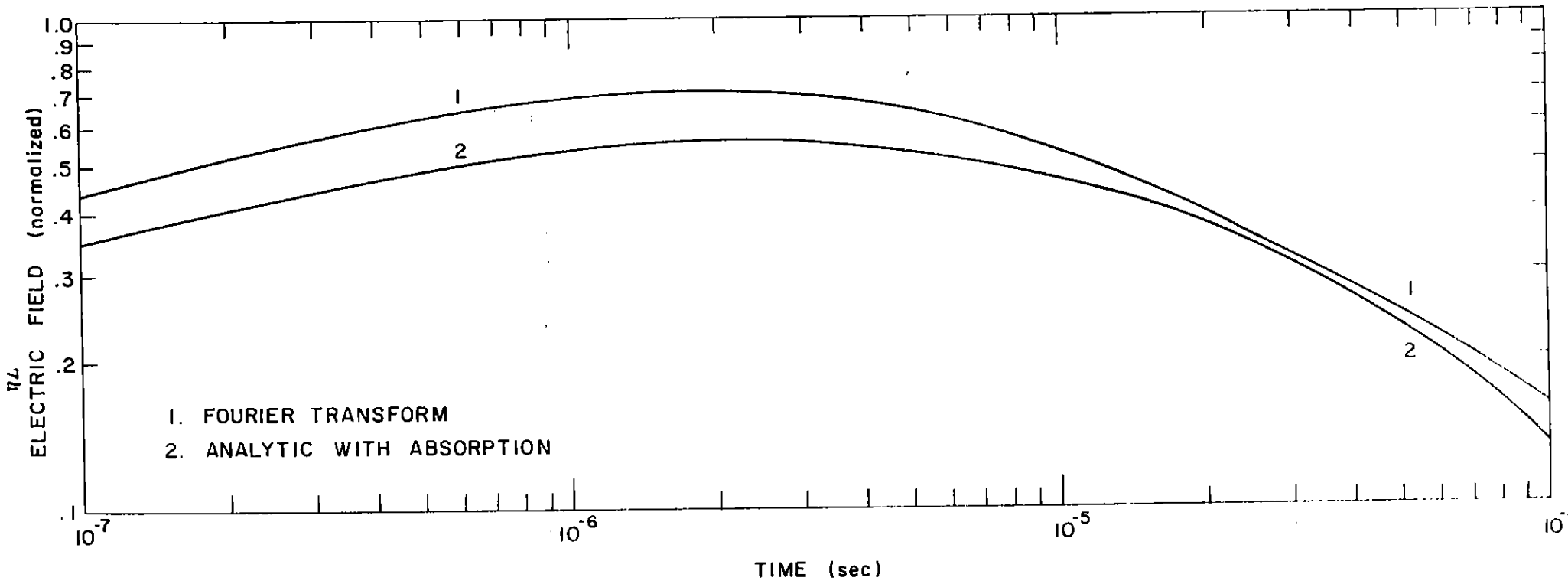

FIGURE 3.4-7 COMPARISON WITH FOURIER TRANSFORM

4. Interaction with Simple Systems

In this section, we investigate the interaction of the propagated fields in terms of (1) the electromagnetic energy delivered to the system and coupled to it (assuming a very simple model for coupling) and (2) the peak fields "seen" by a simple system and the currents induced by these fields. While the models may seem too unrealistic, they are sufficient to predict the order of magnitude and give a feeling for the interrelationships involved.

4.1 Energy Coupling

We will first calculate the fraction of energy transmitted by the ionosphere. Then, modeling the system as a simple band-pass filter, calculate the fraction of this energy which couples into the system.

The total energy density propagating through space is

$$E = \frac{\varepsilon}{2}|E(t)|^2 + \frac{\mu}{2}|H(t)|^2 \qquad (4.1\text{-}1)$$

When propagating through free space, the electric and magnetic field energy densities are equal and

$$E = \varepsilon|E(t)|^2 \qquad (4.1\text{-}2)$$

We will assume this relation to be true for our purposes. The energy passing through a unit area over a given period of time is

$$F = \varepsilon c \int_{t_1}^{t_2} |E(t)|^2 dt \ , \qquad (4.1\text{-}3)$$

where c is the speed of light in vacuo. The total energy passing through a unit area is

$$F_T = \varepsilon c \int_{-\infty}^{\infty} |E(t)|^2 dt \qquad (4.1\text{-}4)$$

Initially, we will ignore geometric attenuation and consider only the reduction of energy content due to the filtering of the ionosphere.

Before proceeding farther, we will derive Parseval's theorem which relates equation 4.1-4 with an equivalent in frequency space. The time dependent electric field is related to its Fourier transform by

$$E(t) = \frac{1}{2\pi}\int_{-\infty}^{\infty} \hat{E}(\omega) e^{i\omega t} d\omega \ . \qquad (4.1\text{-}5)$$

Now,

$$\int_{-\infty}^{\infty} E^2(t)\,dt = \frac{1}{2\pi} \int_{-\infty}^{\infty} E(t) \int_{-\infty}^{\infty} \hat{E}(\omega) e^{i\omega t} d\omega dt \qquad (4.1\text{-}6)$$

or,

$$\int_{-\infty}^{\infty} E^2(t)\,dt = \frac{1}{2\pi} \int_{-\infty}^{\infty} \hat{E}(\omega) \int_{-\infty}^{\infty} E(t) e^{i\omega t} dt d\omega \qquad (4.1\text{-}7)$$

where the order of integration has been reversed. The inside integral is the conjugate of $\hat{E}(\omega)$ so that

$$\int_{-\infty}^{\infty} |E(t)|^2 dt = \frac{1}{2\pi} \int_{-\infty}^{\infty} |\hat{E}(\omega)|^2 d\omega \ . \qquad (4.1\text{-}8)$$

Also, since

$$|\hat{E}(\omega)|^2 = \hat{E}(\omega)\hat{E}^*(\omega)$$

is even,

$$\int_{-\infty}^{\infty} |E(t)|^2 dt = \frac{1}{\pi} \int_{0}^{\infty} |\hat{E}(\omega)|^2 d\omega \qquad (4.1\text{-}9)$$

In frequency space, the total energy per unit area is

$$F_T = \frac{\varepsilon c}{\pi} \int_{0}^{\infty} |\hat{E}(\omega)|^2 d\omega \qquad (4.1\text{-}10)$$

Ignoring absorption, the amplitude of the ionosphere transfer function is the Heaviside step function

$$T(\omega) = H(\omega - \omega_c) \ , \qquad (4.1\text{-}11)$$

where ω_c is the cutoff frequency. The energy delivered per unit area is then

$$F_A = \frac{\varepsilon c}{\pi} \int_{\omega_c}^{\infty} |\hat{E}(\omega)|^2 d\omega \tag{4.1-12}$$

or

$$F_A = F_T - \frac{\varepsilon c}{\pi} \int_{o}^{\omega_c} |\hat{E}(\omega)|^2 d\omega \tag{4.1-13}$$

Consider a time waveform which is a double exponential before ionospheric filtering, i.e.,

$$E(t) = E_o[e^{-\beta t} - e^{-\alpha t}] \tag{4.1-14}$$

with $\alpha >> \beta$. In this case, it is easier to evaluate F_T in the time domain.

$$E^2(t) = E_o^2 \, e^{-\beta t}[e^{-\beta t} - 2e^{-\alpha t}] \tag{4.1-15}$$

$$F_T = \varepsilon c E_o^2 \left| \frac{1}{2\beta} - \frac{2}{\alpha + \beta} \right| , \tag{4.1-16}$$

or, with $\alpha >> \beta$

$$F_T = \varepsilon c \frac{E_o^2}{2\beta} \tag{4.1-17}$$

We must now calculate the amount of energy removed by the ionosphere.

$$|\hat{E}(\omega)|^2 = \frac{E_o^2}{(\alpha^2 + \omega^2)^2 (\beta^2 + \omega^2)^2} \left| [\beta(\alpha^2 + \omega^2) - \alpha(\beta^2 + \omega^2)]^2 + \omega^2(\alpha^2 - \beta^2)^2 \right| \tag{4.1-18}$$

With ω_c and $\beta << \alpha$,

$$|\hat{E}(\omega)|^2 = \frac{E_o^2}{(\beta^2 + \omega^2)^2}\left[\left(\beta - \frac{\beta^2 + \omega^2}{\alpha}\right)^2 + \omega^2\right]$$

or,

$$|\hat{E}(\omega)|^2 \approx \frac{E_o^2}{\beta^2 + \omega^2} \qquad (4.1\text{-}19)$$

Then,

$$F_A = F_T - \frac{\varepsilon c}{\pi} E_o^2 \int_o^{\omega_c} \frac{d\omega}{\beta^2 + \omega^2}$$

or,

$$F_A = \frac{\varepsilon c}{2\beta} E_o^2 \left[1 - \frac{2}{\pi} \tan^{-1}\left(\frac{\omega_c}{\beta}\right)\right] \qquad (4.1\text{-}20)$$

The ratio of transmitted to initial energy is then

$$X = \frac{F_A}{F_T} = 1 - \frac{2}{\pi} \tan^{-1}\left(\frac{\omega_c}{\beta}\right) \qquad (4.1\text{-}21)$$

Figure 4.1-1 shows the value of this transmission factor (in percent transmitted) as a function of ω_c for $\beta = 4 \times 10^6$. Table 4.1-1 shows the energy transmitted to various altitudes, with and without geometric attenuation, for a slant path through a nighttime ionosphere. The path is tangent to the earth from a 400 km burst. The geometric attenuation uses the distance to the earth tangent as the reference distance.

Actually, the amount of energy coupled to an exoatmospheric system can be considerably less than the amount that is transmitted. This is because the satellite will respond only to a certain band or bands of frequencies. As will be shown, the center frequency and bandwidth is quite critical in determining the fraction of energy that actually couples into the system because the bandwidth may overlap the ionosphere cutoff frequency or the center frequency may be at the high end of the spectrum where the spectral content is small. Let the amplitude of the system transfer function be $|\hat{S}(\omega)|$. The energy coupled from the field is then

$$F_S = \frac{\varepsilon c}{\pi} \int_{\omega_c}^{\infty} S(\omega) |\hat{E}(\omega)|^2 d\omega \qquad (4.1\text{-}22)$$

In many cases, as a first approximation, the amplitude of the system transfer function can be modeled as a square bandpass with center frequency ω_o and width $2\Delta\omega$. Then

$$F_S = \frac{\varepsilon c}{\pi} \int_{\omega_o - \Delta\omega}^{\omega_o + \Delta\omega} |\hat{E}(\omega)|^2 d\omega \qquad (4.1\text{-}23)$$

if $\omega_o - \Delta\omega > \omega_c$, or,

$$F_S = \frac{\varepsilon c}{\pi} \int_{\omega_c}^{\omega_o + \Delta\omega} |\hat{E}(\omega)|^2 d\omega \qquad (4.1\text{-}24)$$

otherwise. In terms of the transmitted energy, these equations become

$$F_S = F_A - \frac{\varepsilon c}{\pi} \left[\int_{\omega_c}^{\omega_o - \Delta\omega} |\hat{E}(\omega)|^2 d\omega + \int_{\omega_o + \Delta\omega}^{\infty} |\hat{E}(\omega)|^2 d\omega \right] \qquad (4.1\text{-}25)$$

in the first case, or

$$F_S = F_A - \frac{\varepsilon c}{\pi} \int_{\omega_o + \Delta\omega}^{\infty} |\hat{E}(\omega)|^2 d\omega \qquad (4.1\text{-}26)$$

in the second. Table 4.1-2 shows the effect of the ionosphere cutoff frequency on the amount of energy which can couple into a system. The "Fraction of Available Energy" is the ratio of the energy coupled into a system to the amount which would couple if the ionosphere cutoff frequency was not a consideration. Three cases are considered. In each case, the altitude dependence of the cutoff frequency is demonstrated. The same parameters were used as in constructing Table 4.1-1. In the first case, the center frequency of the system is equal to the ionosphere cutoff frequency above 300 km. The bandwidth is ±5 MHz. The second case uses a higher center frequency, but the bandwidth is allowed to be plus and minus the center frequency itself. The center frequency of the third case is the same as in the second case, but the bandwidth is 10 MHz less in each direction.

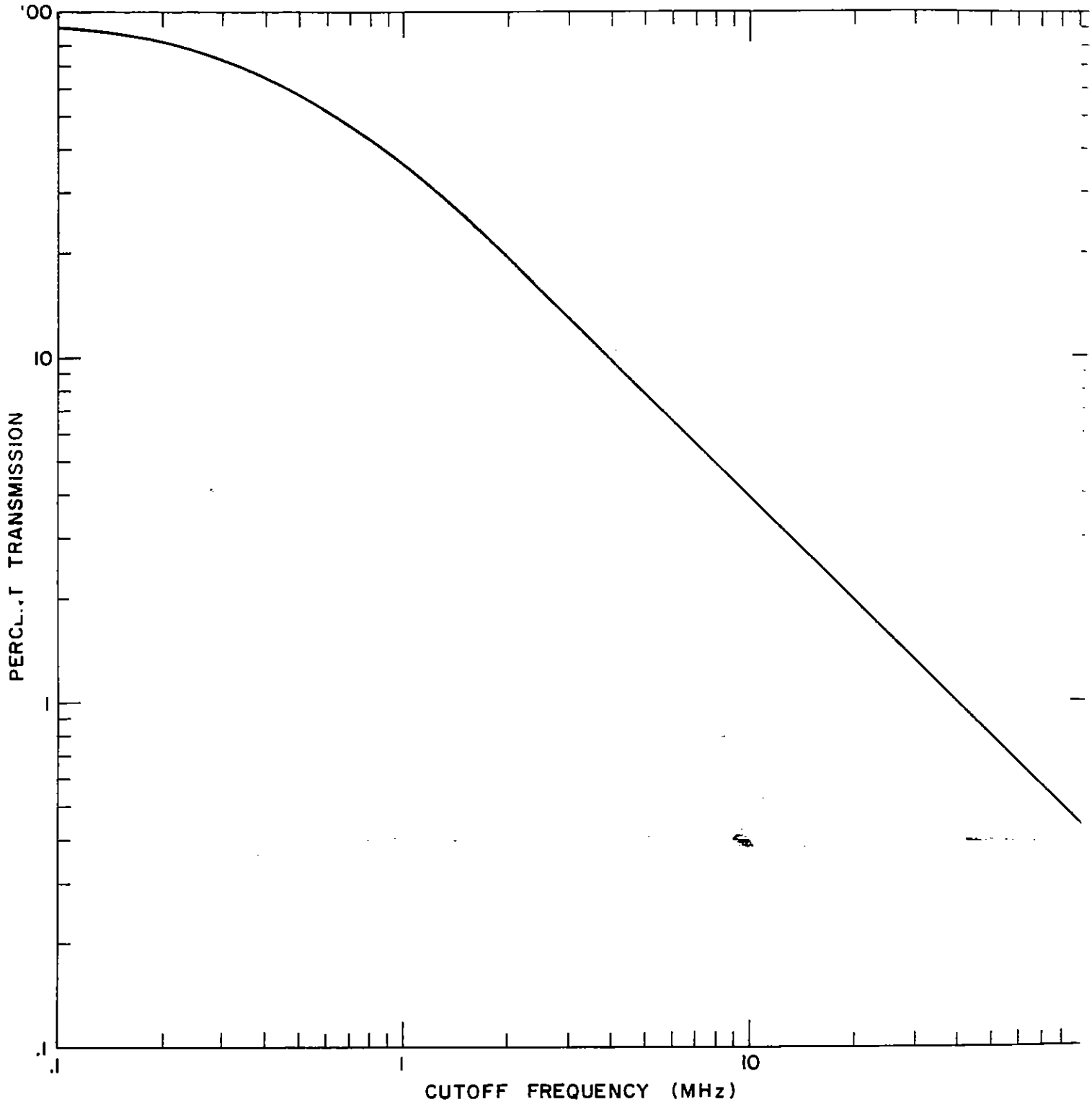

FIGURE 4.1-1 ENERGY TRANSMISSION vs CUTOFF FREQUENCY

Altitude (km)	f_c (MHz)	Ionosphere Transmission	Geometric Factor	Energy Transmission
100	1.6	.25	.45	.113
200	2.3	.17	.35	.060
300	10.1	.04	.29	.012
400	10.1	.04	.25	.010
500	10.1	.04	.22	.0088
1000	10.1	.04	.15	.0060
37000	10.1	.04	.0026	.0001

Table 4.1-1. Ionospheric Energy Transmission Function to Various Observer Altitudes for an Earth Tangent Line-of-Sight from a 400 km Burst

CASE 1: f_o = 10 MHz, Δf = ±5 MHz

Altitude (km)	f_c (MHz)	Fraction of Available Energy
100	1.6	1
200	2.3	1
300-∞	10.1	0.244

CASE 2: f_o = 30 MHz, Δf = ±30 MHz

Altitude (km)	f_c (MHz)	Fraction of Available Energy
100	1.6	0.236
200	2.3	0.166
300-∞	10.1	0.034

CASE 3: f_o = 30 MHz, Δf = ±20 MHz

Altitude (km)	f_c (MHz)	Fraction of Available Energy
100	1.6	1
200	2.3	1
300-∞	10.1	0.988

Table 4.1-2. Fraction of Energy Available for Coupling into Certain Systems due to Ionospheric Filtering. Tangent Line of Sight from 400 km Burst.

4.2 Field Coupling

In this section we look at the maximum voltages and currents developed in a system with narrow band coupling to the incident fields. The maximum electric field coupled into a system will be shown to be of the form

$$E_M = \frac{|\hat{E}(\omega_o)|}{\pi} \Delta \tag{4.2-1}$$

where Δ is an "effective" bandwidth, and $|\hat{E}(\omega_o)|$ is the magnitude of the Fourier transform of the incident field at the bandpass center frequency. It will be shown that Δ equals the system bandwidth for small dispersion and small bandwidths and that it equals a system independent "ionospheric" bandwidth for large dispersion and large system bandwidths. An unsophisticated derivation of Δ will be shown in this section. Appendices II and III derive Δ for two specific bandpasses (step function and Gaussian) in order to show that the same function will be found.

The EMP waveform seen by a system with transfer function $\hat{S}(\omega)$ is

$$E_S(t) = \frac{1}{2\pi} \int_{-\infty}^{\infty} \hat{S}(\omega)\hat{E}(\omega)e^{i\omega t}d\omega \ , \tag{4.2-2}$$

where $\hat{E}(\omega)$ is the Fourier transform of the field incident upon the system. Let $P(\omega)$ be the combined phase of $\hat{S}(\omega) \cdot \hat{E}(\omega)$. Assuming that $\hat{S}(\omega)$ does not distinguish negative frequencies,

$$E_S(t) = \frac{1}{\pi} \int_{o}^{\infty} |S(\omega)||\hat{E}(\omega)|e^{iP(\omega)}e^{i\omega t}d\omega \ . \tag{4.2-3}$$

Let $|S(\omega)|$ provide narrow band characteristics such that $|\hat{E}(\omega)| \approx |\hat{E}(\omega_o)|$ over the bandwidth and $P(\omega)$ can be expanded in a three term Taylor series, i.e.,

$$P(\omega) = P_o - \tau(\omega_o)(\omega - \omega_o) + \frac{D(\omega_o)}{2}(\omega - \omega_o)^2 \tag{4.2-4}$$

where

$$P_o = P(\omega_o) \tag{4.2-5}$$

$$\tau(\omega_o) = -\frac{dP}{d\omega}\bigg|_{\omega_o} \quad \text{(group}$$ (4.2-6)

$$D(\omega_o) = \frac{d^2P}{d\omega^2}\bigg|_{\omega_o} \quad \text{(dispersi}$$ (4.2-7)

The electric field is then

$$E_S(t) = \frac{|\hat{E}(\omega_o)|}{\pi} e^{i(P_o - \omega_o)} \int_{-\omega_o}^{\infty} \cdots e^{-\frac{D}{2}x^2} dx$$ (4.2-8)

where $x = (\omega - \omega_o)$.

The problem is now to study the maximum field seen by the system. Since we are concerned with the envelope of the waveform, the oscillating term (carrier) outside of the integral can be ignored. We wish to put equation (4.2-8) in the form

$$E_M = \frac{|\hat{E}(\omega_o)|}{\pi} \Delta$$ (4.2-9)

where E_M is the maximum field value and Δ is the "effective" bandpass. Let $|S(\omega)|$ have a maximum value of unity at ω_o, i.e., at $x = 0$. For the sake of simplicity, let the bandpass be symmetrical about the center frequency. Define

$$B(\Delta\omega, D) = \int_{-\omega_o}^{\infty} |S(x)| e^{i(\tau - \cdots} e^{-\frac{D}{2}x^2} dx$$ (4.2-10)

so that

$$\Delta = \sup|B| \ .$$ (4.2-11)

Given the function $|S(\omega)|$, one can define a bandwidth such that the maximum value of $B(\Delta\omega, D)$ can be calculated to a good approximation by assuming a step function bandpass $|S_o(x)|$ such that

$$|S_o(x)| = \begin{cases} 1, & -\Delta\omega \leq x \leq \Delta\omega \\ 0, & \text{otherwise} \end{cases} \tag{4.2-12}$$

One way to determine $\Delta\omega$ would be through the relation

$$2\Delta\omega = \int_{-\infty}^{\infty} |S(\omega)| d\omega \ . \tag{4.2-13}$$

Then

$$B(\Delta\omega, D) = \int_{-\Delta\omega}^{\Delta\omega} \exp\left[i\left((t-\tau)x + \frac{D}{2}x^2\right)\right] dx \tag{4.2-14}$$

If dispersion is negligible across the bandpass, the second order term can be ignored and

$$B(\Delta\omega) = \int_{-\Delta\omega}^{\Delta\omega} \exp[i(t-\tau)x]dx \ . \tag{4.2-15}$$

The solution to this equation is

$$B(\Delta\omega) = \frac{\sin[\Delta\omega(t-\tau)]}{t-\tau} \tag{4.2-16}$$

which has the maximum value $\Delta\omega$ so that for small dispersion

$$\Delta = \Delta\omega \ . \tag{4.2-17}$$

If the dispersion is large, the linear phase term can be ignored in the integral and treated as a constant delay so that

$$B(\Delta\omega, D) = \int_{-\Delta\omega}^{\Delta\omega} \exp\left[i\frac{D}{2}x^2\right] dx \ . \tag{4.2-18}$$

The integral can be converted into real and imaginary parts and evaluated in terms of the Fresnel sine and cosine integral functions (see Appendix II) as

$$B = 2\sqrt{\pi/D}\{C(z) + iS(z)\} \tag{4.2-19}$$

where $z = \sqrt{D/\pi}\,\Delta\omega$. In terms of phase and amplitude,

$$B(\Delta\omega,D) = 2\sqrt{\pi/D}\sqrt{C(z)^2 + S(z)^2}\, e^{i\phi} \tag{4.2-20}$$

where

$$\phi = \tan^{-1}\left[\frac{S(z)}{C(z)}\right] .$$

Now,

$$\lim_{z\to\infty} S(z),\ C(z) = 1/2 ,$$

so that for large D and/or $\Delta\omega$,

$$B(\Delta\omega,D) = \sqrt{\frac{2\pi}{D}}\, e^{i\phi} \tag{4.2-21}$$

or

$$\Delta = \sqrt{\frac{2\pi}{D}} . \tag{4.2-22}$$

In the case of large dispersion, the maximum field seen by a system is independent of the system bandwidth and is determined by an "ionospheric" bandwidth given by equation 4.2-22. The maximum amplitude seen by a narrow band receiver

$$B(\Delta\omega) = \Delta = \sqrt{\frac{2\pi}{D(\omega_o)}} . \tag{4.2-23}$$

Thus, for large dispersion

$$E_{MAX} = \frac{|\hat{E}(\omega_o)|}{\pi}\Delta , \tag{4.2-24}$$

with Δ defined above. The expression for Δ can also be calculated using other filter functions (see Appendix II).

It is important to note that Δ is independent of the system bandwidth for large dispersion. The maximum amplitude seen by the system at the frequency ω_o is the value of the envelope of

the propagated signal at the time that the instantaneous frequency ω_o arrives at the system $(t - \tau(\omega_o))$. That this is true can be seen from section 3.4. One can interpret this as being due to the fact that the ionosphere has spread out the frequencies of the pulse so much that the system no longer sees the band

$$\omega_o - \Delta\omega \leq \omega \leq \omega_o + \Delta\omega$$

arriving almost instantaneously and causing a sharp ringing. Instead, this band of frequencies arrives over a long period of time. Over a period of time equal to $1/\Delta\omega$, the system sees a range of frequencies less than $\Delta\omega$ and so the full system bandwidth is never entirely utilized. If the system is intended to couple to the field, e.g., a receiver, one can see that the optimum bandwidth would be $\Delta\omega = \Delta$. Narrower bandwidths will reduce the signal below the amount which could potentially be received and wider bandwidths are wasted, because they do not buy increased resolution or signal strength, but they do buy more background noise. In addition, wider bandwidths allow the receiver to see frequencies whose phases will add destructively and cause distortions.

The maximum fields can be studied in terms of an effective system quality factor defined by

$$Q_E = \frac{\omega_o}{B(\Delta\omega)} \tag{4.2-25}$$

For

$$\Delta\omega << \frac{\Delta t}{D(\omega_o)}$$

the effective quality factor reduces to the familiar

$$Q = \frac{\omega_o}{\Delta\omega}$$

and for large dispersion, i.e., $\Delta\omega >> \Delta t/D$

$$Q_E = \frac{\omega_o}{\Delta} .$$

Then,

$$E_{MAX} = \frac{|\hat{E}(\omega_o)|}{\pi} \frac{\omega_o}{Q_E} . \qquad (4.2\text{-}26)$$

Consider the system to be a dipole antenna. The peak current on that antenna will be approximately

$$I_{MAX} = V/Z \qquad (4.2\text{-}27)$$

where

Z = antenna impedance

$V = E_{MAX}\ell$

ℓ = antenna length.

Then

$$I_{MAX} = \frac{|\hat{E}(\omega_o)|}{\pi Z} \frac{\omega_o \ell}{Q_E} \qquad (4.2\text{-}28)$$

This equation is deceptive because the parameters are not independent and I_{MAX} is more insensitive to them than appearances indicate. The center frequency of the dipole is related to its length by

$$\omega_o = \frac{\pi c}{\ell} , \qquad (4.2\text{-}29)$$

where c is the speed of light in vacuum. Equation 4.2-28 then becomes

$$I_{MAX} = \frac{|\hat{E}(\omega_o)|}{Z} \frac{c}{Q_E} \qquad (4.2\text{-}30)$$

If one is interested in studying the peak fields and currents as a function of altitude, it is simple and useful to use $\Delta\omega$ for the bandwidth for altitudes up to the point where $\Delta\omega = \Delta$ and Δ for higher altitudes. Since Δ will be less than $\Delta\omega$ past this point, Q_E will increase.

The current across a dipole varies with frequency much as the current through a series RLC circuit. We will use this model to investigate more fully the relationship between Z and Q_E for the case of low dispersion ($Q_E = Q$). The complex impedance of a series RLC circuit is

$$Z = R + \frac{i}{\omega C}(\omega^2 LC - 1) \tag{4.2-31}$$

where

R = circuit resistance

L = circuit inductance

C = circuit capacitance.

Resonance occurs at $\omega_o = (LC)^{-1/2}$, in which case Z = R. The Q of such a circuit is given by

$$Q = \frac{|x_L|}{R} \quad \text{or} \quad Q = \frac{|x_C|}{R} \tag{4.2-32}$$

where x_L is the inductive reactance at resonance ($\omega_o L$) and x_C is the capacitive reactance at resonance ($1/\omega_o C$). Either relation can be used to prove the following, but we will choose

$$Q = \frac{|x_L|}{R} \tag{4.2-33}$$

in order to use inductance as a parameter, which seems more appropriate when considering a long wire. Then

$$x_L = \omega_o L = \omega_o L_o \ell \tag{4.2-34}$$

where L_o is the inductance per unit length. Assuming that the dipole sees its resonant frequency,

$$Z(\omega_o) = R$$

and the equation for peak current becomes

$$I_{MAX} = \frac{|\hat{E}(\omega_o)|}{\pi L_o} \tag{4.2-35}$$

The peak current is then quite insensitive to Q and Z for frequencies near ω_o. The reason is quite simple. Increasing Z would tend to decrease the peak current, except that Q is decreased at the same time, resulting in a wider bandwidth which can couple energy from more frequencies.

The above analysis assumed that the system was a good dipole antenna. Most missiles and satellites look more like cylinders, spheres, or things with large paddles pointing outward. Such animals have very broad bandwidths and often more than one resonant mode. In these cases, one can expect to see currents which are one or two orders of magnitude higher than predicted by the simple dipole theory. The coupling mechanisms will be much more complicated and therefore the reader is referred to the many EMP Interaction Notes and Sensor and Simulation Notes for various treatments of coupling problems.

References

Johnson, Francis S., 1965. *Satellite Environment Handbook* (Second Edition), Stanford University Press, California.

Messier, Michael A., 1971. EMP Theoretical Note 117, "A Standard Ionosphere for the Study of Electromagnetic Pulse Propagation," Air Force Weapons Laboratory, New Mexico.

Appendix I. The Impulse Response of a Slab Ionosphere

Consider an impulse function time waveform propagating into and vertically through a planar ionosphere characterized by thickness L and electron density N corresponding to a plasma frequency $\omega_p = 2\pi f_p$. The transfer function of the ionosphere is then (ignoring electron collisions)

$$T(\omega) = \exp\left[-i\frac{\omega L}{c}\sqrt{1 - (\omega_p/\omega)^2}\right] \tag{I-1}$$

$$= \exp\left[-i\frac{L}{c}\sqrt{\omega^2 - \omega_p^2}\right] \tag{I-2}$$

Let $k = L/c$ and $a = i\omega_p$, $s = i\omega$, where c is the speed of light in vacuo. Then in terms of the Laplace transform,

$$T(s) = \exp[-k\sqrt{s^2 - a^2}] \tag{I-3}$$

The Laplace transform of the impulse function is unity, therefore the impulse response of the ionosphere is

$$I(t) = \mathcal{L}^{-1}[T(s)] \tag{I-4}$$

where $\mathcal{L}^{-1}$ denotes the inverse Laplace transform. By (Abramawitz, 1964; eq. 29.3.96)

$$I(t) = \frac{ak}{\sqrt{t^2 - k^2}} I_1(a\sqrt{t^2 - k^2})u(t - k) + \delta(t - k) \tag{I-5}$$

where

$I_1(x)$ = first order modified Bessel function

$u(t - k)$ = unit step function

$\delta(t - k)$ = impulse function.

Since a is imaginary, we must find an equivalent to $I_1(ix)$. By (Abramawitz, 1964; eq. 9.6.3),

$$I_\nu(z) = e^{-(\nu/2)\pi i} J_\nu(z\, e^{(1/2)\pi i}) \tag{I-6}$$

Let $x = -e^{(1/2)\pi i}z$, then

$$I_\nu(-e^{-(1/2)\pi i}x) = i^\nu J_\nu(x) \quad . \tag{I-7}$$

With $\nu = 1$,

$$I_1(ix) = -iJ_1(-x) \quad . \tag{I-8}$$

However, $J_1(x)$ is odd so that

$$I_1(ix) = iJ_1(x) \quad . \tag{I-9}$$

Then

$$I(t) = \frac{-\omega_p k}{\sqrt{t^2 - k^2}} J_1(\omega_p \sqrt{t^2 - k^2})u(t - k) + \delta(t - k) \tag{I-10}$$

It is now useful to translate the time variable so that $\tau = 0$ is the time that light would reach the far side of the ionosphere. Let $\tau = t - k$, where $k = L/c$. Then

$$t^2 - k^2 = \tau(\tau + 2k)$$

and

$$I(\tau) = -\frac{\omega_p k}{\sqrt{\tau(\tau + 2k)}} J_1(\omega_p \sqrt{\tau(\tau + 2k)})u(\tau) + \delta(\tau) \tag{I-11}$$

The last equation is the impulse response of the ionosphere. If one is not interested in frequencies near the cutoff frequency ($\tau << k$), equation I-11 reduces to a simpler form which is more easily convoluted (numerically) with an arbitrary incident waveform, i.e.,

$$I(t) = -\sqrt{\frac{k}{2}} \frac{\omega_p}{\sqrt{\tau}} J_1(\omega_p \sqrt{2k\tau})u(\tau) + \delta(\tau) \tag{I-12}$$

The argument of $J_1(x)$ will normally be large and another good approximation can be made. For large arguments (Abramowitz, 1964; eq. 9.2.1)

$$J_\nu(z) \approx \sqrt{\frac{2}{\pi z}} \cos(z - (\nu/2)\pi - (1/4)\pi) \qquad \text{(I-13)}$$

With $\nu = 1$,

$$J_1(z) \approx \sqrt{\frac{2}{\pi z}} \cos\left(z - \frac{3\pi}{4}\right)$$

and, in the high frequency approximation,

$$I_1(\tau) \approx -\left(\frac{k}{2}\right)^{1/4} \sqrt{\frac{\omega_p}{\pi}} \frac{1}{\tau^{3/4}} \cos\left(\omega_p \sqrt{2k\tau} - \frac{3\pi}{4}\right) u(\tau) + \delta(\tau) \qquad \text{(I-14)}$$

The high frequency approximation allows us to easily characterize the ionosphere in terms of total electron content (TEC) instead of plasma frequency and depth:

$$f_p^2 = 80.6\ N \qquad \text{(I-15)}$$

$$f_p^2 L = 80.6\ NL$$

$$I(t) = -A \sqrt{\frac{TEC}{\tau}}\, J_1(2A\sqrt{(TEC)\,\tau})\, u(\tau) + \delta(\tau) \qquad \text{(I-16)}$$

where

$$A = \pi \sqrt{\frac{2(80.6)}{c}} .$$

When the large argument approximation is used,

$$I(t) = -\sqrt{2}\, B \frac{(TEC)^{1/4}}{\tau^{3/4}} \cos(2A\sqrt{(TEC)\,\tau})\, u(\tau) + \delta(\tau) \qquad \text{(I-17)}$$

where

$$B = \sqrt{\frac{80.6}{2c}} .$$

The envelope of the waveform, in the large argument approximation, can be found by ignoring the cosine term. The TEC will usually be between the limits

$$1.E16 < TEC\ (elec/m^2) < 1.E18$$

and most likely between the limits

$$5.E16 < TEC\ (elec/m^2) < 5.E17\ ,$$

with the lower values corresponding to nighttime ionospheres and the higher ones to daytime ionospheres.

The impulse response of the ionosphere is useful for comparing other calculations against and for convoluting with other input waveforms, but it cannot be used for estimating field strengths and time behavior alone. The fields produced by the impulse are many orders of magnitude higher than typical input waveforms would produce because of its unusual nature.

Appendix II. Effective Bandpass Calculation for a Step Function Bandpass Filter

Consider the system bandpass to be a difference of step functions such that the bandwidth is $2\Delta\omega$ centered about ω_o. The fields coupled into the system are given by

$$E_S(t) = \frac{1}{\pi}\int_{\omega_o-\Delta\omega}^{\omega_o+\Delta\omega} |\hat{E}(\omega)| e^{iP(\omega)} e^{i\omega t} d\omega \qquad \text{(II-1)}$$

where $|\hat{E}(\omega)|$ is the amplitude of the Fourier transform of the field impinging upon the system. The phase of the field and the phase shift due to the filter are combined in $P(\omega)$. Assume that $\Delta\omega$ is small enough to approximate $|\hat{E}(\omega)|$ by $|\hat{E}(\omega_o)|$ and that the phase can be expanded in a three term Taylor expansion about the center frequency. Then

$$P(\omega) = P_o - \tau(\omega_o)(\omega - \omega_o) + \frac{D}{2}(\omega - \omega_o)^2 \qquad \text{(II-2)}$$

where

$$P_o = P(\omega_o)$$

$$\tau(\omega_o) = -\left.\frac{dP}{d\omega}\right|_{\omega_o} \quad \text{(delay)}$$

$$D(\omega_o) = \left.\frac{d^2P}{d\omega^2}\right|_{\omega_o} \quad \text{(dispersion)}$$

and, with $x = (\omega - \omega_o)$,

$$E_S(t) = \frac{|\hat{E}(\omega_o)|}{\pi} e^{i(\omega_o t + \phi(\omega_o))} \int_{-\Delta\omega}^{\Delta\omega} e^{i[(t-\tau)x + \frac{1}{2}Dx^2]} dx \qquad \text{(II-3)}$$

This equation is of the form

$$E_S(t) = \frac{|\hat{E}(\omega_o)|}{\pi} \int_{-\Delta\omega}^{\Delta\omega} e^{i(ax^2+2bx+c)}\,dx \qquad \text{(II-4)}$$

or

$$E_S(t) = \frac{|\hat{E}(\omega_o)|}{\pi} \int_{-\Delta\omega}^{\Delta\omega} e^{-(Ax^2+2Bx+C)}\,dx \qquad \text{(II-5)}$$

$$= \frac{|\hat{E}(\omega_o)|}{\pi} B(\Delta\omega, D) \ , \qquad \text{(II-6)}$$

where

$$a = \frac{D(\omega_o)}{2} \qquad \text{(II-7)}$$

$$b = \frac{1}{2}[t - \tau(\omega_o)] \qquad \text{(II-8)}$$

$$c = \omega_o t + \phi(\omega_o) \ . \qquad \text{(II-9)}$$

The general solution of $B(\Delta\omega, D)$ is (Abramowitz, 1964: eq. 7.4.32)

$$B(\Delta\omega, D) = \frac{1}{2}\sqrt{\frac{\pi}{A}}\, e^{-\frac{B^2-AC}{A}} \operatorname{erf}\left[\sqrt{A}x + \frac{B}{\sqrt{A}}\right]\Bigg|_{-\Delta\omega}^{\Delta\omega} \qquad \text{(II-10)}$$

or,

$$B(\Delta\omega, D) = \frac{1}{2}\sqrt{\frac{\pi}{A}}\, e^{-\frac{ac-b^2}{a}} \{\operatorname{erf}[\sqrt{-i}(\sqrt{a}\Delta\omega + b/\sqrt{a})]$$

$$- \operatorname{erf}[-\sqrt{-i}(\sqrt{a}\Delta\omega - b/\sqrt{a})]\} \ . \qquad \text{(II-11)}$$

The error function is defined by

$$\mathrm{erf}(z) = \frac{2}{\pi}\int_o^z e^{-t^2}dt \ . \qquad \text{(II-12)}$$

From the definition, it is immediately seen that the function is odd. Also, from the definition, an expression for $\mathrm{erf}(\sqrt{\pm i}z)$ can be found. Changing the variable of integration from t to

$$u = \sqrt{\frac{2}{\pi}}\sqrt{\pm i}t \ ,$$

$$\mathrm{erf}(\sqrt{\pm i}z) = \sqrt{\pm i}\sqrt{2}\int_o^{\sqrt{2/\pi}z} e^{\pm i(\pi/2)u^2}du$$

and

$$\mathrm{erf}(\sqrt{\pm i}z) = \sqrt{\pm i}\sqrt{2}[C(\sqrt{2/\pi}z) \pm iS(\sqrt{2/\pi}z)] \ , \qquad \text{(II-13)}$$

where the Fresnel sine and cosine integrals are defined by

$$S(z) = \int_o^z \sin\left(\frac{\pi}{2}t^2\right)dt \qquad \text{(II-14)}$$

$$C(z) = \int_o^z \cos\left(\frac{\pi}{2}t^2\right)dt \ . \qquad \text{(II-15)}$$

With these substitutions,

$$B(\Delta\omega,D) = \sqrt{\frac{\pi}{2a}}\, e^{-i\frac{ac-b^2}{a}}\{[C(z_+) + C(z_-)] - i[S(z_+) + S(z_-)]\} \qquad \text{(II-16)}$$

where

$$z_\pm = \sqrt{\frac{\pi}{2}}[\sqrt{a}\Delta\omega \pm b/\sqrt{a}] \ . \qquad \text{(II-17)}$$

Converting to phase and amplitude notation,

$$B(\Delta\omega,D) = \sqrt{\frac{\pi}{2a}}\sqrt{[C(z_+) + C(z_-)]^2 + [S(z_+) + S(z_-)]^2}\, e^{i\phi} \quad \text{(II-18)}$$

where

$$\phi = -i\left[\frac{ac - b^2}{a} + \tan^{-1}\frac{S(z_+) + S(z_-)}{C(z_+) + C(z_-)}\right] .$$

If the oscillating term is ignored, the effective bandwidth becomes

$$|B(\Delta\omega,D)| = \sqrt{\frac{\pi}{2a}}\sqrt{[C(z_+) + C(z_-)]^2 + [S(z_+) + S(z_-)]^2} \quad \text{(II-19)}$$

where

$$z_{\pm} = \sqrt{\pi/2}[\sqrt{a}\Delta\omega \pm b/\sqrt{a}]$$

$$a = \frac{D(\omega_o)}{2}$$

$$b = \frac{1}{2}[t - \tau(\omega_o)] .$$

When the dispersion is large, i.e., $D\Delta\omega >> \Delta t$, where $\Delta t = \tau(\omega_o) - \tau(\omega_o - \Delta\omega)$,

$$|B(\Delta\omega,D)| = 2\sqrt{\frac{\pi}{D}}\sqrt{C^2(z_o) + S^2(z_o)} \quad \text{(II-20)}$$

where $z_o = \sqrt{a}\Delta\omega$. In the limit of large z_o,

$$C(z_o) = S(z_o) = \frac{1}{2}$$

and the effective bandwidth becomes the ionospheric bandwidth

$$\Delta = \sqrt{\frac{2\pi}{D}} . \quad \text{(II-21)}$$

Appendix III. Effective Bandpass Calculation for a Gaussian Bandpass Filter

In section 4.2, we modeled the system as a step function with center frequency ω_o and bandwidth $2\Delta\omega$. Because this model is so unnatural, it would be encouraging to find that the same peak fields were predicted using a different model, for large dispersion. Let the bandpass be described by the Gaussian function,

$$G(\omega) = e^{-\left(\frac{\omega+\omega_o}{\Delta\omega}\right)^2} \qquad \text{(III-1)}$$

so that the electric field seen by the system is

$$E(t) = \frac{|\hat{E}|}{\pi} \int_{-\infty}^{\infty} e^{i(\phi_o - \tau(\omega-\omega_o) + \frac{D}{2}(\omega-\omega_o)^2} e^{-\left(\frac{\omega-\omega_o}{\Delta\omega}\right)^2} e^{i\omega t} d\omega \qquad \text{(III-2)}$$

where

$$\tau = -\frac{d\phi}{d\omega}$$

$$D = \frac{d^2\phi}{d\omega^2} .$$

The Taylor expansion of the phase is valid for $\Delta\omega$ small enough to force the integral to have negligible contributions very far from ω_o. The integral is of the form

$$E(t) = \frac{|\hat{E}|}{\pi} e^{i(\phi_o + \omega_o t)} \int_{-\infty}^{\infty} e^{-a^2x^2+bx} dx \qquad \text{(III-3)}$$

where

$$x = \omega - \omega_o$$

$$a^2 = \frac{1}{(\Delta\omega)^2} - i\frac{D}{2}$$

$$b = i(t - \tau) \ .$$

Using the notation of section 4.2,

$$B(\Delta\omega) = e^{i(\phi_o + \omega_o t)} \int_{-\infty}^{\infty} e^{-a^2x^2 + bx} dx \qquad \text{(III-4)}$$

and

$$E(t) = \frac{|\hat{E}|}{\pi} B(\Delta\omega) \ . \qquad \text{(III-5)}$$

The integral has the solution

$$W = \frac{\sqrt{\pi}}{a} \exp\left[\frac{b^2}{4a^2}\right] \qquad \text{(III-6)}$$

or

$$W = \frac{\sqrt{\pi}}{\sqrt{\left(\frac{1}{\Delta\omega}\right)^2 - i\,\frac{D}{2}}} \exp\left[-\frac{(t - \tau)^2}{4\left(\left(\frac{1}{\Delta\omega}\right)^2 - i\,\frac{D}{2}\right)}\right]. \qquad \text{(III-7)}$$

Manipulating terms to give W the form of a phase and amplitude,

$$W = e^{iP} \frac{\exp\left\{-\frac{(t - \tau)^2}{4(\Delta\omega)^2\left[\left(\frac{1}{\Delta\omega}\right)^4 + \left(\frac{D}{2}\right)^2\right]}\right\}}{\left[\left(\frac{1}{\Delta\omega}\right)^4 + \left(\frac{D}{2}\right)^2\right]^{1/4}} \qquad \text{(III-8)}$$

where

$$P = \frac{1}{2}\tan^{-1}\left(\frac{D}{2(\Delta\omega)^2}\right) - \frac{D(t - \tau)}{8\left[\left(\frac{1}{\Delta\omega}\right)^4 + \left(\frac{D}{2}\right)^2\right]} \ . \qquad \text{(III-9)}$$

Ignoring the phase terms, the electric field envelope is seen to be

$$E(t) = \frac{|\hat{E}|}{\pi}\sqrt{\frac{2\pi}{D}}\exp\left|-\left[\frac{(t-\tau)}{\Delta\omega D}\right]\right| \qquad \text{(III-10)}$$

for large dispersion, i.e., $D >> 1/(\Delta\omega)^2$. Then, the peak field is given by

$$E_M = \frac{|\hat{E}|}{\pi}\Delta \qquad \text{(III-11)}$$

where the effective bandwidth is

$$\Delta = \sqrt{\frac{2\pi}{D}}\ , \qquad \text{(III-12)}$$

just as calculated in 4.2.

It is interesting to note that the Gaussian bandpass modulates the received signal with a Gaussian envelope. For the low dispersion case, the envelope is of the form

$$\exp\left|-\frac{(\Delta\omega)^2(t-\tau)^2}{4}\right| \qquad \text{(III-13)}$$

instead of the sinusoidal envelope produced by the step function bandpass, i.e.,

$$\frac{\sin[\Delta\omega(t-\tau)]}{t-\tau}\ .$$

Appendix IV. The Fourier Transform of the Double Exponential Pulse

Since the double exponential pulse is often used as an analytic waveform, it is useful to have a ready reference for its Fourier transform. This appendix describes that transform and gives approximations for several ranges of frequency and for some specific frequencies.

The double exponential has the form

$$E(t) = E_o[e^{-\beta t} - e^{-\alpha t}] \tag{IV-1}$$

where α is the rise rate and β is the fall-off rate. Its Fourier transform is

$$\hat{E} = E_o\left|\frac{\alpha - \beta}{(\alpha + i\omega)(\beta + i\omega)}\right| \tag{IV-2}$$

or

$$\hat{E} = \left[\frac{\alpha - \beta}{(\alpha\beta - \omega^2) + i\omega(\alpha + \beta)}\right] \tag{IV-3}$$

The amplitude and phase are given by

$$|\hat{E}| = \frac{E_o(\alpha - \beta)}{\sqrt{(\alpha\beta - \omega^2)^2 + \omega^2(\alpha + \beta)^2}} \tag{IV-4}$$

$$\tan\phi = -\frac{\omega(\alpha + \beta)}{\alpha\beta - \omega^2} . \tag{IV-5}$$

In the following approximations, assume $\alpha >> \beta$ and define $R = |\hat{E}|/E_o$.

Case 1: $\omega << \beta << \alpha$

$$R \simeq 1/\beta \tag{IV-6}$$

$$\tan\phi \simeq \phi \simeq -\omega/\beta$$

Case 2: $\omega = \beta << \alpha$

$$R = \frac{1}{\sqrt{2}\beta} \tag{IV-7}$$

$$= - \pi/4 \tag{IV-8}$$

Case 3: $\omega \sim \beta << \alpha$

$$R \simeq 1/\sqrt{\beta^2 + \omega^2} \tag{IV-9}$$

Case 4: $\beta << \omega << \alpha$

$$R \simeq 1/\omega \tag{IV-10}$$

$$\tan\phi \simeq \frac{-1}{\beta/\omega - \omega/\alpha} \tag{IV-11}$$

Case 5: $\omega = \sqrt{\alpha\beta}$

$$R = 1/\sqrt{\alpha\beta} \tag{IV-12}$$

$$\phi = - \pi/2 \tag{IV-13}$$

Case 6: $\beta << \omega \sim \alpha$

$$R \simeq \frac{\alpha}{\omega\sqrt{\alpha^2 + \omega^2}} \tag{IV-14}$$

$$\tan\phi \simeq - \alpha/\omega \tag{IV-15}$$

Case 7: $\beta << \omega = \alpha$

$$R = 1/\sqrt{2}\alpha \tag{IV-16}$$

$$\tan\phi = -1 \tag{IV-17}$$

$$\phi = - 3\pi/4 \tag{IV-18}$$

Case 8: $\beta << \alpha << \omega$

$$R \simeq \alpha/\omega^2 \tag{IV-19}$$

$$\tan\phi \simeq - \alpha/\omega \tag{IV-20}$$

Case 9: $\lim_{\omega\to\infty} R, \phi$

$$R = 0 \tag{IV-21}$$

$$\phi = -\pi \tag{IV-22}$$